Juniper Publishers
key to the Researchers

ONSITE CONSTRUCTION OF MASS-CONSERVED BOUNDARY CONDITIONS FOR PRESCRIBED VELOCITIES ON SOLID WALLS USING FIRST AND THIRD ORDER MOMENTS FOR LATTICE BOLTZMANN SIMULATIONS

ISBN: 978-1-946628-31-2

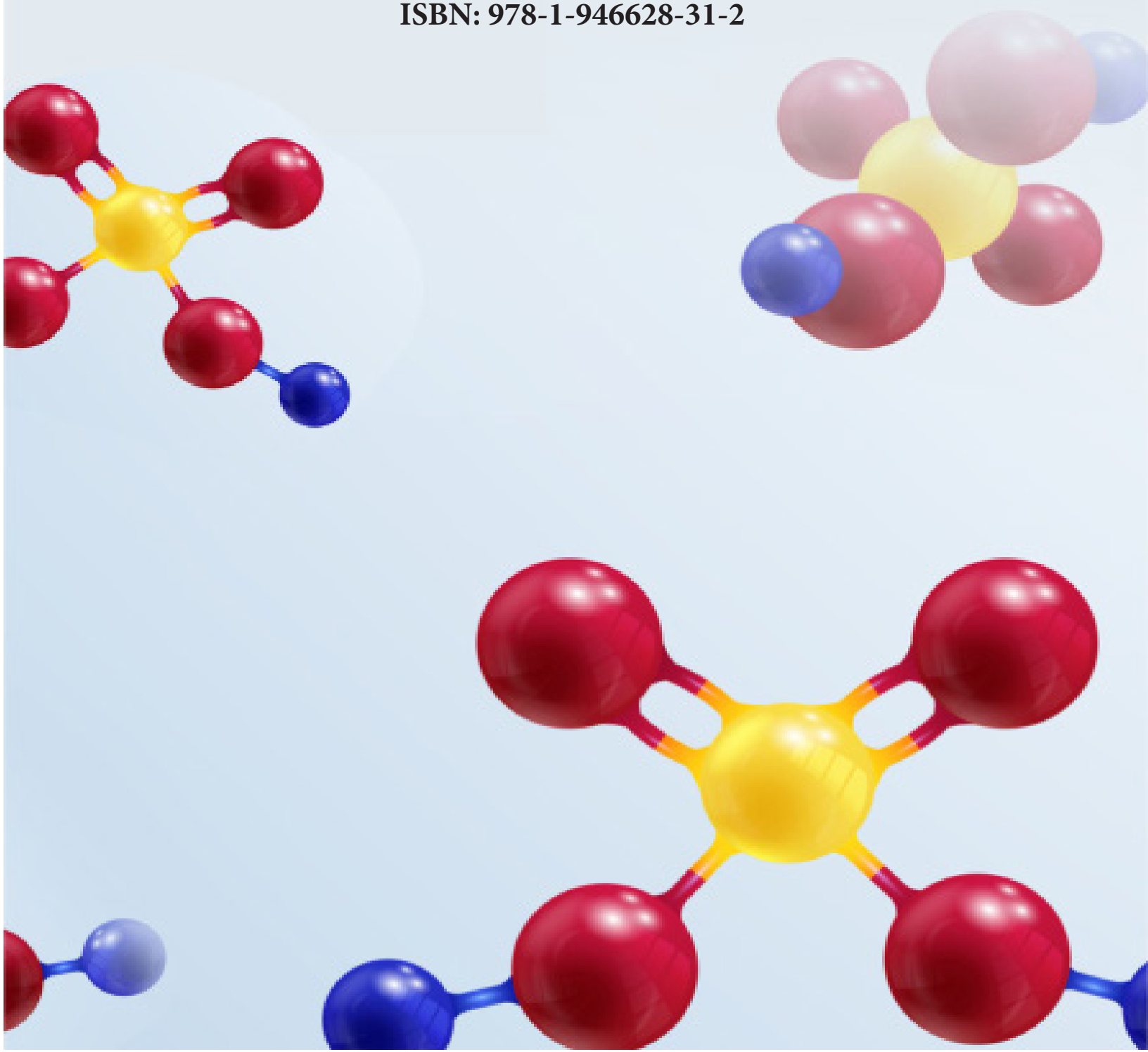

Onsite Construction of Mass-Conserved Boundary Conditions for Prescribed Velocities on Solid Walls Using First and Third Order Moments for Lattice Boltzmann Simulations

Jiujiang Zhu*

School of Civil Engineering and Architecture, Wuyi University, China

***Corresponding Author**

Jiujiang Zhu, School of Civil Engineering and Architecture, Wuyi University, China

Published By

Juniper publishers Inc.
United States
February 04, 2021

Author Biography

Prof. Jiujiang Zhu is an experienced mathematician with thermodynamics and continuum mechanics background; has more than 20 years teaching and research experience in international universities; has worked successfully in several different research areas such as solid and fluid mechanics, materials science, image analysis, computational biology, and computational fluid dynamics, has a particular skill for mathematical modeling and numerical simulation; was awarded “One Hundred Excellent Young Scientists” by Chinese Academy of Sciences in the year 1997.

List of Contents

Abstract

In this monograph, a new scheme for constructing a velocity boundary condition is proposed for Lattice Boltzmann Model: it enables one to prescribe exact nonslip or slip velocity on every shared face between any adjacent fluid and solid cells, defined by a 2/3D binary image. With respect to image cells, a face-center LB lattice is adopted so that each lattice boundary node coincides with the center of a shared face between a pair of adjacent fluid and solid cells. Extended from the 2D off-equilibrium bounce-back scheme proposed by Zou & He [1], this scheme makes use of both first- and third-order moments of Probability Distribution Functions, $\{f_\alpha\}$, also referred to as particle populations, at each node on a boundary face in α velocity directions, to construct every particle population with an unknown/unspecified quantity; it results in that all particle populations become known and specified after the streaming operation. The scheme possesses the following characteristics:

I. On-site as it makes use of particle populations at each node only;

II. Retaining all known particle populations;

III. Nodal mass conservation as it ensures particle populations entered each solid cell and come out it by applying a correction to zero-direction particle population.

It is convenient for parallel implementation and can be used for modeling fluid flow with strong interaction between the fluid and the solid at the wall of a flow domain.

Keywords: Lattice Boltzmann Model; Third-order moments; Boundary condition

Introduction

Lattice Boltzmann Model (LBM) has become a popular approach in Computational Fluid Dynamics. LBM represents a fluid as discrete Probability Distribution Functions (PDF) $\{f_\alpha\}$, or particle populations, at each lattice node on a lattice along with α velocity directions. For low Mach-number fluid flow as considered in this monograph, each particle population f_α can be divided as the sum of non-equilibrium and equilibrium parts, donated as f_α^{non} and f_α^{eq}, respectively (for details see the next section), and LBM simulates fluid flow by colliding particle populations at every node toward equilibrium counterparts and then streaming every particle population of a node to an adjacent node along with its respective velocity directions. Unlike in the standard continuum approach, the fluid is treated as a continuum, and its flow behaviours are characterized by basic physical quantities (e.g., density, velocity, and temperature $\{\rho, \mathbf{u}, \theta\}$) to be solved governing partial differential questions (e.g., Naiver-Stokes equations and heat conduction equations), LBM does not solve basic physical quantities directly but recover them from the moments of PDF.

Given a physical flow domain that contains void space for fluid to occupy and its conjugated solid space, LBM requires that domain be discretized into lattice or mesh. The easiest way to do this is to construct a regular spacing lattice composed of a fluid and solid nodes to fit that domain as tightly as possible. It is known that on a regular spacing, lattice LBM computation can be optimized by many techniques, including efficient parallelisation [2]. However, a regular spacing lattice cannot fit a flow domain that contains an irregular boundary tightly, and that boundary can only be approximated by a set of zigzagged connected surface patches of a regular spacing lattice. In a Cartesian coordinate system, each surface patch is a square; its normal coincides with the cardinal direction of the coordinate system. In LBM fluid and solid interaction is treated by one of two approaches:

1) Implicit surface approximation in which the interaction is assumed to take place on an implicit surface that matches closer to the boundary but cuts through a set of adjacent fluid and solid nodes [3,8], and

2) Explicit patch approximation in which the interaction is assumed to take place on a set of zigzagged connected patches [1,9-12].

The explicit patch approximation has been widely applied in modeling flow in porous media where a physical flow domain cannot be defined precisely but only approximately. The binarization of an X-ray tomography image of a porous sample is a widely adopted process to obtain an approximate flow domain to the unknown actual physical domains [12-15]. In this monograph, this second approach is of concern only, and hereafter an input to LBM is a binary image whose pixel/voxel values of 0 or 1 define fluid (or pore cubic cells) or non-fluid (or solid cells), respectively.

Given a binary image as an input, the explicit patch approximation can take two different pathways depending on how an LB lattice is defined with reference to the cell-based input image. The most common approach is to define a lattice so that each of its nodes is located in the center of a cell, and each shared face between two adjacent fluid and solid cells defines a patch on an approximated solid wall surface. This leads to a so-called cell-center lattice on which nonslip velocity can be 'recovered' on each patch with a zero patch-tangential component simply by applying a bounce-back scheme during the streaming operation. Since the bounce-back scheme can be implemented almost without incurring a further computational cost, this is where claimed advantages of LBM lie for dealing with a complex flow domain. However, the bounce-back scheme results in a nonzero patch-tangential velocity component at each fluid node next to a patch on a cell-center lattice [16-19]. Besides this drawback, a cell-center lattice has another even more critical weakness, that is, one cannot develop velocity boundary conditions to match exactly prescribed velocities on each patch because no lattice node is defined on any patch [16-19]. This limits LBM to be applied where nonslip boundary condition is necessary for modeling flow correctly, such as in tightly confined pore space where the slip flow is dominant [20].

To overcome the drawbacks of the cell-center lattice, we propose here to construct an alternative type of lattice, face-centered lattice, for LBM. In a face-centered lattice, every one of its nodes coincides with the center of one of the shared faces between every pair of adjacent image cells. In effect, such a face-centered lattice expands the fluid domain of the 3D image by half of a lattice unit on every wall face. Appendix A shows all 2D boundary configurations defined by a 2D binary image whose fluid and solid cells/pixels are overlapped by the corresponding face-centered lattice inflated into solid image cells. In this monograph, we develop a method for constructing velocity boundary conditions for the flow domain defined by a 3D binary image on its corresponding face-center lattices.

In LBM, the construction of a velocity boundary condition is often performed in conjunction with the streaming operation to ensure that after streaming, every particle population at a fluid node is defined. After streaming, each undefined/unknown particle population at a fluid node must be adjacent to a solid node along one direction. If that particle population is constructed from known particle populations of the same node only, and prescribed boundary condition on the solid node, we refer it as onsite construction [9], otherwise off-site construction

[10]. The bounce-back scheme on a cell-center lattice is an onsite construction for nonslip velocity condition; it does this by setting each unknown particle population, which would be streamed out of an adjacent wall node at a direction, by the particle population which enters into the wall along the opposite direction. This monograph reports the development of an onsite scheme for a face-centered lattice in 3D that considers all possible combinations of zigzagged patch arrangements.

Some earlier onsite construction schemes for zigzagged boundaries were developed for 2D only or do not satisfy the mass conservation. For a brief review, the reader is referred to Latt et al. [11]. Early work includes Inamuro model [21] and Zou–He model [1]. Inamuro et al. [21] proposed to evaluate the unknown f_α using their equilibrium counterparts with a counter-slip velocity and undetermined density. This scheme is only applicable in 2D, and it is impractical to extend to 3D (see Latt et al. [11]). Based on the boundary conditions developed by Noble et al. [22] and Maier et al. [23], Zou and He [1] proposed an off-equilibrium bounce-back model for the D2Q9 but limited to 2D only as it would induce conflicts in the momentum equations.

Many previous schemes did not satisfy this[24,25]. For example, Inamuro scheme [21], the density was implicitly determined in boundary reconstruction. As pointed by Chopard & Dupuis[24] and Latt et al. [11], "even though these conservation laws guarantee equal mass in the pre- and post-collision state of a cell, they do not guarantee global mass conservation in the system." This defect is related to the non-equilibrium parts of particle populations, and results from the boundary reconstruction which does not guarantee the same amount of mass to be received by a wall will be re-injected in the fluid after streaming. We will show the on-site reconstruction scheme satisfies mass-conservation as it uses the particle population at 0 direction to compensate the induced mass difference.

Almost existing boundary condition reconstruction schemes retain all known particle populations, which are streamed from neighbour fluid nodes, and only reconstruct unknown populations, which are streamed from solid wall nodes, including Inamuro model [21] and Zou-He model [1]. But there are schemes which do not follow this 'rule ' and replace all known populations [11]. The simplest approach is to replace every particle population by corresponding equilibrium particle populations. In this over-simplified approach, only zero and first-order moments of PDF may not be zero, whereas all higher-order moments of PDF are zero. Latt et al. [11] demonstrated this approach is not accurate and proposed to replace all PDFs with each corresponding equilibrium part plus the second-order moment. The second-order moment was reconstructed through an off-equilibrium bounce-back method, and for the reconstructed PDFs, we have nonzero moments up to the second-order only. However, this is not applicable to thermal LBM simulation with an isothermal boundary condition, because the heat flux is generally nonzero and is directly linked to the third-order moments.

Some previous schemes reconstructed unknown particle populations from the second-order moments [10,26-31], which are related to the stress tensor or strain rate tensor. Skordos [10] calculated a stress tensor from the velocity gradient using finite difference, an offset scheme. Taheri et al. [32] used Grad's 13-moment equations to explore how the slip velocity is related to the higher-order moments. These show that the different orders of the moments correspond to different states of the same flow filed at a continuum scale that the boundary conditions are prescribed. Therefore, in order to ensure the prescribed boundary conditions are consistent, we should avoid selecting those orders of the moments that would amount to constrain different states at the same location. It is easy to see that all odd orders of equilibrium PDF moments are linear functions of velocity, whereas all even orders of equilibrium PDF moments are square functions of velocity (see Eq. and Eq. for details). Therefore, we propose to the first and third orders of PDF moments to develop our on-site reconstruction scheme.

More specifically, we extend the off-equilibrium bounce-back model proposed by Zou and He [1] from 2D to 3D and propose zero off-equilibrium third-order moments of the PDF model. We will preserve the known particle populations at boundary nodes, as it is necessary.

To summarise, this monograph proposes a 3D mass conserved reconstruction for prescribing slip and/or nonslip velocity boundary condition on each wall surface. The reconstruction retains all known particle populations which are streamed from neighbour fluid nodes. The reconstruction is onsite, i.e., unknown particle populations are reconstructed using the known particle populations in the current node only. The boundary condition is reconstructed using the first and third-order moments of PDF only. We postulate even and odd moments should not be mixed in the boundary condition reconstruction due to corresponding to different physical quantities.

This monograph is organized as follows: Section 5 gives a brief overview of basic LB equations for D3Q19 lattice. Section 6 reveals non-equilibrium and equilibrium moments up to the third order. In section 7, all possible boundary configurations on a cylindrical channel are reconstructed. Section 8 treats inlet and outlet boundary conditions. Section 9 gives some cases study followed by conclusions in section 10. In Appendix A, it is elaborated how a flow domain in a binary image can be transformed into a face-center LB lattice. 3D face-centre LB lattice can be built from an X-ray CT image in the same manner. All possible boundary configurations in 2D are enumerated, including those which have not been considered in the literature. In 2D, cases 1, 2, and 3 have been considered, whereas cases 4, 5, and 6 have not yet.

Lattice boltzmann model in D3Q19 lattice

Assume the force acting on each particle is $\mathbf{F}'$, the mass of each particle is m, and particle density is n, then the mass density $\rho = \rho(\mathbf{r},t) = mn$, the force applied on unit volume will be $\mathbf{F} = n\mathbf{F}'$. Velocity distribution function $f(\mathbf{r}, \xi, t)$ satisfies the Boltzmann equation as follows:

$$\frac{\partial f(\xi,\mathbf{r},t)}{\partial t} + \xi \cdot \frac{\partial f(\xi,\mathbf{r},t)}{\partial \mathbf{r}} + \frac{1}{\rho}\mathbf{F} \cdot \frac{\partial f(\xi,\mathbf{r},t)}{\partial \xi} = -\frac{f - f^{eq}}{\tau} \tag{1}$$

In which equilibrium distribution

$$f^{eq}(\xi,\mathbf{r},t) = n(\mathbf{r},t)\Gamma(\xi,\mathbf{r},t) = \frac{n(\mathbf{r},t)}{\left[2\pi\theta(\mathbf{r},t)\right]^{D/2}} \exp\left\{-\frac{\left[\xi - \mathbf{u}(\mathbf{r},t)\right]^2}{2\theta(\mathbf{r},t)}\right\} \tag{2}$$

and

$$\Gamma(\xi,\mathbf{r},t) = \frac{1}{\left[2\pi\theta(\mathbf{r},t)\right]^{D/2}} \exp\left\{-\frac{\left[\xi - \mathbf{u}(\mathbf{r},t)\right]^2}{2\theta(\mathbf{r},t)}\right\} \tag{3}$$

Following He et al. [33], we adopt the following approximation

$$\frac{\partial f(\xi,\mathbf{r},t)}{\partial \xi} \approx \frac{\partial f^{eq}(\xi,\mathbf{r},t)}{\partial \xi} = -\frac{(\xi - \mathbf{u})}{\theta} f^{eq}(\xi,\mathbf{r},t) \tag{4}$$

then Eq. can be integrated as

$$f(\xi,\mathbf{r}+\xi\Delta t, t+\Delta t) - f(\xi,\mathbf{r},t) = -\int_t^{t+\Delta t} \frac{f - f^{eq}}{\tau} dt + \int_t^{t+\Delta t} \frac{\mathbf{F}\cdot(\xi - \mathbf{u})}{\rho\theta} f^{eq}(\xi,\mathbf{r},t)\, dt \tag{5}$$

If the trapezoid approximation is adopted to first integration on the right-hand side of Eq. (5) and rectangle approximation to second integration in Eq.(5), we have

$$f(\xi,\mathbf{r}+\xi\Delta t, t+\Delta t) - f(\xi,\mathbf{r},t) = -\frac{\left(f - f^{eq}\right)\big|_t}{\tilde{\tau}^*} + \Delta t \frac{\mathbf{F}\cdot(\xi - \mathbf{u})}{\rho\theta} f^{eq}\big|_t \tag{6}$$

in which

$$\tilde{\tau}^* = \tilde{\tau} + \frac{1}{2} = \frac{\tau}{\Delta t} + \frac{1}{2} \tag{7}$$

The discrete Boltzmann equation may be obtained by discretization Eq. for typical lattice structures, without loss generate, we use D3Q19 in this monograph (Figure 1).

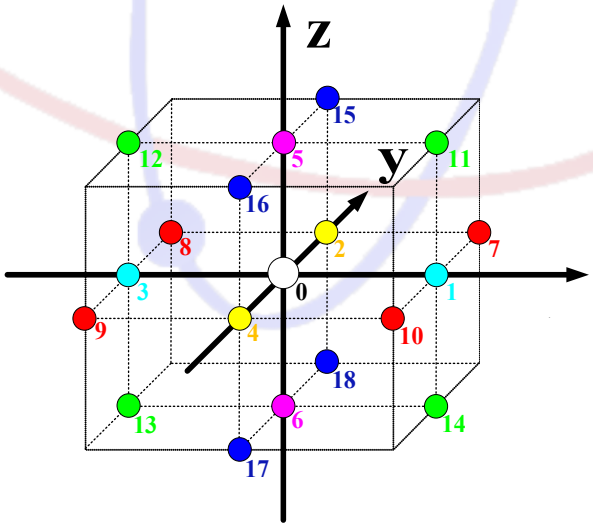

Figure 1: Sketch of D3Q19 Lattice.

The normalized lattice vectors for D3Q19 lattice reads

$$\mathbf{e}_\alpha \quad (\alpha = 0,1,\cdots,18) \tag{8}$$

$\mathbf{e}$	0	1	2	3	4	5	6	7	8	9	10	11	12	13	14	15	16	17	18
x	0	1	0	−1	0	0	0	1	−1	−1	1	1	−1	−1	1	0	0	0	0
y	0	0	1	0	−1	0	0	1	1	−1	−1	0	0	0	0	1	−1	−1	1
z	0	0	0	0	0	1	−1	0	0	0	0	1	1	−1	−1	1	1	−1	−1

(9)

The standard lattice velocity $\hat{\mathbf{e}}_\alpha = \Delta x \ _\alpha \ \Delta x$ is the length of space lattice. Let denote the following discrete functions:

$$\Gamma_\alpha(\mathbf{r},t) = \Gamma(\xi_\alpha,\mathbf{r},t) = w_\alpha\left[1+\frac{\xi_\alpha\cdot\mathbf{u}}{\theta}+\frac{(\xi_\alpha\cdot\mathbf{u})^2}{2\theta^2}-\frac{\mathbf{u}^2}{2\theta}\right] \tag{10}$$

$$w_\alpha = \begin{cases} 1/3 & \alpha=0 \\ 1/18 & \alpha=1,2\cdots,6 \\ 1/36 & \alpha=7,8,\cdots 18 \end{cases} \tag{11}$$

$$f_\alpha = f_\alpha(\mathbf{r},t) \equiv mf(\xi_\alpha,\mathbf{r},t) \tag{12}$$

$$f_\alpha^{eq}(\mathbf{r},t) \equiv mf^{eq}(\xi_\alpha,\mathbf{r},t) \approx \rho\Gamma_\alpha(\mathbf{r},t) \tag{13}$$

Let

$$c = \frac{\Delta x}{\Delta t} \tag{14}$$

introduce the following dimensionless variables

$$\tilde{\tau} = \frac{\tau}{\Delta t},\ \tilde{\tau}^* = \tilde{\tau}+\frac{1}{2},\ \tilde{\mathbf{r}} = \frac{\mathbf{r}}{\Delta x},\ \tilde{t} = \frac{t}{\Delta t} \tag{15}$$

$$\tilde{\mathbf{u}} = \frac{\mathbf{u}}{c},\ \tilde{\theta} = \frac{\theta}{c^2} \equiv \frac{1}{3} \tag{16}$$

$$\tilde{\rho} = \frac{\rho}{\rho_c},\quad \tilde{f}_\alpha = \frac{f_\alpha}{\rho_c},\quad \tilde{f}_\alpha^{eq} = \frac{f_\alpha^{eq}}{\rho_c} \tag{17}$$

$$\tilde{\mathbf{F}} = \frac{\mathbf{F}\Delta t}{\rho_c c} \tag{18}$$

in which ρ_c is the reference density of the system. Then the dimensionless form of Eq. reads

$$\Gamma_\alpha(\tilde{\mathbf{u}}) = w_\alpha\left[1+\frac{\mathbf{e}_\alpha\cdot\tilde{\mathbf{u}}}{\tilde{\theta}}+\frac{(\mathbf{e}_\alpha\cdot\tilde{\mathbf{u}})^2}{2\tilde{\theta}^2}-\frac{\tilde{\mathbf{u}}^2}{2\tilde{\theta}}\right] \tag{19}$$

The dimensionless form of Eq.(13) reads

$$\tilde{f}_\alpha^{eq} = \tilde{\rho}\Gamma_\alpha(\tilde{\mathbf{u}}) \tag{20}$$

The dimensionless discrete form of Eq(6) reads

$$\tilde{f}_\alpha(\tilde{\mathbf{r}}+\mathbf{e}_\alpha,\tilde{t}+1)-\tilde{f}_\alpha(\tilde{\mathbf{r}},\tilde{t}) = -\frac{\tilde{f}_\alpha(\tilde{\mathbf{r}},\tilde{t})-\tilde{f}_\alpha^{eq}(\tilde{\mathbf{r}},\tilde{t})}{\tilde{\tau}^*}+\frac{\tilde{\mathbf{F}}\cdot(\mathbf{e}_\alpha-\tilde{\mathbf{u}})}{\tilde{\theta}}\Gamma_\alpha(\tilde{\mathbf{u}}) \tag{21}$$

Let the collision variable be:

$$\tilde{f}_\alpha^c(\tilde{\mathbf{r}},\tilde{t}+1) = \left(1-\frac{1}{\tilde{\tau}^*}\right)\tilde{f}_\alpha(\tilde{\mathbf{r}},\tilde{t})+\left[\frac{\tilde{\rho}}{\tilde{\tau}^*}+\frac{\tilde{\mathbf{F}}\cdot(\mathbf{e}_\alpha-\tilde{\mathbf{u}})}{\tilde{\theta}}\right]\Gamma_\alpha(\tilde{\mathbf{u}}) \tag{22}$$

Then Eq(21) may be rewritten to define the streaming operation as

$$\tilde{f}_\alpha(\tilde{\mathbf{r}}+\mathbf{e}_\alpha,\tilde{t}+1) = \tilde{f}_\alpha^c(\tilde{\mathbf{r}},\tilde{t}+1) \tag{23}$$

Mass equation reads

$$\sum_{\alpha=0}^{18}\tilde{f}_\alpha(\tilde{\mathbf{r}},\tilde{t}+1) = \tilde{\rho}(\tilde{\mathbf{r}},\tilde{t}+1) \tag{24}$$

Momentum equation reads

$$\sum_{\alpha=0}^{18}\tilde{f}_\alpha(\tilde{\mathbf{r}},\tilde{t}+1)\mathbf{e}_\alpha = \tilde{\rho}(\tilde{\mathbf{r}},\tilde{t}+1)\tilde{\mathbf{u}}(\tilde{\mathbf{r}},\tilde{t}+1) \tag{25}$$

In the node near to the solid wall, if direction $\bar{\alpha}$ ($\bar{\alpha}$ stands for the opposite direction of α) points to the solid node, the zero velocity may be achieved by applying bouncy back boundary condition in the streaming step, i.e.

$$\tilde{f}_\alpha(\tilde{\mathbf{r}},\tilde{t}+1) = \tilde{f}_{\bar{\alpha}}^c(\tilde{\mathbf{r}},\tilde{t}+1) \tag{26}$$

in which $\tilde{f}_{\bar{\alpha}}^{c}(\tilde{\mathbf{r}},\tilde{t}+1)$ can be calculated by Eq.(22),Eqs.(19),(22)-(26)forms a close set of equations for the first-order accuracy of Lattice Boltzmann Model. Eq.(26) is the so-called traditional bounce-back boundary condition.

Moments of probability distribution function

Let introduce the moments of probability distribution function up to the third order, and they take forms as follows:

The zero order moment:

$$\tilde{\mathbf{M}}_0=\sum_{\alpha=0}^{18}\tilde{f}_\alpha=\tilde{\rho} \tag{27}$$

Its component form reads as follows:

$$\tilde{\rho}=\left(\tilde{f}_1+\tilde{f}_7+\tilde{f}_{10}+\tilde{f}_{11}+\tilde{f}_{14}\right)+\tilde{f}_0+\tilde{f}_2+\tilde{f}_3+\tilde{f}_4+\tilde{f}_5+\tilde{f}_6+\tilde{f}_8+\tilde{f}_9+\tilde{f}_{12}+\tilde{f}_{13}+\tilde{f}_{15}+\tilde{f}_{16}+\tilde{f}_{17}+\tilde{f}_{18} \tag{28}$$

The first order moment

$$\tilde{\mathbf{M}}=\sum_{\alpha=0}^{18}\tilde{f}_\alpha\mathbf{e}_\alpha=\tilde{\rho}\tilde{\mathbf{u}} \tag{29}$$

Its component form reads as follows:

$$\tilde{M}_x=\tilde{f}_1+\tilde{f}_7+\tilde{f}_{10}+\tilde{f}_{11}+\tilde{f}_{14}-\tilde{f}_3-\tilde{f}_8-\tilde{f}_9-\tilde{f}_{12}-\tilde{f}_{13}=\tilde{\rho}\tilde{u}_x \tag{30}$$

$$\tilde{M}_y=\tilde{f}_7-\tilde{f}_{10}+\tilde{f}_2-\tilde{f}_4+\tilde{f}_8-\tilde{f}_9+\tilde{f}_{15}+\tilde{f}_{18}-\tilde{f}_{16}-\tilde{f}_{17}=\tilde{\rho}\tilde{u}_y \tag{31}$$

$$\tilde{M}_z=\tilde{f}_{11}-\tilde{f}_{14}+\tilde{f}_5-\tilde{f}_6+\tilde{f}_{12}-\tilde{f}_{13}+\tilde{f}_{15}+\tilde{f}_{16}-\tilde{f}_{17}-\tilde{f}_{18}=\tilde{\rho}\tilde{u}_z \tag{32}$$

The second order moments

$$\tilde{\mathbf{S}}=\sum_{\alpha=0}^{18}\tilde{f}_\alpha\mathbf{e}_\alpha\otimes\mathbf{e}_\alpha \tag{33}$$

The component form reads as follows:

$$\tilde{\mathbf{S}}=\begin{pmatrix}\left(\tilde{f}_1+\tilde{f}_7+\tilde{f}_{10}+\tilde{f}_{11}+\tilde{f}_{14}\right)+\tilde{f}_3+\tilde{f}_8+\tilde{f}_9+\tilde{f}_{12}+\tilde{f}_{13} & \left(\tilde{f}_7-\tilde{f}_{10}\right)+\tilde{f}_9-\tilde{f}_8 & \left(\tilde{f}_{11}-\tilde{f}_{14}\right)+\tilde{f}_{13}-\tilde{f}_{12}\\ \left(\tilde{f}_7-\tilde{f}_{10}\right)+\tilde{f}_9-\tilde{f}_8 & \left(\tilde{f}_7+\tilde{f}_{10}\right)+\tilde{f}_8+\tilde{f}_9+\tilde{f}_2+\tilde{f}_4+\tilde{f}_{15}+\tilde{f}_{16}+\tilde{f}_{17}+\tilde{f}_{18} & \tilde{f}_{15}-\tilde{f}_{16}+\tilde{f}_{17}-\tilde{f}_{18}\\ \left(\tilde{f}_{11}-\tilde{f}_{14}\right)+\tilde{f}_{13}-\tilde{f}_{12} & \tilde{f}_{15}-\tilde{f}_{16}+\tilde{f}_{17}-\tilde{f}_{18} & \left(\tilde{f}_{11}+\tilde{f}_{14}\right)+\tilde{f}_5+\tilde{f}_6+\tilde{f}_{12}+\tilde{f}_{13}+\tilde{f}_{15}+\tilde{f}_{16}+\tilde{f}_{17}+\tilde{f}_{18}\end{pmatrix} \tag{34}$$

The third order moments

$$\tilde{\mathbf{Q}}=\sum_{\alpha=0}^{18}\tilde{f}_\alpha\mathbf{e}_\alpha\otimes\mathbf{e}_\alpha\otimes\mathbf{e}_\alpha \tag{35}$$

The third-order tensor $\tilde{Q}$ can be represented as:

$$\tilde{\mathbf{Q}}=\left(\bar{\tilde{Q}}_{ik}\right)=\left(\tilde{Q}_{i\square k}\right) \tag{36}$$

In which

$$\bar{\tilde{Q}}_{11}=\begin{pmatrix}\tilde{Q}_{111}\\ \tilde{Q}_{121}\\ \tilde{Q}_{131}\end{pmatrix}=\begin{pmatrix}\left(\tilde{f}_1+\tilde{f}_7+\tilde{f}_{10}+\tilde{f}_{11}+\tilde{f}_{14}\right)-\tilde{f}_3-\tilde{f}_8-\tilde{f}_9-\tilde{f}_{12}-\tilde{f}_{13}\\ \left(\tilde{f}_7-\tilde{f}_{10}\right)+\tilde{f}_8-\tilde{f}_9\\ \left(\tilde{f}_{11}-\tilde{f}_{14}\right)+\tilde{f}_{12}-\tilde{f}_{13}\end{pmatrix} \tag{37}$$

$$\bar{\tilde{Q}}_{22}=\begin{pmatrix}\tilde{Q}_{212}\\ \tilde{Q}_{222}\\ \tilde{Q}_{232}\end{pmatrix}=\begin{pmatrix}\left(\tilde{f}_7+\tilde{f}_{10}\right)-\tilde{f}_8-\tilde{f}_9\\ \left(\tilde{f}_7-\tilde{f}_{10}\right)+\tilde{f}_2-\tilde{f}_4+\tilde{f}_8-\tilde{f}_9+\tilde{f}_{15}+\tilde{f}_{18}-\tilde{f}_{16}-\tilde{f}_{17}\\ \tilde{f}_{15}+\tilde{f}_{16}-\tilde{f}_{17}-\tilde{f}_{18}\end{pmatrix} \tag{38}$$

$$\bar{\tilde{Q}}_{33}=\begin{pmatrix}\tilde{Q}_{313}\\ \tilde{Q}_{323}\\ \tilde{Q}_{333}\end{pmatrix}=\begin{pmatrix}\left(\tilde{f}_{11}+\tilde{f}_{14}\right)-\tilde{f}_{12}-\tilde{f}_{13}\\ \tilde{f}_{15}+\tilde{f}_{18}-\tilde{f}_{16}-\tilde{f}_{17}\\ \left(\tilde{f}_{11}-\tilde{f}_{14}\right)+\tilde{f}_5-\tilde{f}_6+\tilde{f}_{12}-\tilde{f}_{13}+\tilde{f}_{15}+\tilde{f}_{16}-\tilde{f}_{17}-\tilde{f}_{18}\end{pmatrix} \tag{39}$$

$$\bar{\tilde{Q}}_{12} = \begin{pmatrix} \tilde{Q}_{112} \\ \tilde{Q}_{122} \\ \tilde{Q}_{132} \end{pmatrix} = \begin{pmatrix} \left(\tilde{f}_7 - \tilde{f}_{10}\right) + \tilde{f}_8 - \tilde{f}_9 \\ \left(\tilde{f}_7 + \tilde{f}_{10}\right) - \tilde{f}_8 - \tilde{f}_9 \\ 0 \end{pmatrix} \quad (40)$$

$$\bar{\tilde{Q}}_{13} = \begin{pmatrix} \tilde{Q}_{113} \\ \tilde{Q}_{123} \\ \tilde{Q}_{133} \end{pmatrix} = \begin{pmatrix} \left(\tilde{f}_{11} - \tilde{f}_{14}\right) + \tilde{f}_{12} - \tilde{f}_{13} \\ 0 \\ \left(\tilde{f}_{11} + \tilde{f}_{14}\right) - \tilde{f}_{12} - \tilde{f}_{13} \end{pmatrix} \quad (41)$$

$$\bar{\tilde{Q}}_{23} = \begin{pmatrix} \tilde{Q}_{213} \\ \tilde{Q}_{223} \\ \tilde{Q}_{233} \end{pmatrix} = \begin{pmatrix} 0 \\ \tilde{f}_{15} + \tilde{f}_{16} - \tilde{f}_{17} - \tilde{f}_{18} \\ \tilde{f}_{15} + \tilde{f}_{18} - \tilde{f}_{16} - \tilde{f}_{17} \end{pmatrix} \quad (42)$$

Note that the following symmetric conditions hold for $\{\bar{\tilde{Q}}_{ik}\}$ and $\{\tilde{Q}_{ijk}\}$, respectively as follows:

$$\bar{\tilde{Q}}_{ik} = \bar{\tilde{Q}}_{ki} \text{ and } \tilde{Q}_{ijk} = \tilde{Q}_{jik} = \tilde{Q}_{kji} = \tilde{Q}_{ikj} \quad (43)$$

Similarly, we may define the moments at equilibrium as

$$\tilde{\mathbf{M}}_0^{eq} = \sum_{\alpha=0}^{18} \tilde{f}_\alpha^{eq} = \tilde{\rho} \quad (44)$$

$$\tilde{\mathbf{M}}^{eq} = \sum_{\alpha=0}^{18} \tilde{f}_\alpha^{eq} \mathbf{e}_\alpha = \tilde{\rho}\tilde{\mathbf{u}} \quad (45)$$

$$\tilde{\mathbf{S}}^{eq} = \sum_{\alpha=0}^{18} \tilde{f}_\alpha^{eq} \mathbf{e}_\alpha \otimes \mathbf{e}_\alpha \quad (46)$$

$$\tilde{\mathbf{Q}}^{eq} = \sum_{\alpha=0}^{18} \tilde{f}_\alpha^{eq} \mathbf{e}_\alpha \otimes \mathbf{e}_\alpha \otimes \mathbf{e}_\alpha \quad (47)$$

Substituting Eq(20) into Eqs.(44)-(47) then Eqs.(44) and (45) are automatically satisfied, and

$$\tilde{\mathbf{S}}^{eq} = \begin{pmatrix} \tilde{\rho}\left(\frac{1}{3} + \tilde{u}_x^2\right) & \tilde{\rho}\tilde{u}_x\tilde{u}_y & \tilde{\rho}\tilde{u}_x\tilde{u}_z \\ \tilde{\rho}\tilde{u}_x\tilde{u}_y & \tilde{\rho}\left(\frac{1}{3} + \tilde{u}_y^2\right) & \tilde{\rho}\tilde{u}_y\tilde{u}_z \\ \tilde{\rho}\tilde{u}_z\tilde{u}_x & \tilde{\rho}\tilde{u}_z\tilde{u}_y & \tilde{\rho}\left(\frac{1}{3} + \tilde{u}_z^2\right) \end{pmatrix} \quad (48)$$

$$\tilde{\mathbf{Q}}^{eq} = \begin{pmatrix} \begin{pmatrix} \tilde{\rho}\tilde{u}_x \\ \tilde{\rho}\tilde{u}_y/3 \\ \tilde{\rho}\tilde{u}_z/3 \end{pmatrix} & \begin{pmatrix} \tilde{\rho}\tilde{u}_y/3 \\ \tilde{\rho}\tilde{u}_x/3 \\ 0 \end{pmatrix} & \begin{pmatrix} \tilde{\rho}\tilde{u}_z/3 \\ 0 \\ \tilde{\rho}\tilde{u}_x/3 \end{pmatrix} \\ \begin{pmatrix} \tilde{\rho}\tilde{u}_y/3 \\ \tilde{\rho}\tilde{u}_x/3 \\ 0 \end{pmatrix} & \begin{pmatrix} \tilde{\rho}\tilde{u}_x/3 \\ \tilde{\rho}\tilde{u}_y \\ \tilde{\rho}\tilde{u}_z/3 \end{pmatrix} & \begin{pmatrix} 0 \\ \tilde{\rho}\tilde{u}_z/3 \\ \tilde{\rho}\tilde{u}_y/3 \end{pmatrix} \\ \begin{pmatrix} \tilde{\rho}\tilde{u}_z/3 \\ 0 \\ \tilde{\rho}\tilde{u}_x/3 \end{pmatrix} & \begin{pmatrix} 0 \\ \tilde{\rho}\tilde{u}_z/3 \\ \tilde{\rho}\tilde{u}_y/3 \end{pmatrix} & \begin{pmatrix} \tilde{\rho}\tilde{u}_x/3 \\ \tilde{\rho}\tilde{u}_y/3 \\ \tilde{\rho}\tilde{u}_z \end{pmatrix} \end{pmatrix} \quad (49)$$

In the case of the low Mach number approximation, one may perform Chapman-Enskog expansion

$$\tilde{f} = \tilde{f}^{(0)} + \varepsilon\tilde{f}^{(1)} + \varepsilon^2\tilde{f}^{(2)} + \cdots \quad (50)$$

For the first-order approximation, we may simply denote

$$\tilde{f} = \tilde{f}^{(0)} + \tilde{f}^{(1)} = \tilde{f}^{eq} + \tilde{f}^{non} \quad (51)$$

Consequently

$$\tilde{\mathbf{S}} = \tilde{\mathbf{S}}^{eq} + \tilde{\mathbf{S}}^{non} \quad (52)$$

$$\tilde{\mathbf{Q}} = \tilde{\mathbf{Q}}^{eq} + \tilde{\mathbf{Q}}^{non} \quad (53)$$

where superscript "non" stands for nonequilibrium. $\tilde{\mathbf{S}}^{non}$ and $\tilde{\mathbf{Q}}^{non}$ are evaluated by Eq.(33) and (35) respectively, using $\tilde{f}^{non}$. It can be approved that shear stress can be expressed as:

$$\boldsymbol{\sigma}=\text{dev}\tilde{\mathbf{S}}^{non} \tag{54}$$

where "dev" stands for deviation part. Applying Chapman-Enskog expansion, one can show the following:

$$\boldsymbol{\sigma}=\text{dev}\tilde{\mathbf{S}}^{non}=2\mu\boldsymbol{\Lambda} \tag{55}$$

where

$$\boldsymbol{\Lambda}=\frac{1}{2}\left[\nabla\mathbf{u}+(\nabla\mathbf{u})^{T}\right] \tag{56}$$

Comparing Eqs.(37) - (42) with Eqs.(53) and (49) we have

$$\tilde{Q}_{111}=\left(\tilde{f}_1+\tilde{f}_7+\tilde{f}_{10}+\tilde{f}_{11}+\tilde{f}_{14}\right)-\tilde{f}_3-\tilde{f}_8-\tilde{f}_9-\tilde{f}_{12}-\tilde{f}_{13}=\tilde{\rho}\tilde{u}_x+\tilde{Q}_{111}^{non} \tag{57}$$

$$\tilde{Q}_{222}=\tilde{f}_7-\tilde{f}_{10}+\tilde{f}_2-\tilde{f}_4+\tilde{f}_8-\tilde{f}_9+\tilde{f}_{15}+\tilde{f}_{18}-\tilde{f}_{16}-\tilde{f}_{17}=\tilde{\rho}\tilde{u}_y+\tilde{Q}_{222}^{non} \tag{58}$$

$$\tilde{Q}_{333}=\tilde{f}_{11}-\tilde{f}_{14}+\tilde{f}_5-\tilde{f}_6+\tilde{f}_{12}-\tilde{f}_{13}+\tilde{f}_{15}+\tilde{f}_{16}-\tilde{f}_{17}-\tilde{f}_{18}=\tilde{\rho}\tilde{u}_z+\tilde{Q}_{333}^{non} \tag{59}$$

$$\tilde{Q}_{121}=\tilde{f}_7+\tilde{f}_8-\tilde{f}_9-\tilde{f}_{10}=\frac{1}{3}\tilde{\rho}\tilde{u}_y+\tilde{Q}_{121}^{non} \tag{60}$$

$$\tilde{Q}_{131}=\tilde{f}_{11}+\tilde{f}_{12}-\tilde{f}_{13}-\tilde{f}_{14}=\frac{1}{3}\tilde{\rho}\tilde{u}_z+\tilde{Q}_{131}^{non} \tag{61}$$

$$\tilde{Q}_{212}=\tilde{f}_7+\tilde{f}_{10}-\tilde{f}_8-\tilde{f}_9=\frac{1}{3}\tilde{\rho}\tilde{u}_x+\tilde{Q}_{212}^{non} \tag{62}$$

$$\tilde{Q}_{232}=\tilde{f}_{15}+\tilde{f}_{16}-\tilde{f}_{17}-\tilde{f}_{18}=\frac{1}{3}\tilde{\rho}\tilde{u}_z+\tilde{Q}_{232}^{non} \tag{63}$$

$$\tilde{Q}_{313}=\tilde{f}_{11}+\tilde{f}_{14}-\tilde{f}_{12}-\tilde{f}_{13}=\frac{1}{3}\tilde{\rho}\tilde{u}_x+\tilde{Q}_{313}^{non} \tag{64}$$

$$\tilde{Q}_{323}=\tilde{f}_{15}+\tilde{f}_{18}-\tilde{f}_{16}-\tilde{f}_{17}=\frac{1}{3}\tilde{\rho}\tilde{u}_y+\tilde{Q}_{323}^{non} \tag{65}$$

Since the first-order moment $\tilde{\mathbf{M}}$ is assumed exactly equal to the momentum $\tilde{\rho}\tilde{\mathbf{u}}$, we have

$$\tilde{Q}_{111}^{non}=\tilde{Q}_{222}^{non}=\tilde{Q}_{333}^{non}\equiv 0 \tag{66}$$

Substituting Eqs.(60) - (65) into Eqs. (57) - (59) we have

$$\tilde{f}_1-\tilde{f}_3=\frac{1}{3}\tilde{\rho}\tilde{u}_x-\tilde{Q}_{212}^{non}-\tilde{Q}_{313}^{non} \tag{67}$$

$$\tilde{f}_2-\tilde{f}_4=\frac{1}{3}\tilde{\rho}\tilde{u}_y-\tilde{Q}_{121}^{non}-\tilde{Q}_{323}^{non} \tag{68}$$

$$\tilde{f}_5-\tilde{f}_6=\frac{1}{3}\tilde{\rho}\tilde{u}_z-\tilde{Q}_{131}^{non}-\tilde{Q}_{232}^{non} \tag{69}$$

Section 7 will demonstrate how the third-order moment equations will be used to close nonslip (or prescribed velocity) boundary conditions.

Boundary reconstruction in 3D

In this section, we reconstruct the velocity boundary condition for each fluid node adjacent to a wall node for all possible boundary configurations on a 3D face-centered lattice, which is defined on a 3D image containing $n\times m\times k$ voxels/cells. In this monograph, we use a local lattice with the nodal numbering system, as shown in Figure 1 to discuss boundary reconstruction. That is for each fluid node, which is adjacent to one or more solid nodes on the boundary walls; we position the local lattice centered on that node with nodal index 0, i.e., node 0, as illustrated in Figure 1. This nodal numbering system consistently defines the velocity directions of the standard D3Q19 stencil (without illustrating the direction arrows on the figure), meaning that nodal indexes are identical to velocity streaming directions. By this nodal numbering system, in the streaming step $f_\alpha\left(\tilde{\mathbf{r}},\tilde{t}+1\right)$, the probability distribution function of node 0 in the direction α is streamed from $f_\alpha\left(\tilde{\mathbf{r}}+\mathbf{e}_{\bar{\alpha}},\tilde{t}+1\right)$ the probability distribution function of a neighboring node with index $\bar{\alpha}$ (opposite to α) in the same velocity direction α.

Table 1 list all opposite pairs of velocity streaming directions $(\alpha,\bar{\alpha})$ in Figure 1. Note that we will mix using terminology velocity streaming directions α with the node α in the rest part of the monograph without confusion. If a neighboring node with index $\bar{\alpha}$ (or $\tilde{\mathbf{r}}+\mathbf{e}_{\bar{\alpha}}$) is a fluid node, $f_\alpha\left(\tilde{\mathbf{r}},\tilde{t}+1\right)$ is known, and if $\tilde{\mathbf{r}}+\mathbf{e}_{\bar{\alpha}}$ is a solid node, $f_\alpha\left(\tilde{\mathbf{r}},\tilde{t}+1\right)$ is unknown and needs to be reconstructed.

Table 1: Opposite Pairs of Velocity Streaming Directions

α	1	2	3	4	5	6	7	8	9	10	11	12	13	14	15	16	17	18
$\overline{\alpha}$	3	4	1	2	6	5	9	10	7	8	13	14	11	12	17	18	15	16

Solid wall cell

Figure 2 shows a configuration of the first case in which nodes 6, 13, 14, 17, and 18 are on the solid wall. According to Table 1, $f_\alpha(\tilde{\mathbf{r}},\tilde{t}+1)$ for $(\alpha=5,11,12,15,16)$ will be streamed out from $f_5(\tilde{\mathbf{r}}+\mathbf{e}_6,\tilde{t}+1)$, $f_{11}(\tilde{\mathbf{r}}+\mathbf{e}_{13},\tilde{t}+1)$, $f_{12}(\tilde{\mathbf{r}}+\mathbf{e}_{14},\tilde{t}+1)$, $f_{15}(\tilde{\mathbf{r}}+\mathbf{e}_{17},\tilde{t}+1)$ and $f_{16}(\tilde{\mathbf{r}}+\mathbf{e}_{18},\tilde{t}+1)$ respectively, or simply by saying, probability distribution function at solid nodes, 6, 13, 14, 17 and 18 at respective mapped velocity directions. Note that in following discussion of each later case we will take the way of the latter expression as long as it does not cause any confusion.

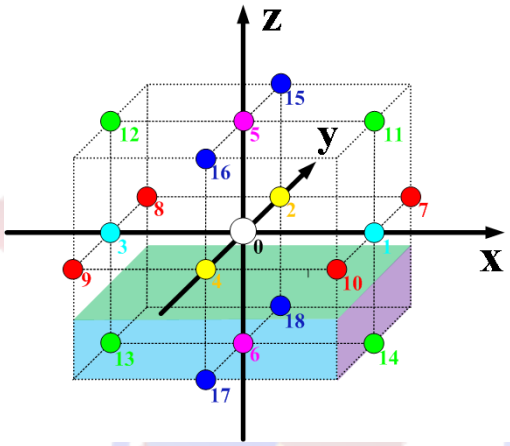

Figure 2: Solid Wall Boundary Cell.

Suppose that $\tilde{\mathbf{u}}=(\tilde{u}_x,\tilde{u}_y,0)$ are prescribed on the boundary. We only need to determine $\tilde{f}_5,\tilde{f}_{11},\tilde{f}_{12},\tilde{f}_{15},\tilde{f}_{16}$ and $\tilde{\rho}$, because all other probability distribution functions $\tilde{f}_i$ $(i\neq 5,11,12,15,16)$ are known, which are streamed from neighbored fluid nodes. In order to determine five unknowns $\tilde{f}_5,\tilde{f}_{11},\tilde{f}_{12},\tilde{f}_{15},\tilde{f}_{16}$, one may use the first-order moments from Eq.(30) - (32). However, we only have three equations for five unknowns. So, we choose the remaining complementary equations from the third-order moments. Since nodes 6, 13, 14, 17 and 18 are solid wall, we assume

$$\tilde{Q}^{non}_{131}=\tilde{Q}^{non}_{232}=0 \tag{70}$$

From Eqs. (61), (63) and (70)

$$\begin{cases}\tilde{f}_{11}+\tilde{f}_{12}-\tilde{f}_{13}-\tilde{f}_{14}=0\\ \tilde{f}_{15}+\tilde{f}_{16}-\tilde{f}_{17}-\tilde{f}_{18}=0\end{cases} \tag{71}$$

From Eqs. (69) and (70)

$$\tilde{f}_5=\tilde{f}_6 \tag{72}$$

Eq.(71) together with Eqs.(30) and (31) lead to the following set of equations:

$$\begin{cases}\tilde{f}_5=\tilde{f}_6\\ \tilde{f}_{11}=\frac{1}{2}\tilde{\rho}\tilde{u}_x+\tilde{f}_{13}+\frac{(\tilde{f}_3+\tilde{f}_8+\tilde{f}_9)-(\tilde{f}_1+\tilde{f}_7+\tilde{f}_{10})}{2}\\ \tilde{f}_{12}=-\frac{1}{2}\tilde{\rho}\tilde{u}_x+\tilde{f}_{14}-\frac{(\tilde{f}_3+\tilde{f}_8+\tilde{f}_9)-(\tilde{f}_1+\tilde{f}_7+\tilde{f}_{10})}{2}\\ \tilde{f}_{15}=\frac{1}{2}\tilde{\rho}\tilde{u}_y+\tilde{f}_{17}+\frac{(\tilde{f}_4+\tilde{f}_9+\tilde{f}_{10})-(\tilde{f}_2+\tilde{f}_7+\tilde{f}_8)}{2}\\ \tilde{f}_{16}=-\frac{1}{2}\tilde{\rho}\tilde{u}_y+\tilde{f}_{18}-\frac{(\tilde{f}_4+\tilde{f}_9+\tilde{f}_{10})-(\tilde{f}_2+\tilde{f}_7+\tilde{f}_8)}{2}\end{cases} \tag{73}$$

To ensure mass conservation, we enforce the total mass that comes out from the wall equal to the total mass that is sent into the wall, i.e.

$$\tilde{f}_5+\tilde{f}_{11}+\tilde{f}_{12}+\tilde{f}_{15}+\tilde{f}_{16}=\tilde{f}_6^c+\tilde{f}_{13}^c+\tilde{f}_{14}^c+\tilde{f}_{17}^c+\tilde{f}_{18}^c \tag{74}$$

Since Eq.(73) cannot guarantee Eq.(74) to be satisfied, we set the probability distribution function at the resting velocity direction, as

$$\tilde{f}_0=\tilde{f}_0^c+\left(\tilde{f}_6^c+\tilde{f}_{13}^c+\tilde{f}_{14}^c+\tilde{f}_{17}^c+\tilde{f}_{18}^c\right)-\left(\tilde{f}_5+\tilde{f}_{11}+\tilde{f}_{12}+\tilde{f}_{15}+\tilde{f}_{16}\right) \tag{75}$$

Substituting Eq.(32) into Eq. (28) and using Eq.(75)

$$\begin{aligned}\tilde{\rho}&=\tilde{f}_0^c+\left(\tilde{f}_1+\tilde{f}_2+\tilde{f}_3+\tilde{f}_4+\tilde{f}_7+\tilde{f}_8+\tilde{f}_9+\tilde{f}_{10}\right)\\&+\left(\tilde{f}_6^c+\tilde{f}_{13}^c+\tilde{f}_{14}^c+\tilde{f}_{17}^c+\tilde{f}_{18}^c\right)+\left(\tilde{f}_6+\tilde{f}_{13}+\tilde{f}_{14}+\tilde{f}_{17}+\tilde{f}_{18}\right)\end{aligned} \tag{76}$$

Similarly, if nodes 5, 11, 12, 15, and 16 are the wall nodes, Eq. (71) together with Eqs.(30) and (31) give rise to

$$\begin{cases}\tilde{f}_6=\tilde{f}_5\\ \tilde{f}_{13}=-\frac{1}{2}\tilde{\rho}\tilde{u}_x+\tilde{f}_{11}-\frac{\left(\tilde{f}_3+\tilde{f}_8+\tilde{f}_9\right)-\left(\tilde{f}_1+\tilde{f}_7+\tilde{f}_{10}\right)}{2}\\ \tilde{f}_{14}=\frac{1}{2}\tilde{\rho}\tilde{u}_x+\tilde{f}_{12}+\frac{\left(\tilde{f}_3+\tilde{f}_8+\tilde{f}_9\right)-\left(\tilde{f}_1+\tilde{f}_7+\tilde{f}_{10}\right)}{2}\\ \tilde{f}_{17}=-\frac{1}{2}\tilde{\rho}\tilde{u}_y+\tilde{f}_{15}-\frac{\left(\tilde{f}_4+\tilde{f}_9+\tilde{f}_{10}\right)-\left(\tilde{f}_2+\tilde{f}_7+\tilde{f}_8\right)}{2}\\ \tilde{f}_{18}=\frac{1}{2}\tilde{\rho}\tilde{u}_y+\tilde{f}_{16}+\frac{\left(\tilde{f}_4+\tilde{f}_9+\tilde{f}_{10}\right)-\left(\tilde{f}_2+\tilde{f}_7+\tilde{f}_8\right)}{2}\end{cases} \tag{77}$$

In order to satisfy the mass conservation condition, the probability function at the resting node could be set as

$$\tilde{f}_0=\tilde{f}_0^c+\left(\tilde{f}_5^c+\tilde{f}_{11}^c+\tilde{f}_{12}^c+\tilde{f}_{15}^c+\tilde{f}_{16}^c\right)-\left(\tilde{f}_6+\tilde{f}_{13}+\tilde{f}_{14}+\tilde{f}_{17}+\tilde{f}_{18}\right) \tag{78}$$

Such that the total mass can be written as

$$\begin{aligned}\tilde{\rho}&=\tilde{f}_0^c+\left(\tilde{f}_1+\tilde{f}_2+\tilde{f}_3+\tilde{f}_4+\tilde{f}_7+\tilde{f}_8+\tilde{f}_9+\tilde{f}_{10}\right)\\&+\left(\tilde{f}_5^c+\tilde{f}_{11}^c+\tilde{f}_{12}^c+\tilde{f}_{15}^c+\tilde{f}_{16}^c\right)+\left(\tilde{f}_5+\tilde{f}_{11}+\tilde{f}_{12}+\tilde{f}_{15}+\tilde{f}_{16}\right)\end{aligned} \tag{79}$$

As shown in Figure 3, if nodes 2, 7, 8, 15, 18 are solid wall nodes, in the streaming step, the probability distribution function at nodes 4, 9, 10, 16 and 17 need to be reconstructed, i.e., $\tilde{\mathbf{u}}=(\tilde{u}_x,0,\tilde{u}_z)$ and the other $\tilde{f}_i(i\neq 4,9,10,16,17)$ are specified. We want to determine $\tilde{f}_4,\tilde{f}_9,\tilde{f}_{10},\tilde{f}_{16},\tilde{f}_{17}$ and $\tilde{\rho}$. In principle, Figure 2 and Figure 3 are the same boundary configuration; one of them can be obtained from another one through a rigid body rotation. We repeat the derivation process above because some equations need to be used later. Since nodes 2, 7, 8, 15, 18 are solid wall nodes, we assume

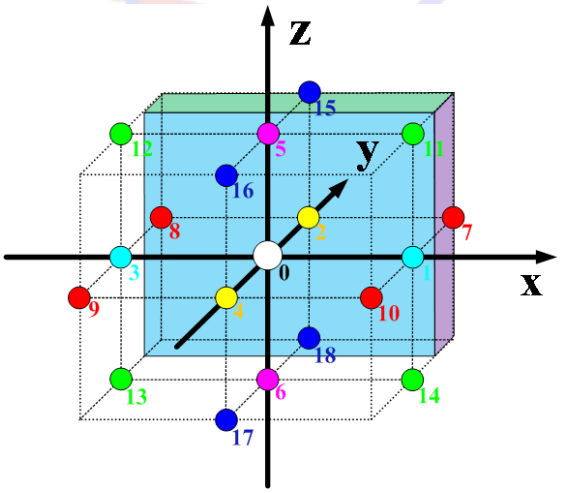

Figure 3: Solid Wall Boundary Cell.

$$\tilde{Q}_{121}^{non} = \tilde{Q}_{323}^{non} = 0 \tag{80}$$

From Eqs.(60), (65) and (80) we have,

$$\begin{cases} \left(\tilde{f}_7 - \tilde{f}_9\right) + \left(\tilde{f}_8 - \tilde{f}_{10}\right) = 0 \\ \left(\tilde{f}_{15} - \tilde{f}_{17}\right) + \left(\tilde{f}_{18} - \tilde{f}_{16}\right) = 0 \end{cases} \tag{81}$$

From Eqs.(68) and (80) we have

$$\tilde{f}_4 = \tilde{f}_2 \tag{82}$$

Eq.(81) together with Eqs.(30) and (32) give rise to

$$\begin{cases} \tilde{f}_4 = \tilde{f}_2 \\ \tilde{f}_9 = -\frac{1}{2}\tilde{\rho}\tilde{u}_x + \tilde{f}_7 - \frac{\left(\tilde{f}_3 + \tilde{f}_{12} + \tilde{f}_{13}\right) - \left(\tilde{f}_1 + \tilde{f}_{11} + \tilde{f}_{14}\right)}{2} \\ \tilde{f}_{10} = \frac{1}{2}\tilde{\rho}\tilde{u}_x + \tilde{f}_8 + \frac{\left(\tilde{f}_3 + \tilde{f}_{12} + \tilde{f}_{13}\right) - \left(\tilde{f}_1 + \tilde{f}_{11} + \tilde{f}_{14}\right)}{2} \\ \tilde{f}_{17} = -\frac{1}{2}\tilde{\rho}\tilde{u}_z + \tilde{f}_{15} - \frac{\left(\tilde{f}_6 + \tilde{f}_{13} + \tilde{f}_{14}\right) - \left(\tilde{f}_5 + \tilde{f}_{11} + \tilde{f}_{12}\right)}{2} \\ \tilde{f}_{16} = \frac{1}{2}\tilde{\rho}\tilde{u}_z + \tilde{f}_{18} + \frac{\left(\tilde{f}_6 + \tilde{f}_{13} + \tilde{f}_{14}\right) - \left(\tilde{f}_5 + \tilde{f}_{11} + \tilde{f}_{12}\right)}{2} \end{cases} \tag{83}$$

In order to satisfy the mass conservation condition, the probability function at the resting node could be set as

$$\tilde{f}_0 = \tilde{f}_0^c + \left(\tilde{f}_2^c + \tilde{f}_7^c + \tilde{f}_8^c + \tilde{f}_{15}^c + \tilde{f}_{18}^c\right) - \left(\tilde{f}_4 + \tilde{f}_9 + \tilde{f}_{10} + \tilde{f}_{17} + \tilde{f}_{16}\right) \tag{84}$$

Such that the total mass can be written as

$$\begin{aligned} \tilde{\rho} &= \tilde{f}_0^c + \left(\tilde{f}_1 + \tilde{f}_3 + \tilde{f}_5 + \tilde{f}_6 + \tilde{f}_{11} + \tilde{f}_{12} + \tilde{f}_{13} + \tilde{f}_{14}\right) \\ &+ \left(\tilde{f}_2^c + \tilde{f}_7^c + \tilde{f}_8^c + \tilde{f}_{15}^c + \tilde{f}_{18}^c\right) + \left(\tilde{f}_2 + \tilde{f}_7 + \tilde{f}_8 + \tilde{f}_{15} + \tilde{f}_{18}\right) \end{aligned} \tag{85}$$

Similarly, if nodes 4, 9, 10, 16 and 17 are solid wall nodes, we have

$$\begin{cases} \tilde{f}_2 = \tilde{f}_4 \\ \tilde{f}_7 = \frac{1}{2}\tilde{\rho}\tilde{u}_x + \tilde{f}_9 + \frac{\left(\tilde{f}_3 + \tilde{f}_{12} + \tilde{f}_{13}\right) - \left(\tilde{f}_1 + \tilde{f}_{11} + \tilde{f}_{14}\right)}{2} \\ \tilde{f}_8 = -\frac{1}{2}\tilde{\rho}\tilde{u}_x + \tilde{f}_{10} - \frac{\left(\tilde{f}_3 + \tilde{f}_{12} + \tilde{f}_{13}\right) - \left(\tilde{f}_1 + \tilde{f}_{11} + \tilde{f}_{14}\right)}{2} \\ \tilde{f}_{15} = \frac{1}{2}\tilde{\rho}\tilde{u}_z + \tilde{f}_{17} + \frac{\left(\tilde{f}_6 + \tilde{f}_{13} + \tilde{f}_{14}\right) - \left(\tilde{f}_5 + \tilde{f}_{11} + \tilde{f}_{12}\right)}{2} \\ \tilde{f}_{18} = -\frac{1}{2}\tilde{\rho}\tilde{u}_z + \tilde{f}_{16} - \frac{\left(\tilde{f}_6 + \tilde{f}_{13} + \tilde{f}_{14}\right) - \left(\tilde{f}_5 + \tilde{f}_{11} + \tilde{f}_{12}\right)}{2} \end{cases} \tag{86}$$

In order to satisfy the mass conservation condition, the probability function at the resting node could be set as

$$\tilde{f}_0 = \tilde{f}_0^c + \left(\tilde{f}_4^c + \tilde{f}_9^c + \tilde{f}_{10}^c + \tilde{f}_{16}^c + \tilde{f}_{17}^c\right) - \left(\tilde{f}_2 + \tilde{f}_7 + \tilde{f}_8 + \tilde{f}_{15} + \tilde{f}_{18}\right) \tag{87}$$

Such that the total mass can be written as

$$\begin{aligned} \tilde{\rho} &= \tilde{f}_0^c + \left(\tilde{f}_1 + \tilde{f}_3 + \tilde{f}_5 + \tilde{f}_6 + \tilde{f}_{11} + \tilde{f}_{12} + \tilde{f}_{13} + \tilde{f}_{14}\right) \\ &+ \left(\tilde{f}_4^c + \tilde{f}_9^c + \tilde{f}_{10}^c + \tilde{f}_{16}^c + \tilde{f}_{17}^c\right) + \left(\tilde{f}_4 + \tilde{f}_9 + \tilde{f}_{10} + \tilde{f}_{16} + \tilde{f}_{17}\right) \end{aligned} \tag{88}$$

Concave edge cell

Figure 4 shows a case containing solid nodes 6, 13, 14, 17, 18, at the bottom, and 2, 7, 8, 15, 18 at the back Given $\tilde{\mathbf{u}} = (0, 0, \tilde{u}_x)$ is specified. $\tilde{f}_i \quad (i \neq 4, 5, 9, 10, 11, 12, 15, 16, 17)$ are streamed from neighboured fluid nodes, so they are known. We want to determine $\tilde{f}_4, \tilde{f}_5, \tilde{f}_9, \tilde{f}_{10}, \tilde{f}_{11}, \tilde{f}_{12}, \tilde{f}_{15}, \tilde{f}_{16}, \tilde{f}_{17}$ and $\tilde{\rho}$. Since nodes 6, 13, 14, 17, 18 are the solid wall, we assume Eq. (70) is satisfied, thus Eq. (71) and Eq. (72) are true. Since nodes 2, 7, 8, 15, 18 are solid wall nodes, we assume Eq.(80) is satisfied, thus Eq. (81) and Eq. (82) are true. From Eqn. (71) and (81) we have

$$\tilde{f}_{16} = \tilde{f}_{18} \tag{89}$$

$$\tilde{f}_{15} = \tilde{f}_{17} \tag{90}$$

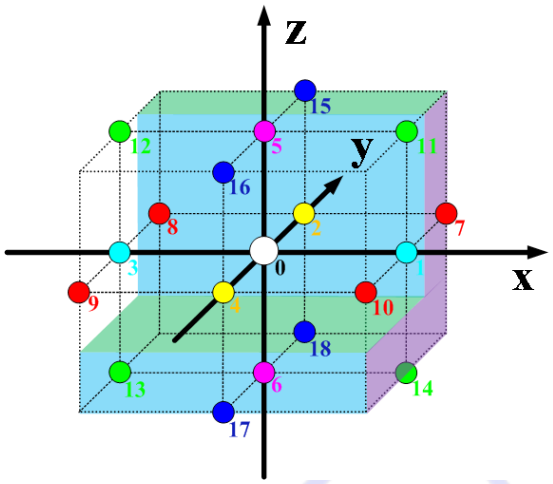

Figure 4: Concave Edge Cell.

Both $\tilde{f}_{15}$ and $\tilde{f}_{17}$ are unknown nodes and they opposite each other; thus, they form a pair of buried links. We made an additional assumption that the sum of the probability distribution function in direction 15 and 17 satisfies the bouncy back condition i.e.

$$\tilde{f}_{15}+\tilde{f}_{17}=\tilde{f}_{15}^{c}+\tilde{f}_{17}^{c} \tag{91}$$

Where $\tilde{f}_{15}^{c}$ and $\tilde{f}_{17}^{c}$ stands for probability distribution function after the collision step. From Eqs. (90) and (91) we have

$$\tilde{f}_{15}=\tilde{f}_{17}=\frac{\tilde{f}_{15}^{c}+\tilde{f}_{17}^{c}}{2} \tag{92}$$

From Eq.(30) we have

$$\tilde{f}_{1}+\tilde{f}_{7}+\tilde{f}_{10}+\tilde{f}_{11}+\tilde{f}_{14}-\tilde{f}_{3}-\tilde{f}_{8}-\tilde{f}_{9}-\tilde{f}_{12}-\tilde{f}_{13}=\tilde{\rho}\tilde{u}_{x} \tag{93}$$

Because the x direction is not towards the solid wall, either $\tilde{Q}_{212}^{non}$ or $\tilde{Q}_{313}^{non}$ may not be zero. However, since the y axis and the z axis are symmetry, we may assume

$$\tilde{Q}_{212}^{non}=\tilde{Q}_{313}^{non} \tag{94}$$

From Eqs.(62), (64) and (94) we have

$$\tilde{f}_{7}+\tilde{f}_{10}-\tilde{f}_{8}-\tilde{f}_{9}=\tilde{f}_{11}+\tilde{f}_{14}-\tilde{f}_{12}-\tilde{f}_{13} \tag{95}$$

From Eqs.(93), (95) we have

$$\left(\tilde{f}_{1}-\tilde{f}_{3}\right)+2\left(\tilde{f}_{7}+\tilde{f}_{10}-\tilde{f}_{8}-\tilde{f}_{9}\right)=\tilde{\rho}\tilde{u}_{x} \tag{96}$$

From the first equation of Eq.(81) and Eq.(96) we have

$$\begin{cases}\tilde{f}_{9}=-\dfrac{1}{4}\tilde{\rho}\tilde{u}_{x}+\tilde{f}_{7}+\dfrac{\tilde{f}_{1}-\tilde{f}_{3}}{4}\\ \tilde{f}_{10}=\dfrac{1}{4}\tilde{\rho}\tilde{u}_{x}+\tilde{f}_{8}-\dfrac{\tilde{f}_{1}-\tilde{f}_{3}}{4}\end{cases} \tag{97}$$

From Eqs.(93) and (96) we have

$$\left(\tilde{f}_{1}-\tilde{f}_{3}\right)+2\left(\tilde{f}_{11}+\tilde{f}_{14}-\tilde{f}_{12}-\tilde{f}_{13}\right)=\tilde{\rho}\tilde{u}_{x} \tag{98}$$

From the first equation of Eq. (71) and Eq.(98) we have

$$\begin{cases}\tilde{f}_{11}=\dfrac{1}{4}\tilde{\rho}\tilde{u}_{x}+\tilde{f}_{13}-\dfrac{\tilde{f}_{1}-\tilde{f}_{3}}{4}\\ \tilde{f}_{12}=-\dfrac{1}{4}\tilde{\rho}\tilde{u}_{x}+\tilde{f}_{14}+\dfrac{\tilde{f}_{1}-\tilde{f}_{3}}{4}\end{cases} \tag{99}$$

To summarize we have

$$\begin{cases} \tilde{f}_4 = \tilde{f}_2 \\ \tilde{f}_5 = \tilde{f}_6 \\ \tilde{f}_{16} = \tilde{f}_{18} \\ \tilde{f}_{15} = \tilde{f}_{17} = \dfrac{\tilde{f}_{15}^c + \tilde{f}_{17}^c}{2} \\ \tilde{f}_9 = -\dfrac{1}{4}\tilde{\rho}\tilde{u}_x + \tilde{f}_7 + \dfrac{\tilde{f}_1 - \tilde{f}_3}{4} \\ \tilde{f}_{10} = \dfrac{1}{4}\tilde{\rho}\tilde{u}_x + \tilde{f}_8 - \dfrac{\tilde{f}_1 - \tilde{f}_3}{4} \\ \tilde{f}_{11} = \dfrac{1}{4}\tilde{\rho}\tilde{u}_x + \tilde{f}_{13} - \dfrac{\tilde{f}_1 - \tilde{f}_3}{4} \\ \tilde{f}_{12} = -\dfrac{1}{4}\tilde{\rho}\tilde{u}_x + \tilde{f}_{14} + \dfrac{\tilde{f}_1 - \tilde{f}_3}{4} \end{cases} \quad (100)$$

In order to satisfy mass conservation condition, the probability function at the resting node could be set as

$$\tilde{f}_0 = \tilde{f}_0^c + \left(\tilde{f}_2^c + \tilde{f}_6^c + \tilde{f}_7^c + \tilde{f}_8^c + \tilde{f}_{13}^c + \tilde{f}_{14}^c + \tilde{f}_{18}^c\right) - \left(\tilde{f}_4 + \tilde{f}_5 + \tilde{f}_9 + \tilde{f}_{10} + \tilde{f}_{11} + \tilde{f}_{12} + \tilde{f}_{16}\right) \quad (101)$$

Such that the total mass can be written as

$$\tilde{\rho} = \tilde{f}_0^c + \left(\tilde{f}_2^c + \tilde{f}_6^c + \tilde{f}_7^c + \tilde{f}_8^c + \tilde{f}_{13}^c + \tilde{f}_{14}^c + \tilde{f}_{18}^c\right) + \left(\tilde{f}_{15}^c + \tilde{f}_{17}^c\right) + \left(\tilde{f}_1 + \tilde{f}_3\right) + \left(\tilde{f}_2 + \tilde{f}_6 + \tilde{f}_7 + \tilde{f}_8 + \tilde{f}_{13} + \tilde{f}_{14} + \tilde{f}_{18}\right) \quad (102)$$

Similarly, if nodes 5, 11, 12, 15 and 16 are on a solid wall, so do noses 4, 9, 10, 16, 17, then

$$\begin{cases} \tilde{f}_2 = \tilde{f}_4 \\ \tilde{f}_6 = \tilde{f}_5 \\ \tilde{f}_{18} = \tilde{f}_{16} \\ \tilde{f}_{15} = \tilde{f}_{17} = \dfrac{\tilde{f}_{15}^c + \tilde{f}_{17}^c}{2} \\ \tilde{f}_7 = \dfrac{1}{4}\tilde{\rho}\tilde{u}_x + \tilde{f}_9 - \dfrac{\tilde{f}_1 - \tilde{f}_3}{4} \\ \tilde{f}_8 = -\dfrac{1}{4}\tilde{\rho}\tilde{u}_x + \tilde{f}_{10} + \dfrac{\tilde{f}_1 - \tilde{f}_3}{4} \\ \tilde{f}_{13} = -\dfrac{1}{4}\tilde{\rho}\tilde{u}_x + \tilde{f}_{11} + \dfrac{\tilde{f}_1 - \tilde{f}_3}{4} \\ \tilde{f}_{14} = \dfrac{1}{4}\tilde{\rho}\tilde{u}_x + \tilde{f}_{12} - \dfrac{\tilde{f}_1 - \tilde{f}_3}{4} \end{cases} \quad (103)$$

In order to satisfy the mass conservation condition, the probability function at the resting node could be set as

$$\tilde{f}_0 = \tilde{f}_0^c + \left(\tilde{f}_4^c + \tilde{f}_5^c + \tilde{f}_9^c + \tilde{f}_{10}^c + \tilde{f}_{11}^c + \tilde{f}_{12}^c + \tilde{f}_{16}^c\right) - \left(\tilde{f}_2 + \tilde{f}_6 + \tilde{f}_7 + \tilde{f}_8 + \tilde{f}_{13} + \tilde{f}_{14} + \tilde{f}_{18}\right) \quad (104)$$

Such that the total mass can be written as

$$\tilde{\rho} = \tilde{f}_0^c + \left(\tilde{f}_4^c + \tilde{f}_5^c + \tilde{f}_9^c + \tilde{f}_{10}^c + \tilde{f}_{11}^c + \tilde{f}_{12}^c + \tilde{f}_{16}^c\right) + \left(\tilde{f}_{15}^c + \tilde{f}_{17}^c\right) + \left(\tilde{f}_1 + \tilde{f}_3\right) + \left(\tilde{f}_4 + \tilde{f}_5 + \tilde{f}_9 + \tilde{f}_{10} + \tilde{f}_{11} + \tilde{f}_{12} + \tilde{f}_{16}\right) \quad (105)$$

If nodes 5, 11, 12, 15 and 16 are solid wall, and so do nodes 2, 7, 8, 15, 18, then

$$\begin{cases} \tilde{f}_4 = \tilde{f}_2 \\ \tilde{f}_6 = \tilde{f}_5 \\ \tilde{f}_{17} = \tilde{f}_{15} \\ \tilde{f}_{16} = \tilde{f}_{18} = \dfrac{\tilde{f}_{16}^c + \tilde{f}_{18}^c}{2} \\ \tilde{f}_9 = -\dfrac{1}{4}\tilde{\rho}\tilde{u}_x + \tilde{f}_7 + \dfrac{\tilde{f}_1 - \tilde{f}_3}{4} \\ \tilde{f}_{10} = \dfrac{1}{4}\tilde{\rho}\tilde{u}_x + \tilde{f}_8 - \dfrac{\tilde{f}_1 - \tilde{f}_3}{4} \\ \tilde{f}_{13} = -\dfrac{1}{4}\tilde{\rho}\tilde{u}_x + \tilde{f}_{11} + \dfrac{\tilde{f}_1 - \tilde{f}_3}{4} \\ \tilde{f}_{14} = \dfrac{1}{4}\tilde{\rho}\tilde{u}_x + \tilde{f}_{12} - \dfrac{\tilde{f}_1 - \tilde{f}_3}{4} \end{cases} \quad (106)$$

In order to satisfy the mass conservation condition, the probability function at the resting node could be set as

$$\tilde{f}_0 = \tilde{f}_0^c + \left(\tilde{f}_2^c + \tilde{f}_5^c + \tilde{f}_7^c + \tilde{f}_8^c + \tilde{f}_{11}^c + \tilde{f}_{12}^c + \tilde{f}_{15}^c\right) - \left(\tilde{f}_4 + \tilde{f}_6 + \tilde{f}_9 + \tilde{f}_{10} + \tilde{f}_{13} + \tilde{f}_{14} + \tilde{f}_{17}\right) \tag{107}$$

Such that the total mass can be written as

$$\tilde{\rho} = \tilde{f}_0^c + \left(\tilde{f}_2^c + \tilde{f}_5^c + \tilde{f}_7^c + \tilde{f}_8^c + \tilde{f}_{11}^c + \tilde{f}_{12}^c + \tilde{f}_{15}^c\right) + \left(\tilde{f}_{16}^c + \tilde{f}_{18}^c\right) + \left(\tilde{f}_1 + \tilde{f}_3\right) + \left(\tilde{f}_2 + \tilde{f}_5 + \tilde{f}_7 + \tilde{f}_8 + \tilde{f}_{11} + \tilde{f}_{12} + \tilde{f}_{15}\right) \tag{108}$$

Similarly, if nodes 6, 13, 14, 17, 18 are solid wall, and so do noses 4, 9, 10, 16, 17, then

$$\begin{cases} \tilde{f}_2 = \tilde{f}_4 \\ \tilde{f}_5 = \tilde{f}_6 \\ \tilde{f}_{15} = \tilde{f}_{17} \\ \tilde{f}_{16} = \tilde{f}_{18} = \dfrac{\tilde{f}_{16}^c + \tilde{f}_{18}^c}{2} \\ \tilde{f}_7 = \dfrac{1}{4}\tilde{\rho}\tilde{u}_x + \tilde{f}_9 - \dfrac{\tilde{f}_1 - \tilde{f}_3}{4} \\ \tilde{f}_8 = -\dfrac{1}{4}\tilde{\rho}\tilde{u}_x + \tilde{f}_{10} + \dfrac{\tilde{f}_1 - \tilde{f}_3}{4} \\ \tilde{f}_{11} = \dfrac{1}{4}\tilde{\rho}\tilde{u}_x + \tilde{f}_{13} - \dfrac{\tilde{f}_1 - \tilde{f}_3}{4} \\ \tilde{f}_{12} = -\dfrac{1}{4}\tilde{\rho}\tilde{u}_x + \tilde{f}_{14} + \dfrac{\tilde{f}_1 - \tilde{f}_3}{4} \end{cases} \tag{109}$$

In order to satisfy the mass conservation condition, the probability function at the resting node could be set as

$$\tilde{f}_0 = \tilde{f}_0^c + \left(\tilde{f}_4^c + \tilde{f}_6^c + \tilde{f}_9^c + \tilde{f}_{10}^c + \tilde{f}_{13}^c + \tilde{f}_{14}^c + \tilde{f}_{17}^c\right) - \left(\tilde{f}_2 + \tilde{f}_6 + \tilde{f}_7 + \tilde{f}_8 + \tilde{f}_{13} + \tilde{f}_{14} + \tilde{f}_{18}\right) \tag{110}$$

Such that the total mass can be written as

$$\tilde{\rho} = \tilde{f}_0^c + \left(\tilde{f}_4^c + \tilde{f}_6^c + \tilde{f}_9^c + \tilde{f}_{10}^c + \tilde{f}_{13}^c + \tilde{f}_{14}^c + \tilde{f}_{17}^c\right) + \left(\tilde{f}_{16}^c + \tilde{f}_{18}^c\right) + \left(\tilde{f}_1 + \tilde{f}_3\right) + \left(\tilde{f}_4 + \tilde{f}_6 + \tilde{f}_9 + \tilde{f}_{10} + \tilde{f}_{13} + \tilde{f}_{14} + \tilde{f}_{17}\right) \tag{111}$$

Concave three corner cell

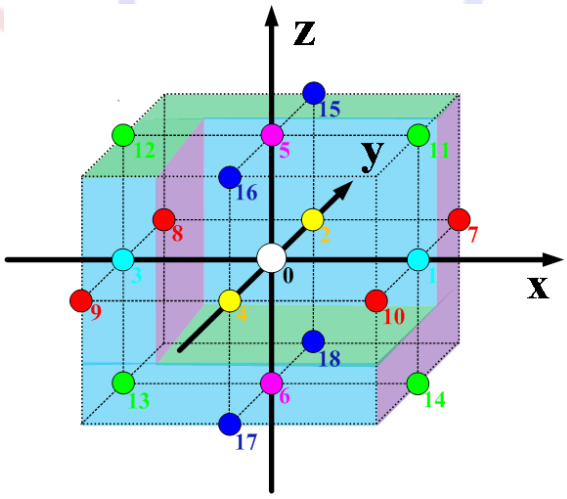

Figure 5: Concave three corner cell.

As shown in Figure 5, nodes 2, 3, 6 all towards a solid wall, further to Eq.(100) we have

$$\begin{cases} \tilde{f}_1 = \tilde{f}_3 \\ \tilde{f}_4 = \tilde{f}_2 \\ \tilde{f}_5 = \tilde{f}_6 \\ \tilde{f}_{10} = \tilde{f}_8 \\ \tilde{f}_{11} = \tilde{f}_{13} \\ \tilde{f}_{16} = \tilde{f}_{18} \\ \\ \tilde{f}_{15} = \tilde{f}_{17} = \dfrac{\tilde{f}_{15}^c + \tilde{f}_{17}^c}{2} \\ \tilde{f}_9 = \tilde{f}_7 = \dfrac{\tilde{f}_9^c + \tilde{f}_7^c}{2} \\ \tilde{f}_{12} = \tilde{f}_{14} = \dfrac{\tilde{f}_{12}^c + \tilde{f}_{14}^c}{2} \end{cases} \tag{112}$$

In order to satisfy mass conservation condition, the probability function at the resting node could be set as

$$\tilde{f}_0 = \tilde{f}_0^c + \left(\tilde{f}_2^c + \tilde{f}_3^c + \tilde{f}_6^c + \tilde{f}_8^c + \tilde{f}_{13}^c + \tilde{f}_{18}^c\right) - \left(\tilde{f}_1 + \tilde{f}_4 + \tilde{f}_5 + \tilde{f}_{10} + \tilde{f}_{11} + \tilde{f}_{16}\right) \tag{113}$$

Such that the total mass can be written as

$$\tilde{\rho} = \tilde{f}_0^c + \left(\tilde{f}_7^c + \tilde{f}_9^c\right) + \left(\tilde{f}_{12}^c + \tilde{f}_{14}^c\right) + \left(\tilde{f}_{15}^c + \tilde{f}_{17}^c\right) + \left(\tilde{f}_2^c + \tilde{f}_3^c + \tilde{f}_6^c + \tilde{f}_8^c + \tilde{f}_{13}^c + \tilde{f}_{18}^c\right) + \left(\tilde{f}_2 + \tilde{f}_3 + \tilde{f}_6 + \tilde{f}_8 + \tilde{f}_{13} + \tilde{f}_{18}\right) \tag{114}$$

Edge cell with partial wall

If some boundary nodes are partially adjacent to a pure solid wall, some additional assumptions are needed to closure the problem. The additional assumptions can be made based on the symmetry of the cell geometrical structure. For simplicity, we focus on flow within the cylinder along x axis direction.

Edge cell with one partial wall: As shown in Figure 6, if nodes 2, 7, 8, 18 are solid wall nodes, after the streaming step, the probability distribution function at nodes 4, 9, 10, and 16 need to be reconstructed, i.e., $\tilde{\mathbf{u}} = \left(\tilde{u}_x, 0, \tilde{u}_z\right)$ and the other $\tilde{f}_i \left(i \neq 4,\ 9, 10, 16, 17\right)$ are specified. We want determined $\tilde{f}_4, \tilde{f}_9, \tilde{f}_{10}, \tilde{f}_{16}$ and $\tilde{\rho}$.

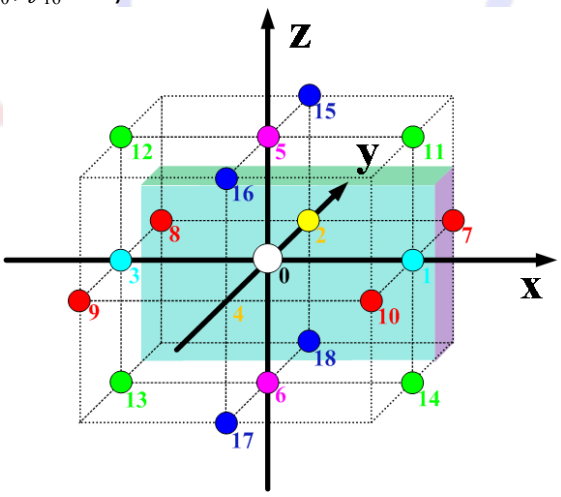

Figure 6: Edge cell with one partial wall

From Eq.(32) we have

$$\tilde{f}_{16} = \tilde{\rho}\tilde{u}_z + \tilde{f}_{18} + \tilde{f}_{17} - \tilde{f}_{15} + \tilde{f}_6 - \tilde{f}_5 + \tilde{f}_{13} + \tilde{f}_{14} - \tilde{f}_{11} - \tilde{f}_{12} \tag{115}$$

From the symmetry of cell geometry, an additional assumption can be made as

$$\tilde{Q}_{121}^{non} = 0 \tag{116}$$

From Eq.(60) and (116) we have

$$\tilde{f}_7 + \tilde{f}_8 - \tilde{f}_9 - \tilde{f}_{10} = 0 \tag{117}$$

From Eq. (31) and (117) and using Eq. (115) we have

$$\tilde{f}_4 = -\tilde{\rho}\tilde{u}_z + \tilde{f}_2 + \tilde{f}_5 - \tilde{f}_6 + \tilde{f}_{11} + \tilde{f}_{12} - \tilde{f}_{13} - \tilde{f}_{14} + 2\left(\tilde{f}_{15} - \tilde{f}_{17}\right) \tag{118}$$

From Eq.(30)

$$\tilde{f}_1 + \tilde{f}_7 + \tilde{f}_{10} + \tilde{f}_{11} + \tilde{f}_{14} - \tilde{f}_3 - \tilde{f}_8 - \tilde{f}_9 - \tilde{f}_{12} - \tilde{f}_{13} = \tilde{\rho}\tilde{u}_x \tag{119}$$

From Eq.(117) and (119) we have

$$\tilde{f}_{10} = \frac{1}{2}\tilde{\rho}\tilde{u}_x + \tilde{f}_8 - \frac{\tilde{f}_1 - \tilde{f}_3 + \tilde{f}_{11} + \tilde{f}_{14} - \tilde{f}_{12} - \tilde{f}_{13}}{2} \tag{120}$$

$$\tilde{f}_9 = -\frac{1}{2}\tilde{\rho}\tilde{u}_x + \tilde{f}_7 + \frac{\tilde{f}_1 - \tilde{f}_3 + \tilde{f}_{11} + \tilde{f}_{14} - \tilde{f}_{12} - \tilde{f}_{13}}{2} \tag{121}$$

To summarize we have

$$\begin{cases} \tilde{f}_4 = -\tilde{\rho}\tilde{u}_z + \tilde{f}_2 + \tilde{f}_5 - \tilde{f}_6 + \tilde{f}_{11} + \tilde{f}_{12} - \tilde{f}_{13} - \tilde{f}_{14} + 2\left(\tilde{f}_{15} - \tilde{f}_{17}\right) \\ \tilde{f}_9 = -\frac{1}{2}\tilde{\rho}\tilde{u}_x + \tilde{f}_7 + \frac{\tilde{f}_1 - \tilde{f}_3 + \tilde{f}_{11} + \tilde{f}_{14} - \tilde{f}_{12} - \tilde{f}_{13}}{2} \\ \tilde{f}_{10} = \frac{1}{2}\tilde{\rho}\tilde{u}_x + \tilde{f}_8 - \frac{\tilde{f}_1 - \tilde{f}_3 + \tilde{f}_{11} + \tilde{f}_{14} - \tilde{f}_{12} - \tilde{f}_{13}}{2} \\ \tilde{f}_{16} = \tilde{\rho}\tilde{u}_z + \tilde{f}_{18} + \tilde{f}_{17} - \tilde{f}_{15} + \tilde{f}_6 - \tilde{f}_5 + \tilde{f}_{13} + \tilde{f}_{14} - \tilde{f}_{11} - \tilde{f}_{12} \end{cases} \tag{122}$$

To ensure mass conservation, the probability distribution function at the resting node should be corrected as

$$\tilde{f}_0 = \tilde{f}_0^c + \left(\tilde{f}_2^c + \tilde{f}_7^c + \tilde{f}_8^c + \tilde{f}_{18}^c\right) - \left(\tilde{f}_4 + \tilde{f}_9 + \tilde{f}_{10} + \tilde{f}_{16}\right) \tag{123}$$

Thus, total mass reads

$$\begin{aligned} \tilde{\rho} = \tilde{f}_0^c + \left(\tilde{f}_2^c + \tilde{f}_7^c + \tilde{f}_8^c + \tilde{f}_{18}^c\right) + \tilde{f}_1 + \tilde{f}_2 + \tilde{f}_3 + \tilde{f}_5 + \tilde{f}_6 + \tilde{f}_7 + \tilde{f}_8 \\ + \tilde{f}_{11} + \tilde{f}_{12} + \tilde{f}_{13} + \tilde{f}_{14} + \tilde{f}_{15} + \tilde{f}_{17} + \tilde{f}_{18} \end{aligned} \tag{124}$$

Corner cell with two adjacent partial walls

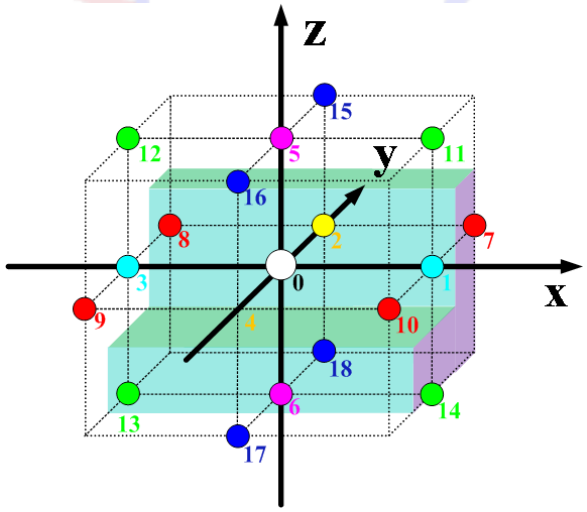

Figure 7: Corner cell with two adjacent partial walls

As shown in Figure 7, if nodes 6, 13, 14, and nodes 2, 7, 8, and 18 are solid wall $\tilde{\mathbf{u}}=(\tilde{u}_x,0,0)$ is specified. All others $\tilde{f}_i \quad (i\neq 4,9,10,5,11,12,16)$ can be obtained through the streaming step from neighbored fluid nodes. We want to determine $\tilde{f}_4,\tilde{f}_9,\tilde{f}_{10},\tilde{f}_5,\tilde{f}_{11},\tilde{f}_{12},\tilde{f}_{16}$ and $\tilde{\rho}$. As shown in Figure 7, the y axis and z axis are symmetry, in terms of the symmetry of the geometric structure of the cell, we can make the following additional assumption

$$\tilde{Q}_{121}^{non}=0 \tag{125}$$

$$\tilde{Q}_{131}^{non}=0 \tag{126}$$

$$\tilde{Q}_{232}^{non}=\tilde{Q}_{323}^{non} \tag{127}$$

$$\tilde{Q}_{212}^{non}=\tilde{Q}_{313}^{non} \tag{128}$$

From Eq.(63) and Eq.(65).

$$\begin{cases}\tilde{f}_{15}+\tilde{f}_{16}-\tilde{f}_{17}-\tilde{f}_{18}=\tilde{Q}_{232}^{non}\\ \tilde{f}_{15}+\tilde{f}_{18}-\tilde{f}_{16}-\tilde{f}_{17}=\tilde{Q}_{323}^{non}\end{cases} \tag{129}$$

From Eq.(127) and (129) we have

$$\tilde{f}_{16}=\tilde{f}_{18} \tag{130}$$

From Eq. (60) and Eq.(125)

$$\tilde{f}_7+\tilde{f}_8-\tilde{f}_9-\tilde{f}_{10}=0 \tag{131}$$

Substituting Eq.(131) and Eq.(130) into Eq. (31) we have

$$\tilde{f}_4=\tilde{f}_2+\tilde{f}_{15}-\tilde{f}_{17} \tag{132}$$

From Eq.(61) and Eq. (126)

$$\tilde{f}_{11}+\tilde{f}_{12}-\tilde{f}_{13}-\tilde{f}_{14}=0 \tag{133}$$

Substituting Eq.(133) and Eq.(130) into Eq.(32) we have

$$\tilde{f}_5=\tilde{f}_6-\tilde{f}_{15}+\tilde{f}_{17} \tag{134}$$

From Eq.(61) and Eq.(64)

$$\begin{cases}\tilde{f}_7+\tilde{f}_{10}-\tilde{f}_8-\tilde{f}_9=\dfrac{1}{3}\tilde{\rho}\tilde{u}_x+\tilde{Q}_{212}^{non}\\ \tilde{f}_{11}+\tilde{f}_{14}-\tilde{f}_{12}-\tilde{f}_{13}=\dfrac{1}{3}\tilde{\rho}\tilde{u}_x+\tilde{Q}_{313}^{non}\end{cases} \tag{135}$$

From Eq.(128) and Eq.(135)

$$\tilde{f}_7+\tilde{f}_{10}-\tilde{f}_8-\tilde{f}_9=\tilde{f}_{11}+\tilde{f}_{14}-\tilde{f}_{12}-\tilde{f}_{13} \tag{136}$$

From Eq.(30)

$$\tilde{f}_1+\tilde{f}_7+\tilde{f}_{10}+\tilde{f}_{11}+\tilde{f}_{14}-\tilde{f}_3-\tilde{f}_8-\tilde{f}_9-\tilde{f}_{12}-\tilde{f}_{13}=\tilde{\rho}\tilde{u}_x \tag{137}$$

Solve simultaneous equations of Eq.(137), Eq.(136), Eq.(131)and Eq (133) we have

$$\tilde{f}_9=-\frac{1}{4}\tilde{\rho}\tilde{u}_x+\tilde{f}_7+\frac{\tilde{f}_1-\tilde{f}_3}{4} \tag{138}$$

$$\tilde{f}_{10}=\frac{1}{4}\tilde{\rho}\tilde{u}_x+\tilde{f}_8-\frac{\tilde{f}_1-\tilde{f}_3}{4} \tag{139}$$

$$\tilde{f}_{11}=\frac{1}{4}\tilde{\rho}\tilde{u}_x+\tilde{f}_{13}-\frac{\tilde{f}_1-\tilde{f}_3}{4} \tag{140}$$

$$\tilde{f}_{12}=-\frac{1}{4}\tilde{\rho}\tilde{u}_x+\tilde{f}_{14}+\frac{\tilde{f}_1-\tilde{f}_3}{4} \tag{141}$$

To summarize

$$\begin{cases} \tilde{f}_{16} = \tilde{f}_{18} \\ \tilde{f}_4 = \tilde{f}_2 + \tilde{f}_{15} - \tilde{f}_{17} \\ \tilde{f}_5 = \tilde{f}_6 - \tilde{f}_{15} + \tilde{f}_{17} \\ \tilde{f}_9 = -\frac{1}{4}\tilde{\rho}\tilde{u}_x + \tilde{f}_7 + \frac{\tilde{f}_1 - \tilde{f}_3}{4} \\ \tilde{f}_{10} = \frac{1}{4}\tilde{\rho}\tilde{u}_x + \tilde{f}_8 - \frac{\tilde{f}_1 - \tilde{f}_3}{4} \\ \tilde{f}_{11} = \frac{1}{4}\tilde{\rho}\tilde{u}_x + \tilde{f}_{13} - \frac{\tilde{f}_1 - \tilde{f}_3}{4} \\ \tilde{f}_{12} = -\frac{1}{4}\tilde{\rho}\tilde{u}_x + \tilde{f}_{14} + \frac{\tilde{f}_1 - \tilde{f}_3}{4} \end{cases} \quad (142)$$

The total mass comes out from the solid wall is $\tilde{f}_4 + \tilde{f}_5 + \tilde{f}_9 + \tilde{f}_{10} + \tilde{f}_{11} + \tilde{f}_{12} + \tilde{f}_{16}$. Total mass sent to the solid wall after the collision is $\tilde{f}_2^c + \tilde{f}_6^c + \tilde{f}_7^c + \tilde{f}_8^c + \tilde{f}_{13}^c + \tilde{f}_{14}^c + \tilde{f}_{18}^c$. To ensure mass conservation, the probability distribution function at the resting node should be corrected as

$$\tilde{f}_0 = \tilde{f}_0^c + \tilde{f}_2^c + \tilde{f}_6^c + \tilde{f}_7^c + \tilde{f}_8^c + \tilde{f}_{13}^c + \tilde{f}_{14}^c + \tilde{f}_{18}^c - \left(\tilde{f}_4 + \tilde{f}_5 + \tilde{f}_9 + \tilde{f}_{10} + \tilde{f}_{11} + \tilde{f}_{12} + \tilde{f}_{16}\right) \quad (143)$$

Thus, total mass reads

$$\begin{aligned} \tilde{\rho} = {} & \tilde{f}_0^c + \tilde{f}_2^c + \tilde{f}_6^c + \tilde{f}_7^c + \tilde{f}_8^c + \tilde{f}_{13}^c + \tilde{f}_{14}^c + \tilde{f}_{18}^c \\ & + \tilde{f}_1 + \tilde{f}_3 + \tilde{f}_5 + \tilde{f}_9 + \tilde{f}_{10} + \tilde{f}_{11} + \tilde{f}_{12} + \tilde{f}_{15} + \tilde{f}_{16} + \tilde{f}_{17} \end{aligned} \quad (144)$$

Concave edge cell with one full wall and an adjacent partial wall

As shown in Figure 8, if nodes 6, 13, 14, 17, 18 and nodes 2, 7, 8 are solid wall $\tilde{\mathbf{u}} = (\tilde{u}_x, 0, 0)$ is specified. $\tilde{f}_i \quad (i \neq 4, 9, 10, 5, 11, 12, 15, 16)$ may be obtained through streaming step from neighbored fluid nodes. We want to determine $\tilde{f}_4, \tilde{f}_9, \tilde{f}_{10}, \tilde{f}_5, \tilde{f}_{11}, \tilde{f}_{12}, \tilde{f}_{15}, \tilde{f}_{16}$ and $\tilde{\rho}$.

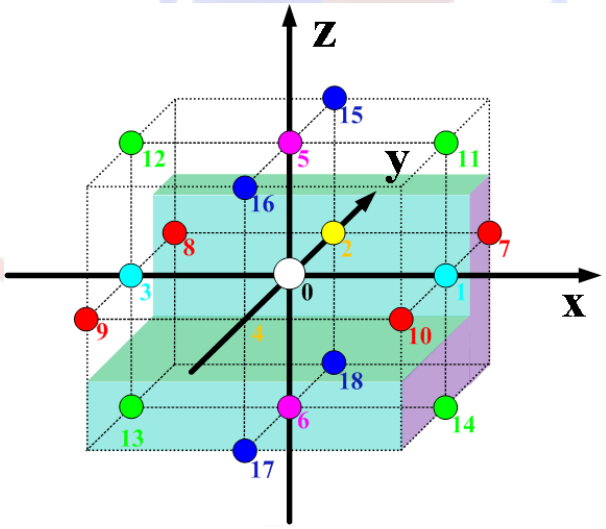

Figure 8: Concave edge cell with one full wall and an adjacent partial wall

If we replace solid node 17 as a fluid node, then Figure 8 becomes as same as Figure 7, i.e., if $\tilde{f}_{15}$ is known, then Eq.(142) is applicable here. Since the whole bottom surface is a solid wall, additional to assumptions made in the last section, we assume

$$\tilde{Q}_{232}^{non} = 0 \quad (145)$$

Substituting Eq.(145) into Eq.(63) we have

$$\tilde{f}_{15} + \tilde{f}_{16} - \tilde{f}_{17} - \tilde{f}_{18} = 0 \quad (146)$$

Eq. (146) together with Eq.(142) give rise to

$$\begin{cases} \tilde{f}_4 = \tilde{f}_2 \\ \tilde{f}_5 = \tilde{f}_6 \\ \tilde{f}_{15} = \tilde{f}_{17} \\ \tilde{f}_{16} = \tilde{f}_{18} \\ \tilde{f}_9 = -\frac{1}{4}\tilde{\rho}\tilde{u}_x + \tilde{f}_7 + \frac{\tilde{f}_1 - \tilde{f}_3}{4} \\ \tilde{f}_{10} = \frac{1}{4}\tilde{\rho}\tilde{u}_x + \tilde{f}_8 - \frac{\tilde{f}_1 - \tilde{f}_3}{4} \\ \tilde{f}_{11} = \frac{1}{4}\tilde{\rho}\tilde{u}_x + \tilde{f}_{13} - \frac{\tilde{f}_1 - \tilde{f}_3}{4} \\ \tilde{f}_{12} = -\frac{1}{4}\tilde{\rho}\tilde{u}_x + \tilde{f}_{14} + \frac{\tilde{f}_1 - \tilde{f}_3}{4} \end{cases} \quad (147)$$

The total mass comes out from the solid wall is $\tilde{f}_4 + \tilde{f}_5 + \tilde{f}_9 + \tilde{f}_{10} + \tilde{f}_{11} + \tilde{f}_{12} + \tilde{f}_{15} + \tilde{f}_{16}$. Total mass sent to the solid wall after the collision is $\tilde{f}_2^c + \tilde{f}_6^c + \tilde{f}_7^c + \tilde{f}_8^c + \tilde{f}_{13}^c + \tilde{f}_{14}^c + \tilde{f}_{17}^c + \tilde{f}_{18}^c$, to ensure mass conservation, the probability distribution function at the resting node should be corrected as

$$\begin{aligned} \tilde{f}_0 = \tilde{f}_0^c + \tilde{f}_2^c + \tilde{f}_6^c + \tilde{f}_7^c + \tilde{f}_8^c + \tilde{f}_{13}^c + \tilde{f}_{14}^c + \tilde{f}_{17}^c + \tilde{f}_{18}^c \\ -\left(\tilde{f}_4 + \tilde{f}_5 + \tilde{f}_9 + \tilde{f}_{10} + \tilde{f}_{11} + \tilde{f}_{12} + \tilde{f}_{15} + \tilde{f}_{16}\right) \end{aligned} \quad (148)$$

Thus, total mass reads

$$\begin{aligned} \tilde{\rho} = \tilde{f}_0^c + \tilde{f}_2^c + \tilde{f}_6^c + \tilde{f}_7^c + \tilde{f}_8^c + \tilde{f}_{13}^c + \tilde{f}_{14}^c + \tilde{f}_{18}^c \\ + \tilde{f}_1 + \tilde{f}_3 + \tilde{f}_5 + \tilde{f}_9 + \tilde{f}_{10} + \tilde{f}_{11} + \tilde{f}_{12} + \tilde{f}_{15} + \tilde{f}_{16} + \tilde{f}_{17} \end{aligned} \quad (149)$$

Convex edge cell

As shown in Figure 9. If node 18 is a convex node only, the probability distribution function on direction 16 need to be reconstruction, the probability distribution function on all other nodes may be obtained through streaming from neighbored fluid nodes. In general, it is impossible to satisfy exactly nonslip boundary condition, since we have only one unknown variable $\tilde{f}_{16}$. In this case, we simply assume

$$\tilde{f}_{16} = \tilde{f}_{18} \quad (150)$$

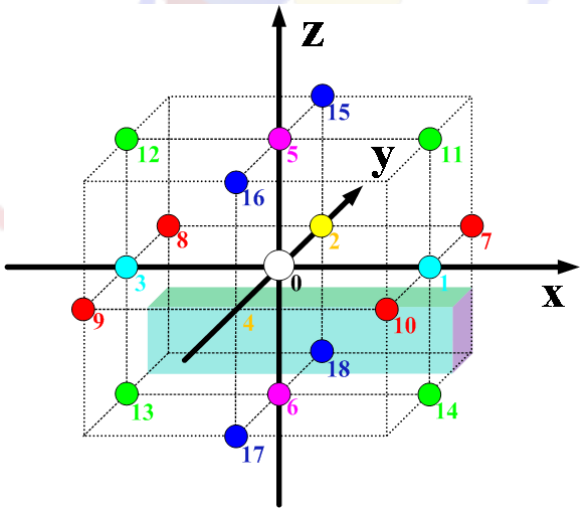

Figure 9: Convex edge cell

The mass comes out from the wall is $\tilde{f}_{16} = \tilde{f}_{18}$, the mass sent into the wall is $\tilde{f}_{18}^c$, in order keeps mass conservation the probability distribution function at the resting node should be corrected as

$$\tilde{f}_0 = \tilde{f}_0^c + \tilde{f}_{18}^c - \tilde{f}_{16} \quad (151)$$

Thus, total mass reads

$$\begin{aligned} \tilde{\rho} = \tilde{f}_0^c + \tilde{f}_1 + \tilde{f}_2 + \tilde{f}_3 + \tilde{f}_4 + \tilde{f}_5 + \tilde{f}_6 + \tilde{f}_7 + \tilde{f}_8 + \tilde{f}_9 \\ + \tilde{f}_{10} + \tilde{f}_{11} + \tilde{f}_{12} + \tilde{f}_{13} + \tilde{f}_{14} + \tilde{f}_{15} + \tilde{f}_{18}^c + \tilde{f}_{17} + \tilde{f}_{18} \end{aligned} \quad (152)$$

Simple rule for density update in nonslip boundary condition

In section 7.1 – section 7.5, we presented some cases to demonstrate how to user third-order moment to closure nonslip boundary condition. Here we show that the rule to determine density on the boundary node is very simple. Define direction set U as $U=\{\beta|,\tilde{f}_\beta(\tilde{\mathbf{r}},\tilde{t}+1)\text{ is unknown}\}$. Then the total masses come to the current boundary node from all wall nodes (pure solid nodes) is $\sum_{\beta\in U}\tilde{f}_\beta(\tilde{\mathbf{r}},\tilde{t}+1)$, in which the summation of β is carried out over U. On the other hand, the total mass sent to all wall nodes from the current boundary node in the last collision step is $\sum_{\beta\in U}\tilde{f}^c_{\bar{\beta}}(\tilde{\mathbf{r}},\tilde{t}+1)$. To ensure mass conservation, the probability distribution function at the resting node should be corrected as

$$\tilde{f}_0(\tilde{\mathbf{r}},\tilde{t}+1)=\tilde{f}^c_0(\tilde{\mathbf{r}},\tilde{t}+1)+\sum_{\beta\in U}\tilde{f}^c_{\bar{\beta}}(\tilde{\mathbf{r}},\tilde{t}+1)-\sum_{\beta\in U}\tilde{f}_\beta(\tilde{\mathbf{r}},\tilde{t}+1) \tag{153}$$

thus, the density at $\tilde{t}+1$ step reads

$$\tilde{\rho}(\tilde{\mathbf{r}},\tilde{t}+1)=\tilde{f}^c_0(\tilde{\mathbf{r}},\tilde{t}+1)+\sum_{\beta\in U}\tilde{f}^c_{\bar{\beta}}(\tilde{\mathbf{r}},\tilde{t}+1)+\sum_{\alpha\neq 0;\alpha\notin U}\tilde{f}_\alpha(\tilde{\mathbf{r}},\tilde{t}+1) \tag{154}$$

in which $\bar{\beta}$ stands for the opposite direction of β direction. Summation of β is carried out over all directions, which come out from the solid wall, while summation of α is carried out over all directions, which come out from fluid nodes (pure fluid nodes and other boundary nodes). Eq.(152) shows that, if the probability distribution function is known, which is streamed into the current node from other boundary nodes or fluid nodes, and then this probability distribution function simply appears in density formulation. If the probability distribution function is unknown, which is streamed to the current boundary node from solid wall nodes, in the density formulation, it is replaced by the last post-collision probability distribution function in its opposite direction. Since on the boundary node, the velocity $\tilde{\mathbf{u}}(\tilde{\mathbf{r}},\tilde{t}+1)$ is prescribed, it is very simple to update equilibrium probability distribution function with Eq.(154).

Inlet and outlet boundary condition

It should be mentioned that, for inlet (or outlet) boundary, due to the moving of inlet (outlet) boundary, some volume of current voxel change into the outside of fluid domain from inside of the fluid domain. In a one-time step, the amount of changed volume equals $\tilde{\rho}\tilde{u}_x$. Thus, the simple rule for density calculation Eq.(154) needs to be modified accordingly on the inlet (or outlet) boundary. The details will be given in section 8.8

Middle inlet cell

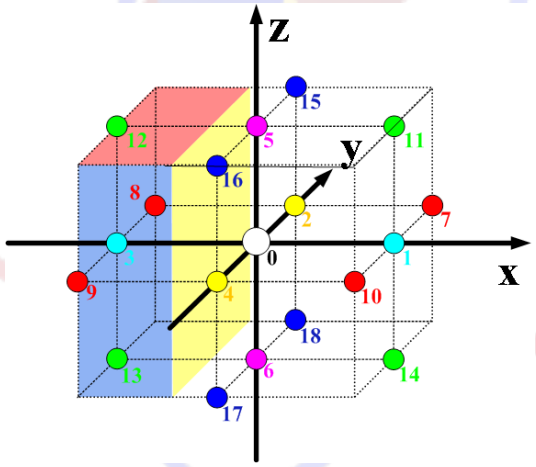

Figure 10: Middle Inlet Cell

For inlet cell shown as Figure 10, $\tilde{\mathbf{u}}=(\tilde{u}_x,\tilde{u}_y,\tilde{u}_z)$ is specified on the boundary. Nodes 3,8,9,12,13 are outside of the simulation domain. Different colors are used here so that to distinguished inlet boundary from solid wall boundary. In the streaming step, the distribution function on inlet node towards directions 1, 7, 10, 11, and 14 dependents upon the value on unknown nodes 3, 8, 9, 12, and 13, therefore they are in need to be reconstructed. All other probability distribution function $\tilde{f}_i$ $(i\neq 1,7,10,11,14)$ can be obtained through the streaming step from neighbored fluid nodes.

From Eq.(67)

$$\tilde{f}_1-\tilde{f}_3=\frac{1}{3}\tilde{\rho}\tilde{u}_x-\tilde{Q}^{non}_{212}-\tilde{Q}^{non}_{313} \tag{155}$$

Eq.(62) combined with Eq.(31) give rise to

$$\tilde{f}_7 = \tilde{f}_9 + \frac{\tilde{\rho}\tilde{u}_x}{6} + \frac{\tilde{\rho}\tilde{u}_y}{2} + \frac{\left(\tilde{f}_4 + \tilde{f}_{16} + \tilde{f}_{17}\right) - \left(\tilde{f}_2 + \tilde{f}_{15} + \tilde{f}_{18}\right)}{2} + \frac{1}{2}\tilde{Q}_{212}^{non} \tag{156}$$

$$\tilde{f}_{10} = \tilde{f}_8 + \frac{\tilde{\rho}\tilde{u}_x}{6} - \frac{\tilde{\rho}\tilde{u}_y}{2} - \frac{\left(\tilde{f}_4 + \tilde{f}_{16} + \tilde{f}_{17}\right) - \left(\tilde{f}_2 + \tilde{f}_{15} + \tilde{f}_{18}\right)}{2} + \frac{1}{2}\tilde{Q}_{212}^{non} \tag{157}$$

Eq.(64) combined with Eq.(32) give rise to

$$\tilde{f}_{11} = \tilde{f}_{13} + \frac{\tilde{\rho}\tilde{u}_x}{6} + \frac{\tilde{\rho}\tilde{u}_z}{2} + \frac{\left(\tilde{f}_6 + \tilde{f}_{17} + \tilde{f}_{18}\right) - \left(\tilde{f}_5 + \tilde{f}_{15} + \tilde{f}_{16}\right)}{2} + \frac{1}{2}\tilde{Q}_{313}^{non} \tag{158}$$

$$\tilde{f}_{14} = \tilde{f}_{12} + \frac{\tilde{\rho}\tilde{u}_x}{6} - \frac{\tilde{\rho}\tilde{u}_z}{2} - \frac{\left(\tilde{f}_6 + \tilde{f}_{17} + \tilde{f}_{18}\right) - \left(\tilde{f}_5 + \tilde{f}_{15} + \tilde{f}_{16}\right)}{2} + \frac{1}{2}\tilde{Q}_{313}^{non} \tag{159}$$

In principle, in order to get high order accuracy, we need to specify energy flux, i.e., $\tilde{Q}_{212}^{non}$ and $\tilde{Q}_{313}^{non}$ in the inlet and outlet boundary. Without known the detail information of energy flux, for first-order approximation, we may set

$$\tilde{Q}_{212}^{non} = \tilde{Q}_{313}^{non} = 0 \tag{160}$$

To summarize we have

$$\begin{cases} \tilde{f}_1 = \tilde{f}_3 + \frac{\tilde{\rho}\tilde{u}_x}{3} \\ \tilde{f}_7 = \tilde{f}_9 + \frac{\tilde{\rho}\tilde{u}_x}{6} + \frac{\tilde{\rho}\tilde{u}_y}{2} + \frac{\left(\tilde{f}_4 + \tilde{f}_{16} + \tilde{f}_{17}\right) - \left(\tilde{f}_2 + \tilde{f}_{15} + \tilde{f}_{18}\right)}{2} \\ \tilde{f}_{10} = \tilde{f}_8 + \frac{\tilde{\rho}\tilde{u}_x}{6} - \frac{\tilde{\rho}\tilde{u}_y}{2} - \frac{\left(\tilde{f}_4 + \tilde{f}_{16} + \tilde{f}_{17}\right) - \left(\tilde{f}_2 + \tilde{f}_{15} + \tilde{f}_{18}\right)}{2} \\ \tilde{f}_{11} = \tilde{f}_{13} + \frac{\tilde{\rho}\tilde{u}_x}{6} + \frac{\tilde{\rho}\tilde{u}_z}{2} + \frac{\left(\tilde{f}_6 + \tilde{f}_{17} + \tilde{f}_{18}\right) - \left(\tilde{f}_5 + \tilde{f}_{15} + \tilde{f}_{16}\right)}{2} \\ \tilde{f}_{14} = \tilde{f}_{12} + \frac{\tilde{\rho}\tilde{u}_x}{6} - \frac{\tilde{\rho}\tilde{u}_z}{2} - \frac{\left(\tilde{f}_6 + \tilde{f}_{17} + \tilde{f}_{18}\right) - \left(\tilde{f}_5 + \tilde{f}_{15} + \tilde{f}_{16}\right)}{2} \end{cases} \tag{161}$$

The mass sent into unknown nodes (nodes 3, 8, 9, 12, 13) from the current node in the last collision step is $\tilde{f}_3^c + \tilde{f}_8^c + \tilde{f}_9^c + \tilde{f}_{12}^c + \tilde{f}_{13}^c$. The mass sent out from unknown nodes into the current node is $\tilde{f}_1 + \tilde{f}_7 + \tilde{f}_{10} + \tilde{f}_{11} + \tilde{f}_{14}$. Since in one time step, current voxel reduce the volume by $\tilde{\rho}\tilde{u}_x$ (this amount volume inside of fluid domain was replaced by outside of fluid domain), therefore in order to keep mass conservation, the probability function at the resting node should be set as

$$\tilde{f}_0 = \tilde{f}_0^c + \left(\tilde{f}_3^c + \tilde{f}_8^c + \tilde{f}_9^c + \tilde{f}_{12}^c + \tilde{f}_{13}^c\right) - \left(\tilde{f}_1 + \tilde{f}_7 + \tilde{f}_{10} + \tilde{f}_{11} + \tilde{f}_{14}\right) - \tilde{\rho}\tilde{u}_x \tag{162}$$

Substituting Eq.(162) into Eq.(28)

$$\tilde{\rho} = -\tilde{\rho}\tilde{u}_x + \tilde{f}_0^c + \left(\tilde{f}_3^c + \tilde{f}_8^c + \tilde{f}_9^c + \tilde{f}_{12}^c + \tilde{f}_{13}^c\right) + \tilde{f}_2 + \tilde{f}_3 + \tilde{f}_4 + \tilde{f}_5 + \tilde{f}_6 + \tilde{f}_8 + \tilde{f}_9 + \tilde{f}_{12} + \tilde{f}_{13} + \tilde{f}_{15} + \tilde{f}_{16} + \tilde{f}_{17} + \tilde{f}_{18} \tag{163}$$

The total density

$$\tilde{\rho} = \frac{\left(\begin{array}{c} \tilde{f}_0^c + \tilde{f}_3^c + \tilde{f}_8^c + \tilde{f}_9^c + \tilde{f}_{12}^c + \tilde{f}_{13}^c + \tilde{f}_2 + \tilde{f}_3 + \tilde{f}_4 + \tilde{f}_5 \\ + \tilde{f}_6 + \tilde{f}_8 + \tilde{f}_9 + \tilde{f}_{12} + \tilde{f}_{13} + \tilde{f}_{15} + \tilde{f}_{16} + \tilde{f}_{17} + \tilde{f}_{18} \end{array}\right)}{\left(1 + \tilde{u}_x\right)} \tag{164}$$

If $\tilde{\rho}$ is given

$$\tilde{u}_x = \frac{\left(\begin{array}{c} \tilde{f}_0^c + \tilde{f}_3^c + \tilde{f}_8^c + \tilde{f}_9^c + \tilde{f}_{12}^c + \tilde{f}_{13}^c + \tilde{f}_2 + \tilde{f}_3 + \tilde{f}_4 + \tilde{f}_5 \\ + \tilde{f}_6 + \tilde{f}_8 + \tilde{f}_9 + \tilde{f}_{12} + \tilde{f}_{13} + \tilde{f}_{15} + \tilde{f}_{16} + \tilde{f}_{17} + \tilde{f}_{18} \end{array}\right)}{\tilde{\rho}} - 1 \tag{165}$$

It should be emphasized that in Figure 10 rectangular at left represent an inlet boundary, one should not confuse it with a solid wall, which is shown in a different color. The same situations also will be in the next few sections; the rectangular with yellow surface represents an inlet boundary rather than a solid wall boundary.

Inlet cell along a surface boundary

For example as shown as Figure 11, $\tilde{\mathbf{u}}=(\tilde{u}_x,\tilde{u}_y,0)$ is specified on the boundary. Again, different colors are used to distinguished inlet boundary from solid wall boundary. If down edge (nodes 6, 13, 14, 17, 18) is a solid wall. The probability distribution function in directions 5, 11, 12, 15, 16 are unknown. The probability distribution function in directions 1, 7, 10, 11, 14 come from the outside fluid domain, and they are also unknown. We need to determine $\tilde{f}_1,\tilde{f}_5,\tilde{f}_7,\tilde{f}_{10},\tilde{f}_{11},\tilde{f}_{12},\tilde{f}_{14},\tilde{f}_{15},\tilde{f}_{16}$ and. All other probability distribution function can be obtained through the streaming step from neighbored fluid nodes. Due to the geometrical symmetry, we assume

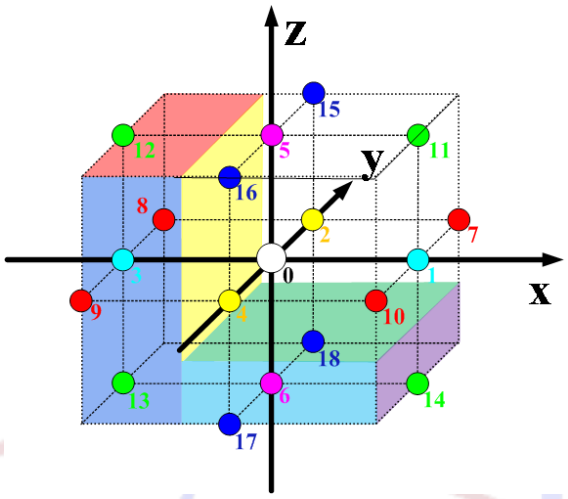

Figure 11: Inlet Cell along A Surface Boundary

$$\tilde{Q}^{non}_{212}=\tilde{Q}^{non}_{313}=0 \quad (166)$$

$$\tilde{Q}^{non}_{131}=\tilde{Q}^{non}_{232}=0 \quad (167)$$

$$\tilde{Q}^{non}_{121}=\tilde{Q}^{non}_{323} \quad (168)$$

Substituting Eq.(166) into Eq.(67)

$$\tilde{f}_1=\frac{1}{3}\tilde{\rho}\tilde{u}_x+\tilde{f}_3 \quad (169)$$

Substituting Eq.(167) into Eq.(69)

$$\tilde{f}_5=\tilde{f}_6 \quad (170)$$

Substituting Eq.(168) into Eq.(68)

$$\tilde{Q}^{non}_{121}=\tilde{Q}^{non}_{323}=\frac{1}{6}\tilde{\rho}\tilde{u}_y-\frac{\tilde{f}_2-\tilde{f}_4}{2} \quad (171)$$

Substituting Eq. (171) into Eq.(60)

$$\tilde{f}_7+\tilde{f}_8-\tilde{f}_9-\tilde{f}_{10}=\frac{1}{2}\tilde{\rho}\tilde{u}_y-\frac{\tilde{f}_2-\tilde{f}_4}{2} \quad (172)$$

From Eq.(62) and Eq.(166)

$$\tilde{f}_7+\tilde{f}_{10}-\tilde{f}_8-\tilde{f}_9=\frac{1}{3}\tilde{\rho}\tilde{u}_x \quad (173)$$

Eq.(172) and Eq.(173) give rise to

$$\tilde{f}_7=\frac{1}{6}\tilde{\rho}\tilde{u}_x+\frac{1}{4}\tilde{\rho}\tilde{u}_y-\frac{\tilde{f}_2-\tilde{f}_4}{4}+\tilde{f}_9 \quad (174)$$

$$\tilde{f}_{10}=\frac{1}{6}\tilde{\rho}\tilde{u}_x-\frac{1}{4}\tilde{\rho}\tilde{u}_y+\tilde{f}_8+\frac{\tilde{f}_2-\tilde{f}_4}{4} \quad (175)$$

Substituting Eq.(171) into Eq.(65)

$$\tilde{f}_{15}+\tilde{f}_{18}-\tilde{f}_{16}-\tilde{f}_{17}=\frac{1}{2}\tilde{\rho}\tilde{u}_y-\frac{\tilde{f}_2-\tilde{f}_4}{2} \quad (176)$$

From Eq. (63) and Eq.(167)

$$\tilde{f}_{15}+\tilde{f}_{16}-\tilde{f}_{17}-\tilde{f}_{18}=0 \tag{177}$$

Eq.(176) and Eq.(177) give rise to

$$\tilde{f}_{15}=\frac{1}{4}\tilde{\rho}\tilde{u}_y+\tilde{f}_{17}-\frac{\tilde{f}_2-\tilde{f}_4}{4} \tag{178}$$

$$\tilde{f}_{16}=-\frac{1}{4}\tilde{\rho}\tilde{u}_y+\tilde{f}_{18}+\frac{\tilde{f}_2-\tilde{f}_4}{4} \tag{179}$$

Substituting Eq.(167) into Eq.(61)

$$\tilde{f}_{11}+\tilde{f}_{12}-\tilde{f}_{13}-\tilde{f}_{14}=0 \tag{180}$$

Substituting Eq. (166) into Eq.(64)

$$\tilde{f}_{11}+\tilde{f}_{14}-\tilde{f}_{12}-\tilde{f}_{13}=\frac{1}{3}\tilde{\rho}\tilde{u}_x \tag{181}$$

Eq.(180) and Eq.(181) give rise to

$$\tilde{f}_{11}=\frac{1}{6}\tilde{\rho}\tilde{u}_x+\tilde{f}_{13} \tag{182}$$

$$\tilde{f}_{14}=\frac{1}{6}\tilde{\rho}\tilde{u}_x+\tilde{f}_{12} \tag{183}$$

Made additional assumption

$$\tilde{f}_{12}+\tilde{f}_{14}=\tilde{f}_{12}^{c}+\tilde{f}_{14}^{c} \tag{184}$$

then

$$\tilde{f}_{14}=\frac{1}{12}\tilde{\rho}\tilde{u}_x+\frac{\tilde{f}_{12}^{c}+\tilde{f}_{14}^{c}}{2} \tag{185}$$

$$\tilde{f}_{12}=-\frac{1}{12}\tilde{\rho}\tilde{u}_x+\frac{\tilde{f}_{12}^{c}+\tilde{f}_{14}^{c}}{2} \tag{186}$$

To summarize we have

$$\begin{cases}
\tilde{f}_1=\frac{1}{3}\tilde{\rho}\tilde{u}_x+\tilde{f}_3\\
\tilde{f}_5=\tilde{f}_6\\
\tilde{f}_7=\frac{1}{6}\tilde{\rho}\tilde{u}_x+\frac{1}{4}\tilde{\rho}\tilde{u}_y-\frac{\tilde{f}_2-\tilde{f}_4}{4}+\tilde{f}_9\\
\tilde{f}_{10}=\frac{1}{6}\tilde{\rho}\tilde{u}_x-\frac{1}{4}\tilde{\rho}\tilde{u}_y+\tilde{f}_8+\frac{\tilde{f}_2-\tilde{f}_4}{4}\\
\tilde{f}_{11}=\frac{1}{6}\tilde{\rho}\tilde{u}_x+\tilde{f}_{13}\\
\tilde{f}_{12}=-\frac{1}{12}\tilde{\rho}\tilde{u}_x+\frac{\tilde{f}_{12}^{c}+\tilde{f}_{14}^{c}}{2}\\
\tilde{f}_{14}=\frac{1}{12}\tilde{\rho}\tilde{u}_x+\frac{\tilde{f}_{12}^{c}+\tilde{f}_{14}^{c}}{2}\\
\tilde{f}_{15}=\frac{1}{4}\tilde{\rho}\tilde{u}_y+\tilde{f}_{17}-\frac{\tilde{f}_2-\tilde{f}_4}{4}\\
\tilde{f}_{16}=-\frac{1}{4}\tilde{\rho}\tilde{u}_y+\tilde{f}_{18}+\frac{\tilde{f}_2-\tilde{f}_4}{4}
\end{cases} \tag{187}$$

The buried link is 12-14. The mass sent into unknown nodes (nodes 3, 6, 8, 9, 12, 13, 14, 17, 18) from the current node in the last collision step is $\tilde{f}_3^{c}+\tilde{f}_6^{c}+\tilde{f}_8^{c}+\tilde{f}_9^{c}+\tilde{f}_{12}^{c}+\tilde{f}_{13}^{c}+\tilde{f}_{14}^{c}+\tilde{f}_{17}^{c}+\tilde{f}_{18}^{c}$. The mass sent out from unknown nodes into the current node is $\tilde{f}_1+\tilde{f}_5+\tilde{f}_7+\tilde{f}_{10}+\tilde{f}_{11}+\tilde{f}_{12}+\tilde{f}_{14}+\tilde{f}_{15}+\tilde{f}_{16}$. The current voxel reduces the volume by $\tilde{\rho}\tilde{u}_x$. To keep mass conservation, the probability function at the resting node could be set as

$$\begin{aligned}\tilde{f}_0=&\tilde{f}_0^{c}+\left(\tilde{f}_3^{c}+\tilde{f}_6^{c}+\tilde{f}_8^{c}+\tilde{f}_9^{c}+\tilde{f}_{13}^{c}+\tilde{f}_{17}^{c}+\tilde{f}_{18}^{c}\right)\\&-\left(\tilde{f}_1+\tilde{f}_5+\tilde{f}_7+\tilde{f}_{10}+\tilde{f}_{11}+\tilde{f}_{15}+\tilde{f}_{16}\right)-\tilde{\rho}\tilde{u}_x\end{aligned} \tag{188}$$

Substituting Eq. (188) into Eq.(28), the total density reads

$$\tilde{\rho}=\frac{\left(\begin{array}{l}\tilde{f}_0^c+\tilde{f}_3^c+\tilde{f}_6^c+\tilde{f}_8^c+\tilde{f}_9^c+\tilde{f}_{13}^c+\tilde{f}_{17}^c+\tilde{f}_{18}^c+\tilde{f}_{12}^c+\\ \tilde{f}_{14}^c+\tilde{f}_2+\tilde{f}_3+\tilde{f}_4+\tilde{f}_6+\tilde{f}_8+\tilde{f}_9+\tilde{f}_{13}+\tilde{f}_{17}+\tilde{f}_{18}\end{array}\right)}{(1+\tilde{u}_x)} \tag{189}$$

If $\tilde{\rho}$ is given

$$\tilde{u}_x=\frac{\left(\begin{array}{l}\tilde{f}_0^c+\tilde{f}_3^c+\tilde{f}_6^c+\tilde{f}_8^c+\tilde{f}_9^c+\tilde{f}_{13}^c+\tilde{f}_{17}^c+\tilde{f}_{18}^c+\tilde{f}_{12}^c+\\ \tilde{f}_{14}^c+\tilde{f}_2+\tilde{f}_3+\tilde{f}_4+\tilde{f}_6+\tilde{f}_8+\tilde{f}_9+\tilde{f}_{13}+\tilde{f}_{17}+\tilde{f}_{18}\end{array}\right)}{\tilde{\rho}}-1 \tag{190}$$

Inlet cell along an edge boundary

As shown as Figure 12, nodes 2, 7, 15, 18 are solid wall, and nodes 6, 14, 17, 18 are solid wall. Thus the probability distribution function in directions 4, 9, 17, 16, 5, 12, 15 are unknown. The probability distribution function in directions 1, 7, 10, 11, 14 come from the outside fluid domain, and they are also unknown. Inlet velocity on the corner is along x direction, which is specified as $\tilde{\mathbf{u}}=(\tilde{u}_x,0,0)$, we need to determine $\tilde{f}_1,\tilde{f}_4,\tilde{f}_5,\tilde{f}_7,\tilde{f}_9,\tilde{f}_{10},\tilde{f}_{11},\tilde{f}_{12},\tilde{f}_{14},\tilde{f}_{15},\tilde{f}_{16},\tilde{f}_{17}$ and ρ. This boundary condition could be achieved by setting nodes 2, 7, 8, 15, 18 as solid wall, and nodes 6, 13, 14, 17, 18 as solid wall; thus Eq.(100) is applicable here

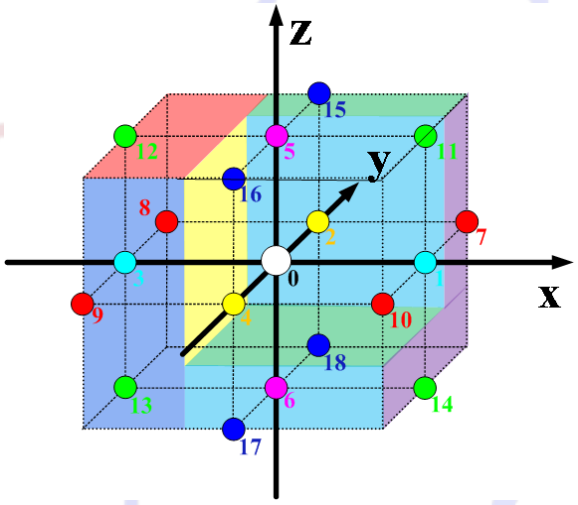

Figure 12: Inlet cell along an edge

$$\begin{cases}\tilde{f}_4=\tilde{f}_2\\ \tilde{f}_5=\tilde{f}_6\\ \tilde{f}_{16}=\tilde{f}_{18}\\ \tilde{f}_{15}=\tilde{f}_{17}=\dfrac{\tilde{f}_{15}^c+\tilde{f}_{17}^c}{2}\\ \tilde{f}_9=-\dfrac{1}{4}\tilde{\rho}\tilde{u}_x+\tilde{f}_7+\dfrac{\tilde{f}_1-\tilde{f}_3}{4}\\ \tilde{f}_{10}=\dfrac{1}{4}\tilde{\rho}\tilde{u}_x+\tilde{f}_8-\dfrac{\tilde{f}_1-\tilde{f}_3}{4}\\ \tilde{f}_{11}=\dfrac{1}{4}\tilde{\rho}\tilde{u}_x+\tilde{f}_{13}-\dfrac{\tilde{f}_1-\tilde{f}_3}{4}\\ \tilde{f}_{12}=-\dfrac{1}{4}\tilde{\rho}\tilde{u}_x+\tilde{f}_{14}+\dfrac{\tilde{f}_1-\tilde{f}_3}{4}\end{cases} \tag{191}$$

However $\tilde{f}_1$ is still unknown; both $\tilde{f}_7$ and $\tilde{f}_9$ are also unknown, they form a buried link; so does the pair of $\tilde{f}_{12}$ and $\tilde{f}_{14}$; Additional assumption is needed to closure the problem. For corner boundary, substituting Eq.(94) into Eq.(67) we have

$$\tilde{f}_1-\tilde{f}_3=\frac{1}{3}\tilde{\rho}\tilde{u}_x-2\tilde{Q}_{212}^{non} \tag{192}$$

In principle, for an incoming fluid particle on inlet corner $\tilde{Q}_{212}^{non}$ should be prescribed, without this information, we assume.

$$\tilde{Q}_{212}^{non} = \tilde{Q}_{313}^{non} = 0 \tag{193}$$

Thus

$$\tilde{f}_1 = \frac{1}{3}\tilde{\rho}\tilde{u}_x + \tilde{f}_3 \tag{194}$$

For buried links we assume

$$\tilde{f}_7 + \tilde{f}_9 = \tilde{f}_7^c + \tilde{f}_9^c \tag{195}$$

$$\tilde{f}_{12} + \tilde{f}_{14} = \tilde{f}_{12}^c + \tilde{f}_{14}^c \tag{196}$$

Eq. (191) together with Eqs. (194) – (196) give rise to

$$\begin{cases} \tilde{f}_1 = \frac{1}{3}\tilde{\rho}\tilde{u}_x + \tilde{f}_3 \\ \tilde{f}_4 = \tilde{f}_2 \\ \tilde{f}_5 = \tilde{f}_6 \\ \tilde{f}_7 = \frac{1}{12}\tilde{\rho}\tilde{u}_x + \frac{\tilde{f}_7^c + \tilde{f}_9^c}{2} \\ \tilde{f}_9 = -\frac{1}{12}\tilde{\rho}\tilde{u}_x + \frac{\tilde{f}_7^c + \tilde{f}_9^c}{2} \\ \tilde{f}_{10} = \frac{1}{6}\tilde{\rho}\tilde{u}_x + \tilde{f}_8 \\ \tilde{f}_{11} = \frac{1}{6}\tilde{\rho}\tilde{u}_x + \tilde{f}_{13} \\ \tilde{f}_{12} = -\frac{1}{12}\tilde{\rho}\tilde{u}_x + \frac{\tilde{f}_{12}^c + \tilde{f}_{14}^c}{2} \\ \tilde{f}_{14} = \frac{1}{12}\tilde{\rho}\tilde{u}_x + \frac{\tilde{f}_{12}^c + \tilde{f}_{14}^c}{2} \\ \tilde{f}_{16} = \tilde{f}_{18} \\ \tilde{f}_{15} = \frac{\tilde{f}_{15}^c + \tilde{f}_{17}^c}{2} \\ \tilde{f}_{17} = \frac{\tilde{f}_{15}^c + \tilde{f}_{17}^c}{2} \end{cases} \tag{197}$$

The buried links are 7-9, 12-14 and 15-17. The mass sent into unknown nodes (nodes 2, 3, 6, 7, 8, 9, 12, 13, 14, 15, 17, 18) from current node in last collision step is $\tilde{f}_2^c + \tilde{f}_3^c + \tilde{f}_6^c + \tilde{f}_7^c + \tilde{f}_8^c + \tilde{f}_9^c + \tilde{f}_{12}^c + \tilde{f}_{13}^c + \tilde{f}_{14}^c + \tilde{f}_{15}^c + \tilde{f}_{17}^c + \tilde{f}_{18}^c$. The mass sent out from unknown nodes into the current node is $\tilde{f}_1 + \tilde{f}_4 + \tilde{f}_5 + \tilde{f}_7 + \tilde{f}_9 + \tilde{f}_{10} + \tilde{f}_{11} + \tilde{f}_{12} + \tilde{f}_{14} + \tilde{f}_{15} + \tilde{f}_{16} + \tilde{f}_{17}$. Due to the moving of the inlet boundary, current voxel reduces the volume by $\tilde{\rho}\tilde{u}_x$. To keep mass conservation, the probability function at the resting node could be set as

$$\tilde{f}_0 = \tilde{f}_0^c + \left(\tilde{f}_2^c + \tilde{f}_3^c + \tilde{f}_6^c + \tilde{f}_8^c + \tilde{f}_{13}^c + \tilde{f}_{18}^c\right) - \left(\tilde{f}_1 + \tilde{f}_4 + \tilde{f}_5 + \tilde{f}_{10} + \tilde{f}_{11} + \tilde{f}_{16}\right) - \tilde{\rho}\tilde{u}_x \tag{198}$$

Substituting Eq. (198) into Eq.(28), the total density reads

$$\tilde{\rho} = \frac{\left[\begin{array}{c} \tilde{f}_0^c + \tilde{f}_2^c + \tilde{f}_3^c + \tilde{f}_6^c + \tilde{f}_8^c + \tilde{f}_{13}^c + \tilde{f}_{18}^c + \left(\tilde{f}_7^c + \tilde{f}_9^c\right) + \\ \left(\tilde{f}_{12}^c + \tilde{f}_{14}^c\right) + \left(\tilde{f}_{15}^c + \tilde{f}_{17}^c\right) + \tilde{f}_2 + \tilde{f}_3 + \tilde{f}_6 + \tilde{f}_8 + \tilde{f}_{13} + \tilde{f}_{18} \end{array}\right]}{(1+\tilde{u}_x)} \tag{199}$$

If $\tilde{\rho}$ is given

$$\tilde{u}_x = \frac{\left[\begin{array}{c} \tilde{f}_0^c + \tilde{f}_2^c + \tilde{f}_3^c + \tilde{f}_6^c + \tilde{f}_8^c + \tilde{f}_{13}^c + \tilde{f}_{18}^c + \left(\tilde{f}_7^c + \tilde{f}_9^c\right) + \\ \left(\tilde{f}_{12}^c + \tilde{f}_{14}^c\right) + \left(\tilde{f}_{15}^c + \tilde{f}_{17}^c\right) + \tilde{f}_2 + \tilde{f}_3 + \tilde{f}_6 + \tilde{f}_8 + \tilde{f}_{13} + \tilde{f}_{18} \end{array}\right]}{\tilde{\rho}} - 1 \tag{200}$$

Inlet cell along a boundary with partial wall

As shown as Figure 13, inlet cell along a boundary with a partial wall, nodes 2, 7, 18 are solid wall nodes, the probability distribution function in the direction 4, 9 and 16 need to be reconstructed, The probability distribution function in directions 1, 7, 10, 11, 14 come from the outside fluid domain, they are also unknown. Inlet velocity on the corner is along x direction, which is specified as $\tilde{\mathbf{u}} = \left(\tilde{u}_x, \tilde{u}_z, 0\right)$, we need to determine $\tilde{f}_1, \tilde{f}_4, \tilde{f}_7, \tilde{f}_9, \tilde{f}_{10}, \tilde{f}_{11}, \tilde{f}_{14}, \tilde{f}_{16}$ and ρ. If $\tilde{f}_4, \tilde{f}_9, \tilde{f}_{16}$ are known (equivalent to replace solid nodes 2, 7, 18 as fluid nodes), then Figure 13 becomes into Figure 10, then from Eq.(161) we have

$$\begin{cases} \tilde{f}_1 = \tilde{f}_3 + \frac{\tilde{\rho}\tilde{u}_x}{3} \\ \tilde{f}_7 = \tilde{f}_9 + \frac{\tilde{\rho}\tilde{u}_x}{6} + \frac{\left(\tilde{f}_4 + \tilde{f}_{16} + \tilde{f}_{17}\right) - \left(\tilde{f}_2 + \tilde{f}_{15} + \tilde{f}_{18}\right)}{2} \\ \tilde{f}_{10} = \tilde{f}_8 + \frac{\tilde{\rho}\tilde{u}_x}{6} - \frac{\left(\tilde{f}_4 + \tilde{f}_{16} + \tilde{f}_{17}\right) - \left(\tilde{f}_2 + \tilde{f}_{15} + \tilde{f}_{18}\right)}{2} \\ \tilde{f}_{11} = \tilde{f}_{13} + \frac{\tilde{\rho}\tilde{u}_x}{6} + \frac{\tilde{\rho}\tilde{u}_z}{2} + \frac{\left(\tilde{f}_6 + \tilde{f}_{17} + \tilde{f}_{18}\right) - \left(\tilde{f}_5 + \tilde{f}_{15} + \tilde{f}_{16}\right)}{2} \\ \tilde{f}_{14} = \tilde{f}_{12} + \frac{\tilde{\rho}\tilde{u}_x}{6} - \frac{\tilde{\rho}\tilde{u}_z}{2} - \frac{\left(\tilde{f}_6 + \tilde{f}_{17} + \tilde{f}_{18}\right) - \left(\tilde{f}_5 + \tilde{f}_{15} + \tilde{f}_{16}\right)}{2} \end{cases} \tag{201}$$

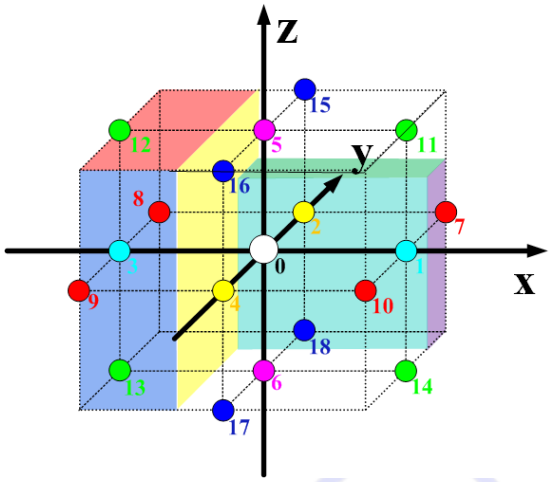

Figure 13: Inlet cell along a boundary with partial wall

We need additional assumptions to find out $\tilde{f}_4, \tilde{f}_9, \tilde{f}_{16}$. Eq.(201) [or Eq.(161)] was derived based on assumptions

$$\tilde{Q}^{non}_{212} = \tilde{Q}^{non}_{313} = 0 \tag{202}$$

Similar to section 7.4.1, we assume

$$\tilde{Q}^{non}_{121} = 0 \tag{203}$$

This results in Eq.(122), i.e.

$$\begin{cases} \tilde{f}_4 = -\tilde{\rho}\tilde{u}_z + \tilde{f}_2 + \tilde{f}_5 - \tilde{f}_6 + \tilde{f}_{11} + \tilde{f}_{12} - \tilde{f}_{13} - \tilde{f}_{14} + 2\left(\tilde{f}_{15} - \tilde{f}_{17}\right) \\ \tilde{f}_9 = -\frac{1}{2}\tilde{\rho}\tilde{u}_x + \tilde{f}_7 + \frac{\tilde{f}_1 - \tilde{f}_3 + \tilde{f}_{11} + \tilde{f}_{14} - \tilde{f}_{12} - \tilde{f}_{13}}{2} \\ \tilde{f}_{10} = \frac{1}{2}\tilde{\rho}\tilde{u}_x + \tilde{f}_8 - \frac{\tilde{f}_1 - \tilde{f}_3 + \tilde{f}_{11} + \tilde{f}_{14} - \tilde{f}_{12} - \tilde{f}_{13}}{2} \\ \tilde{f}_{16} = \tilde{\rho}\tilde{u}_z + \tilde{f}_{18} + \tilde{f}_{17} - \tilde{f}_{15} + \tilde{f}_6 - \tilde{f}_5 + \tilde{f}_{13} + \tilde{f}_{14} - \tilde{f}_{11} - \tilde{f}_{12} \end{cases} \tag{204}$$

From Eq. (160) and Eq.(64)

$$\tilde{f}_{11} + \tilde{f}_{14} - \tilde{f}_{12} - \tilde{f}_{13} = \frac{1}{3}\tilde{\rho}\tilde{u}_x \tag{205}$$

Substituting Eq.(205) and first equation of Eq.(201) into Eq.(204) we have

$$\begin{cases} \tilde{f}_4 = -\tilde{\rho}\tilde{u}_z + \tilde{f}_2 + \tilde{f}_5 - \tilde{f}_6 + \tilde{f}_{11} + \tilde{f}_{12} - \tilde{f}_{13} - \tilde{f}_{14} + 2\left(\tilde{f}_{15} - \tilde{f}_{17}\right) \\ \tilde{f}_9 = -\frac{1}{6}\tilde{\rho}\tilde{u}_x + \tilde{f}_7 \\ \tilde{f}_{10} = \frac{1}{6}\tilde{\rho}\tilde{u}_x + \tilde{f}_8 \\ \tilde{f}_{16} = \tilde{\rho}\tilde{u}_z + \tilde{f}_{18} + \tilde{f}_{17} - \tilde{f}_{15} + \tilde{f}_6 - \tilde{f}_5 + \tilde{f}_{13} + \tilde{f}_{14} - \tilde{f}_{11} - \tilde{f}_{12} \end{cases} \tag{206}$$

From first and last equations of Eq.(206) we have

$$\tilde{f}_4 + \tilde{f}_{16} = \tilde{f}_2 + \tilde{f}_{15} - \tilde{f}_{17} + \tilde{f}_{18} \tag{207}$$

Made additional assumption

$$\tilde{Q}^{non}_{232} = 0 \tag{208}$$

Substituting Eq. (208) into Eq.(63) we have

$$\tilde{f}_{16} = \frac{1}{3}\tilde{\rho}\tilde{u}_z + \tilde{f}_{17} + \tilde{f}_{18} - \tilde{f}_{15} \tag{209}$$

Eq. (207) – Eq.(209) give rise to

$$\tilde{f}_4 = -\frac{1}{3}\tilde{\rho}\tilde{u}_z + \tilde{f}_2 + 2\left(\tilde{f}_{15} - \tilde{f}_{17}\right) \tag{210}$$

Since $\tilde{f}_7, \tilde{f}_9$ form a buried links, we assume

$$\tilde{f}_7 + \tilde{f}_9 = \tilde{f}^c_7 + \tilde{f}^c_9 \tag{211}$$

The second equation of Eq. (206) and Eq.(211) give rise to

$$\begin{cases} \tilde{f}_9 = -\frac{1}{12}\tilde{\rho}\tilde{u}_x + \frac{\tilde{f}_7^c + \tilde{f}_9^c}{2} \\ \tilde{f}_7 = \frac{1}{12}\tilde{\rho}\tilde{u}_x + \frac{\tilde{f}_7^c + \tilde{f}_9^c}{2} \end{cases} \tag{212}$$

Third equation of Eq. (206) reads

$$\tilde{f}_{10} = \frac{1}{6}\tilde{\rho}\tilde{u}_x + \tilde{f}_8 \tag{213}$$

Substituting Eq.(209) into last two equations of Eq.(201) we have

$$\begin{cases} \tilde{f}_{11} = \tilde{f}_{13} + \frac{\tilde{\rho}\tilde{u}_x}{6} + \frac{\tilde{\rho}\tilde{u}_z}{3} + \frac{\tilde{f}_6 - \tilde{f}_5}{2} \\ \tilde{f}_{14} = \tilde{f}_{12} + \frac{\tilde{\rho}\tilde{u}_x}{6} - \frac{\tilde{\rho}\tilde{u}_z}{3} - \frac{\tilde{f}_6 - \tilde{f}_5}{2} \end{cases} \tag{214}$$

To summarize we have

$$\begin{cases} \tilde{f}_1 = \tilde{f}_3 + \frac{\tilde{\rho}\tilde{u}_x}{3} \\ \tilde{f}_4 = -\frac{1}{3}\tilde{\rho}\tilde{u}_z + \tilde{f}_2 + 2\left(\tilde{f}_{15} - \tilde{f}_{17}\right) \\ \tilde{f}_7 = \frac{1}{12}\tilde{\rho}\tilde{u}_x + \frac{\tilde{f}_7^c + \tilde{f}_9^c}{2} \\ \tilde{f}_9 = -\frac{1}{12}\tilde{\rho}\tilde{u}_x + \frac{\tilde{f}_7^c + \tilde{f}_9^c}{2} \\ \tilde{f}_{10} = \frac{1}{6}\tilde{\rho}\tilde{u}_x + \tilde{f}_8 \\ \tilde{f}_{11} = \tilde{f}_{13} + \frac{\tilde{\rho}\tilde{u}_x}{6} + \frac{\tilde{\rho}\tilde{u}_z}{3} + \frac{\tilde{f}_6 - \tilde{f}_5}{2} \\ \tilde{f}_{14} = \tilde{f}_{12} + \frac{\tilde{\rho}\tilde{u}_x}{6} - \frac{\tilde{\rho}\tilde{u}_z}{3} - \frac{\tilde{f}_6 - \tilde{f}_5}{2} \\ \tilde{f}_{16} = \frac{1}{3}\tilde{\rho}\tilde{u}_z + \tilde{f}_{17} + \tilde{f}_{18} - \tilde{f}_{15} \end{cases} \tag{215}$$

The buried link is 7-9. The mass sent into unknown nodes (nodes 2, 3, 7, 8, 9, 12, 13, 18) from the current node in the last collision step is $\tilde{f}_2^c + \tilde{f}_3^c + \tilde{f}_7^c + \tilde{f}_8^c + \tilde{f}_9^c + \tilde{f}_{12}^c + \tilde{f}_{13}^c + \tilde{f}_{18}^c$. The mass sent out from unknown nodes into the current node is $\tilde{f}_1 + \tilde{f}_4 + \tilde{f}_7 + \tilde{f}_9 + \tilde{f}_{10} + \tilde{f}_{11} + \tilde{f}_{14} + \tilde{f}_{16}$. Due to the moving of the inlet boundary, current voxel reduces the volume by $\tilde{\rho}\tilde{u}_x$. To keep mass conservation, the probability function at the resting node could be set as

$$\tilde{f}_0 = \tilde{f}_0^c + \left(\tilde{f}_2^c + \tilde{f}_3^c + \tilde{f}_8^c + \tilde{f}_{12}^c + \tilde{f}_{13}^c + \tilde{f}_{18}^c\right) - \left(\tilde{f}_1 + \tilde{f}_4 + \tilde{f}_{10} + \tilde{f}_{11} + \tilde{f}_{14} + \tilde{f}_{16}\right) - \tilde{\rho}\tilde{u}_x \tag{216}$$

Substituting Eq.(216) into Eq.(28), we have

$$\begin{aligned} \tilde{\rho} = -\tilde{\rho}\tilde{u}_x + \tilde{f}_0^c + \left(\tilde{f}_2^c + \tilde{f}_3^c + \tilde{f}_8^c + \tilde{f}_{12}^c + \tilde{f}_{13}^c + \tilde{f}_{18}^c\right) + \left(\tilde{f}_7^c + \tilde{f}_9^c\right) \\ + \tilde{f}_2 + \tilde{f}_3 + \tilde{f}_5 + \tilde{f}_6 + \tilde{f}_8 + \tilde{f}_{12} + \tilde{f}_{13} + \tilde{f}_{15} + \tilde{f}_{17} + \tilde{f}_{18} \end{aligned} \tag{217}$$

The total density reads

$$\tilde{\rho} = \frac{\left[\begin{array}{l} \tilde{f}_0^c + \left(\tilde{f}_2^c + \tilde{f}_3^c + \tilde{f}_8^c + \tilde{f}_{12}^c + \tilde{f}_{13}^c + \tilde{f}_{18}^c\right) + \left(\tilde{f}_7^c + \tilde{f}_9^c\right) \\ + \tilde{f}_2 + \tilde{f}_3 + \tilde{f}_5 + \tilde{f}_6 + \tilde{f}_8 + \tilde{f}_{12} + \tilde{f}_{13} + \tilde{f}_{15} + \tilde{f}_{17} + \tilde{f}_{18} \end{array}\right]}{1 + \tilde{u}_x} \tag{218}$$

If $\tilde{\rho}$ is given

$$\tilde{u}_x = \frac{\left[\begin{array}{l} \tilde{f}_0^c + \left(\tilde{f}_2^c + \tilde{f}_3^c + \tilde{f}_8^c + \tilde{f}_{12}^c + \tilde{f}_{13}^c + \tilde{f}_{18}^c\right) + \left(\tilde{f}_7^c + \tilde{f}_9^c\right) \\ + \tilde{f}_2 + \tilde{f}_3 + \tilde{f}_5 + \tilde{f}_6 + \tilde{f}_8 + \tilde{f}_{12} + \tilde{f}_{13} + \tilde{f}_{15} + \tilde{f}_{17} + \tilde{f}_{18} \end{array}\right]}{\tilde{\rho}} - 1 \tag{219}$$

Inlet cell along a boundary with two adjacent partial walls

As shown as Figure 14, if inlet cell along a boundary with two adjacent partial walls, nodes 2, 7, 18 are solid wall nodes, so do nodes 6, 14, 18. The probability distribution function in the direction 4, 9, 5, 12 and 16 need to be reconstructed, the probability distribution function in

directions 1, 7, 10, 11, 14 come from the outside fluid domain, they are also unknown. Inlet velocity on the corner is along x direction, which is specified as $\tilde{\mathbf{u}} = (\tilde{u}_x, 0, 0)$, we need to determine $\tilde{f}_1, \tilde{f}_4, \tilde{f}_5, \tilde{f}_7, \tilde{f}_9, \tilde{f}_{10}, \tilde{f}_{11}, \tilde{f}_{12}, \tilde{f}_{14}, \tilde{f}_{16}$ and ρ.

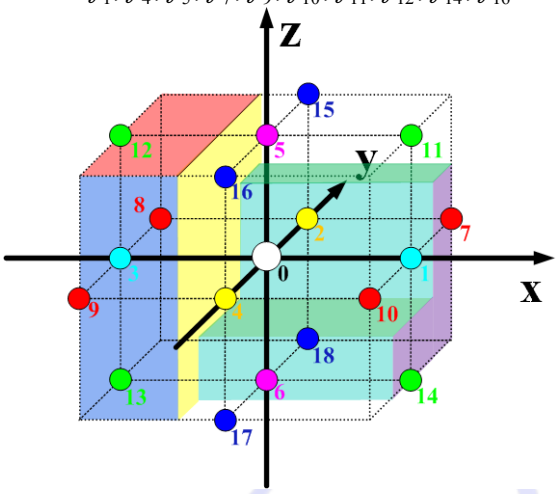

Figure 14: Inlet cell along an edge boundary with two adjacent partial walls

From Eq.(161) we have

$$\begin{cases} \tilde{f}_1 = \tilde{f}_3 + \frac{\tilde{\rho}\tilde{u}_x}{3} \\ \tilde{f}_7 = \tilde{f}_9 + \frac{\tilde{\rho}\tilde{u}_x}{6} + \frac{\left(\tilde{f}_4 + \tilde{f}_{16} + \tilde{f}_{17}\right) - \left(\tilde{f}_2 + \tilde{f}_{15} + \tilde{f}_{18}\right)}{2} \\ \tilde{f}_{10} = \tilde{f}_8 + \frac{\tilde{\rho}\tilde{u}_x}{6} - \frac{\left(\tilde{f}_4 + \tilde{f}_{16} + \tilde{f}_{17}\right) - \left(\tilde{f}_2 + \tilde{f}_{15} + \tilde{f}_{18}\right)}{2} \\ \tilde{f}_{11} = \tilde{f}_{13} + \frac{\tilde{\rho}\tilde{u}_x}{6} + \frac{\left(\tilde{f}_6 + \tilde{f}_{17} + \tilde{f}_{18}\right) - \left(\tilde{f}_5 + \tilde{f}_{15} + \tilde{f}_{16}\right)}{2} \\ \tilde{f}_{14} = \tilde{f}_{12} + \frac{\tilde{\rho}\tilde{u}_x}{6} - \frac{\left(\tilde{f}_6 + \tilde{f}_{17} + \tilde{f}_{18}\right) - \left(\tilde{f}_5 + \tilde{f}_{15} + \tilde{f}_{16}\right)}{2} \end{cases} \quad (220)$$

However more assumptions are needed to find out $\tilde{f}_5, \tilde{f}_9, \tilde{f}_{12}, \tilde{f}_{16}$. As same as section 7.4.2, we assume

$$\tilde{Q}^{non}_{121} = 0 \quad (221)$$

$$\tilde{Q}^{non}_{131} = 0 \quad (222)$$

$$\tilde{Q}^{non}_{232} = \tilde{Q}^{non}_{323} \quad (223)$$

$$\tilde{Q}^{non}_{212} = \tilde{Q}^{non}_{313} \quad (224)$$

From Eq.(142) we have

$$\begin{cases} \tilde{f}_{16} = \tilde{f}_{18} \\ \tilde{f}_4 = \tilde{f}_2 + \tilde{f}_{15} - \tilde{f}_{17} \\ \tilde{f}_5 = \tilde{f}_6 - \tilde{f}_{15} + \tilde{f}_{17} \\ \tilde{f}_9 = -\frac{1}{4}\tilde{\rho}\tilde{u}_x + \tilde{f}_7 + \frac{\tilde{f}_1 - \tilde{f}_3}{4} \\ \tilde{f}_{10} = \frac{1}{4}\tilde{\rho}\tilde{u}_x + \tilde{f}_8 - \frac{\tilde{f}_1 - \tilde{f}_3}{4} \\ \tilde{f}_{11} = \frac{1}{4}\tilde{\rho}\tilde{u}_x + \tilde{f}_{13} - \frac{\tilde{f}_1 - \tilde{f}_3}{4} \\ \tilde{f}_{12} = -\frac{1}{4}\tilde{\rho}\tilde{u}_x + \tilde{f}_{14} + \frac{\tilde{f}_1 - \tilde{f}_3}{4} \end{cases} \quad (225)$$

Eq.(220) and Eq.(225) give rise to

$$\begin{cases} \tilde{f}_1 = \tilde{f}_3 + \dfrac{\tilde{\rho}\tilde{u}_x}{3} \\ \tilde{f}_4 = \tilde{f}_2 + \tilde{f}_{15} - \tilde{f}_{17} \\ \tilde{f}_5 = \tilde{f}_6 - \tilde{f}_{15} + \tilde{f}_{17} \\ \tilde{f}_7 = \tilde{f}_9 + \dfrac{\tilde{\rho}\tilde{u}_x}{6} \\ \tilde{f}_{10} = \tilde{f}_8 + \dfrac{\tilde{\rho}\tilde{u}_x}{6} \\ \tilde{f}_{11} = \tilde{f}_{13} + \dfrac{\tilde{\rho}\tilde{u}_x}{6} \\ \tilde{f}_{14} = \tilde{f}_{12} + \dfrac{\tilde{\rho}\tilde{u}_x}{6} \\ \tilde{f}_{16} = \tilde{f}_{18} \end{cases} \tag{226}$$

Since $\tilde{f}_7, \tilde{f}_9$ form a buried link, so do $\tilde{f}_{12}, \tilde{f}_{14}$ we assume

$$\tilde{f}_7 + \tilde{f}_9 = \tilde{f}_7^c + \tilde{f}_9^c \tag{227}$$

$$\tilde{f}_{12} + \tilde{f}_{14} = \tilde{f}_{12}^c + \tilde{f}_{14}^c \tag{228}$$

Finally, we have

$$\begin{cases} \tilde{f}_1 = \tilde{f}_3 + \dfrac{\tilde{\rho}\tilde{u}_x}{3} \\ \tilde{f}_4 = \tilde{f}_2 + \tilde{f}_{15} - \tilde{f}_{17} \\ \tilde{f}_5 = \tilde{f}_6 - \tilde{f}_{15} + \tilde{f}_{17} \\ \tilde{f}_7 = \dfrac{\tilde{\rho}\tilde{u}_x}{12} + \dfrac{\tilde{f}_7^c + \tilde{f}_9^c}{2} \\ \tilde{f}_9 = -\dfrac{\tilde{\rho}\tilde{u}_x}{12} + \dfrac{\tilde{f}_7^c + \tilde{f}_9^c}{2} \\ \tilde{f}_{10} = \tilde{f}_8 + \dfrac{\tilde{\rho}\tilde{u}_x}{6} \\ \tilde{f}_{11} = \tilde{f}_{13} + \dfrac{\tilde{\rho}\tilde{u}_x}{6} \\ \tilde{f}_{14} = \dfrac{\tilde{\rho}\tilde{u}_x}{12} + \dfrac{\tilde{f}_{12}^c + \tilde{f}_{14}^c}{2} \\ \tilde{f}_{12} = -\dfrac{\tilde{\rho}\tilde{u}_x}{12} + \dfrac{\tilde{f}_{12}^c + \tilde{f}_{14}^c}{2} \\ \tilde{f}_{16} = \tilde{f}_{18} \end{cases} \tag{229}$$

The buried links are 7-9 and 12-14. The mass sent into unknown nodes (nodes2, 3, 6, 7, 8, 9, 12, 13, 14, 18) from current node in last collision step is $\tilde{f}_2^c + \tilde{f}_3^c + \tilde{f}_6^c + \tilde{f}_7^c + \tilde{f}_8^c + \tilde{f}_9^c + \tilde{f}_{12}^c + \tilde{f}_{13}^c + \tilde{f}_{14}^c + \tilde{f}_{18}^c$. The mass sent out from unknown nodes into the current node is $\tilde{f}_1 + \tilde{f}_4 + \tilde{f}_5 + \tilde{f}_7 + \tilde{f}_9 + \tilde{f}_{10} + \tilde{f}_{11} + \tilde{f}_{12} + \tilde{f}_{14} + \tilde{f}_{16}$. Due to the moving of the inlet boundary, current voxel reduces the volume by $\tilde{\rho}\tilde{u}_x$. To keep mass conservation, the probability function at the resting node could be set as

$$\tilde{f}_0 = \tilde{f}_0^c + \left(\tilde{f}_2^c + \tilde{f}_3^c + \tilde{f}_6^c + \tilde{f}_8^c + \tilde{f}_{13}^c + \tilde{f}_{18}^c\right) - \left(\tilde{f}_1 + \tilde{f}_4 + \tilde{f}_5 + \tilde{f}_{10} + \tilde{f}_{11} + \tilde{f}_{16}\right) - \tilde{\rho}\tilde{u}_x \tag{230}$$

Substituting Eq.(230)into Eq.(28),

$$\begin{aligned} \tilde{\rho} = -\tilde{\rho}\tilde{u}_x + \tilde{f}_0^c + \left(\tilde{f}_2^c + \tilde{f}_3^c + \tilde{f}_6^c + \tilde{f}_8^c + \tilde{f}_{13}^c + \tilde{f}_{18}^c\right) + \left(\tilde{f}_7^c + \tilde{f}_9^c\right) \\ + \left(\tilde{f}_{12}^c + \tilde{f}_{14}^c\right) + \tilde{f}_2 + \tilde{f}_3 + \tilde{f}_6 + \tilde{f}_8 + \tilde{f}_{13} + \tilde{f}_{15} + \tilde{f}_{17} + \tilde{f}_{18} \end{aligned} \tag{231}$$

The total density reads

$$\tilde{\rho}=\frac{\left[\begin{array}{l}\tilde{f}_0^c+\left(\tilde{f}_2^c+\tilde{f}_3^c+\tilde{f}_6^c+\tilde{f}_8^c+\tilde{f}_{13}^c+\tilde{f}_{18}^c\right)+\left(\tilde{f}_7^c+\tilde{f}_9^c\right)\\+\left(\tilde{f}_{12}^c+\tilde{f}_{14}^c\right)+\tilde{f}_2+\tilde{f}_3+\tilde{f}_6+\tilde{f}_8+\tilde{f}_{13}+\tilde{f}_{15}+\tilde{f}_{17}+\tilde{f}_{18}\end{array}\right]}{1+\tilde{u}_x} \tag{232}$$

If $\tilde{\rho}$ is given

$$\tilde{u}_x=\frac{\left[\begin{array}{l}\tilde{f}_0^c+\left(\tilde{f}_2^c+\tilde{f}_3^c+\tilde{f}_6^c+\tilde{f}_8^c+\tilde{f}_{13}^c+\tilde{f}_{18}^c\right)+\left(\tilde{f}_7^c+\tilde{f}_9^c\right)\\+\left(\tilde{f}_{12}^c+\tilde{f}_{14}^c\right)+\tilde{f}_2+\tilde{f}_3+\tilde{f}_6+\tilde{f}_8+\tilde{f}_{13}+\tilde{f}_{15}+\tilde{f}_{17}+\tilde{f}_{18}\end{array}\right]}{\tilde{\rho}}-1 \tag{233}$$

Inlet cell along a boundary with a full wall and a partial wall

As shown as Figure 15, if inlet cell along a boundary with a full wall adjacent to a partial walls, nodes 2, 7, 18 are solid wall nodes, nodes 6, 14, 17, 18. The probability distribution function in the direction 4, 9, 5, 12, 15 and 16 need to be reconstructed, The probability distribution function in directions 1, 7, 10, 11, 14 come from the outside fluid domain, they are also unknown. Inlet velocity on the corner is along x direction, which is specified as $\tilde{\mathbf{u}}=(\tilde{u}_x,0,0)$, we need to determine $\tilde{f}_1,\tilde{f}_4,\tilde{f}_5,\tilde{f}_7,\tilde{f}_9,\tilde{f}_{10},\tilde{f}_{11},\tilde{f}_{12},\tilde{f}_{14},\tilde{f}_{15},\tilde{f}_{16}$ and ρ.

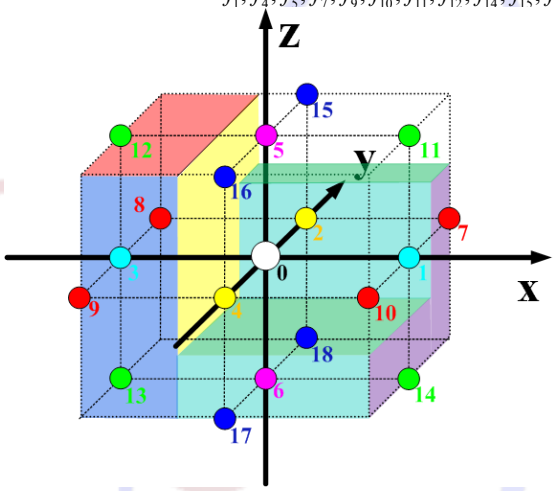

Figure 15: Inlet cell along an edge boundary with a full wall and a partial wall

Similar to section 7.4.3, further to Eq.(229) we assume

$$\tilde{Q}_{232}^{non}=0 \tag{234}$$

Substituting Eq.(234) into Eq.(63) we have

$$\tilde{f}_{15}+\tilde{f}_{16}-\tilde{f}_{17}-\tilde{f}_{18}=0 \tag{235}$$

Eq.(235) together with Eq.(229) give rise to

$$\begin{cases}\tilde{f}_1=\tilde{f}_3+\frac{\tilde{\rho}\tilde{u}_x}{3}\\ \tilde{f}_4=\tilde{f}_2\\ \tilde{f}_5=\tilde{f}_6\\ \tilde{f}_7=\frac{\tilde{\rho}\tilde{u}_x}{12}+\frac{\tilde{f}_7^c+\tilde{f}_9^c}{2}\\ \tilde{f}_9=-\frac{\tilde{\rho}\tilde{u}_x}{12}+\frac{\tilde{f}_7^c+\tilde{f}_9^c}{2}\\ \tilde{f}_{10}=\tilde{f}_8+\frac{\tilde{\rho}\tilde{u}_x}{6}\\ \tilde{f}_{11}=\tilde{f}_{13}+\frac{\tilde{\rho}\tilde{u}_x}{6}\\ \tilde{f}_{14}=\frac{\tilde{\rho}\tilde{u}_x}{12}+\frac{\tilde{f}_{12}^c+\tilde{f}_{14}^c}{2}\\ \tilde{f}_{12}=-\frac{\tilde{\rho}\tilde{u}_x}{12}+\frac{\tilde{f}_{12}^c+\tilde{f}_{14}^c}{2}\\ \tilde{f}_{15}=\tilde{f}_{17}\\ \tilde{f}_{16}=\tilde{f}_{18}\end{cases} \tag{236}$$

The buried links are 7-9 and 12-14. The mass sent into unknown nodes (2, 3, 6, 7, 8, 9, 12, 13, 14, 17, 18) from current node in last collision step is $\tilde{f}_2^c+\tilde{f}_3^c+\tilde{f}_6^c+\tilde{f}_7^c+\tilde{f}_8^c+\tilde{f}_9^c+\tilde{f}_{12}^c+\tilde{f}_{13}^c+\tilde{f}_{14}^c+\tilde{f}_{17}^c+\tilde{f}_{18}^c$. The mass sent out from unknown nodes into the current node is $\tilde{f}_1+\tilde{f}_4+\tilde{f}_5+\tilde{f}_7+\tilde{f}_9+\tilde{f}_{10}+\tilde{f}_{11}+\tilde{f}_{12}+\tilde{f}_{14}+\tilde{f}_{15}+\tilde{f}_{16}$. Due to the moving of the inlet boundary, current voxel reduces the volume by $\tilde{\rho}\tilde{u}_x$. To keep mass conservation, the probability function at the resting node could be set as

$$\tilde{f}_0=\tilde{f}_0^c+\left(\tilde{f}_2^c+\tilde{f}_3^c+\tilde{f}_6^c+\tilde{f}_8^c+\tilde{f}_{13}^c+\tilde{f}_{17}^c+\tilde{f}_{18}^c\right)-\left(\tilde{f}_1+\tilde{f}_4+\tilde{f}_5+\tilde{f}_{10}+\tilde{f}_{11}+\tilde{f}_{15}+\tilde{f}_{16}\right)-\tilde{\rho}\tilde{u}_x \tag{237}$$

Substituting Eq.(237) into Eq.(28),

$$\tilde{\rho}=-\tilde{\rho}\tilde{u}_x+\tilde{f}_0^c+\left(\tilde{f}_2^c+\tilde{f}_3^c+\tilde{f}_6^c+\tilde{f}_8^c+\tilde{f}_{13}^c+\tilde{f}_{17}^c+\tilde{f}_{18}^c\right)+\left(\tilde{f}_7^c+\tilde{f}_9^c\right)+\left(\tilde{f}_{12}^c+\tilde{f}_{14}^c\right)+\tilde{f}_2+\tilde{f}_3+\tilde{f}_6+\tilde{f}_8+\tilde{f}_{13}+\tilde{f}_{17}+\tilde{f}_{18} \tag{238}$$

The total density reads

$$\tilde{\rho}=\frac{\left[\begin{array}{c}\tilde{f}_0^c+\left(\tilde{f}_2^c+\tilde{f}_3^c+\tilde{f}_6^c+\tilde{f}_8^c+\tilde{f}_{13}^c+\tilde{f}_{17}^c+\tilde{f}_{18}^c\right)+\left(\tilde{f}_7^c+\tilde{f}_9^c\right)\\+\left(\tilde{f}_{12}^c+\tilde{f}_{14}^c\right)+\tilde{f}_2+\tilde{f}_3+\tilde{f}_6+\tilde{f}_8+\tilde{f}_{13}+\tilde{f}_{17}+\tilde{f}_{18}\end{array}\right]}{1+\tilde{u}_x} \tag{239}$$

If $\tilde{\rho}$ is given

$$\tilde{u}_x=\frac{\left[\begin{array}{c}\tilde{f}_0^c+\left(\tilde{f}_2^c+\tilde{f}_3^c+\tilde{f}_6^c+\tilde{f}_8^c+\tilde{f}_{13}^c+\tilde{f}_{17}^c+\tilde{f}_{18}^c\right)+\left(\tilde{f}_7^c+\tilde{f}_9^c\right)\\+\left(\tilde{f}_{12}^c+\tilde{f}_{14}^c\right)+\tilde{f}_2+\tilde{f}_3+\tilde{f}_6+\tilde{f}_8+\tilde{f}_{13}+\tilde{f}_{17}+\tilde{f}_{18}\end{array}\right]}{\tilde{\rho}}-1 \tag{240}$$

Inlet cell along a boundary with a convex edge

As shown in Figure 16, if inlet cell along a boundary with a convex edge, node18 are a solid wall. The probability distribution function in the direction 16 need to be reconstructed, the probability distribution function in directions 1, 7, 10, 11, 14 come from the outside fluid domain, they are also unknown. Inlet velocity is specified as $\tilde{\mathbf{u}}=\left(\tilde{u}_x,\tilde{u}_y,\tilde{u}_z\right)$, we need to determine $\tilde{f}_1,\tilde{f}_7,\tilde{f}_{10},\tilde{f}_{11},\tilde{f}_{14},\tilde{f}_{16}$ and ρ. Similar to section 7.5 we may assume

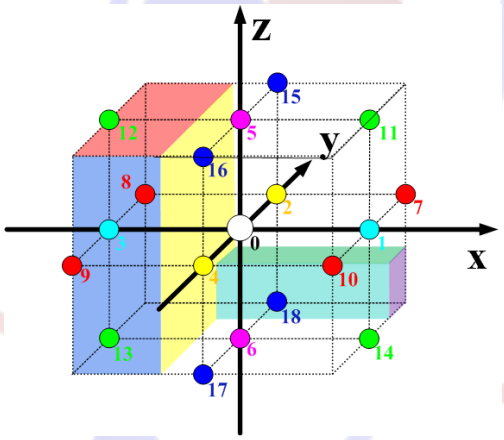

Figure 16: Inlet cell along a boundary with a convex edge

$$\tilde{f}_{16}=\tilde{f}_{18} \tag{241}$$

Eq.(241) together with Eq.(161) gives rise to

$$\begin{cases}\tilde{f}_1=\tilde{f}_3+\dfrac{\tilde{\rho}\tilde{u}_x}{3}\\ \tilde{f}_7=\tilde{f}_9+\dfrac{\tilde{\rho}\tilde{u}_x}{6}+\dfrac{\tilde{\rho}\tilde{u}_y}{2}+\dfrac{\left(\tilde{f}_4+\tilde{f}_{17}\right)-\left(\tilde{f}_2+\tilde{f}_{15}\right)}{2}\\ \tilde{f}_{10}=\tilde{f}_8+\dfrac{\tilde{\rho}\tilde{u}_x}{6}-\dfrac{\tilde{\rho}\tilde{u}_y}{2}-\dfrac{\left(\tilde{f}_4+\tilde{f}_{17}\right)-\left(\tilde{f}_2+\tilde{f}_{15}\right)}{2}\\ \tilde{f}_{11}=\tilde{f}_{13}+\dfrac{\tilde{\rho}\tilde{u}_x}{6}+\dfrac{\tilde{\rho}\tilde{u}_z}{2}+\dfrac{\left(\tilde{f}_6+\tilde{f}_{17}\right)-\left(\tilde{f}_5+\tilde{f}_{15}\right)}{2}\\ \tilde{f}_{14}=\tilde{f}_{12}+\dfrac{\tilde{\rho}\tilde{u}_x}{6}-\dfrac{\tilde{\rho}\tilde{u}_z}{2}-\dfrac{\left(\tilde{f}_6+\tilde{f}_{17}\right)-\left(\tilde{f}_5+\tilde{f}_{15}\right)}{2}\\ \tilde{f}_{16}=\tilde{f}_{18}\end{cases} \tag{242}$$

The mass sent into unknown nodes (nodes3, 8, 9, 12, 13, 18) from the current node in the last collision step is $\tilde{f}_3^c+\tilde{f}_9^c+\tilde{f}_8^c+\tilde{f}_{13}^c+\tilde{f}_{12}^c+\tilde{f}_{18}^c$. The mass sent out from unknown nodes into the current node is $\tilde{f}_1+\tilde{f}_7+\tilde{f}_{10}+\tilde{f}_{11}+\tilde{f}_{14}+\tilde{f}_{16}$. Due to the moving of the inlet boundary, current voxel reduces the volume by $\tilde{\rho}\tilde{u}_x$. To keep mass conservation, the probability function at the resting node could be set as

$$\tilde{f}_0=\tilde{f}_0^c+\left(\tilde{f}_3^c+\tilde{f}_9^c+\tilde{f}_8^c+\tilde{f}_{13}^c+\tilde{f}_{12}^c+\tilde{f}_{18}^c\right)-\left(\tilde{f}_1+\tilde{f}_7+\tilde{f}_{10}+\tilde{f}_{11}+\tilde{f}_{14}+\tilde{f}_{16}\right)-\tilde{\rho}\tilde{u}_x \tag{243}$$

Substituting Eq.(243) into Eq.(28)

$$\tilde{\rho}=-\tilde{\rho}\tilde{u}_x+\tilde{f}_0^c+\left(\tilde{f}_3^c+\tilde{f}_9^c+\tilde{f}_8^c+\tilde{f}_{13}^c+\tilde{f}_{12}^c+\tilde{f}_{18}^c\right)+\tilde{f}_2+\tilde{f}_3+\tilde{f}_4+\tilde{f}_5+\tilde{f}_6+\tilde{f}_8+\tilde{f}_9+\tilde{f}_{12}+\tilde{f}_{13}+\tilde{f}_{15}+\tilde{f}_{17}+\tilde{f}_{18} \tag{244}$$

the total density reads

$$\tilde{\rho}=\frac{\left[\begin{array}{l}\tilde{f}_0^c+\left(\tilde{f}_3^c+\tilde{f}_9^c+\tilde{f}_8^c+\tilde{f}_{13}^c+\tilde{f}_{12}^c+\tilde{f}_{18}^c\right)+\tilde{f}_2+\tilde{f}_3+\\ \tilde{f}_4+\tilde{f}_5+\tilde{f}_6+\tilde{f}_8+\tilde{f}_9+\tilde{f}_{12}+\tilde{f}_{13}+\tilde{f}_{15}+\tilde{f}_{17}+\tilde{f}_{18}\end{array}\right]}{1+\tilde{u}_x} \tag{245}$$

If $\tilde{\rho}$ is given

$$\tilde{u}_x=\frac{\left[\begin{array}{l}\tilde{f}_0^c+\left(\tilde{f}_3^c+\tilde{f}_9^c+\tilde{f}_8^c+\tilde{f}_{13}^c+\tilde{f}_{12}^c+\tilde{f}_{18}^c\right)+\tilde{f}_2+\tilde{f}_3+\\ \tilde{f}_4+\tilde{f}_5+\tilde{f}_6+\tilde{f}_8+\tilde{f}_9+\tilde{f}_{12}+\tilde{f}_{13}+\tilde{f}_{15}+\tilde{f}_{17}+\tilde{f}_{18}\end{array}\right]}{\tilde{\rho}}-1 \tag{246}$$

Density update on inlet boundary

Similar to section 7.6, again, we define direction set U as $U=\{\beta|,\tilde{f}_\beta(\tilde{\mathbf{r}},\tilde{t}+1)\text{ is unknown}\}$, here $\tilde{f}_\beta$ come out from either wall nodes (pure solid nodes) or the nodes which are outside of the fluid domain. Then the total masses come to current boundary node from all unknown nodes is $\sum_{\beta\in U}\tilde{f}_\beta(\tilde{\mathbf{r}},\tilde{t}+1)$, in which the summation of β is carried out over all pure solid wall nodes and the nodes outside of the fluid domain. On the other hand, the total mass sent into all unknown nodes from the current boundary node in the last collision step is $\sum_{\beta\in U}\tilde{f}_{\bar{\beta}}^c(\tilde{\mathbf{r}},\tilde{t}+1)$. Due to the moving of inlet boundary, current voxel reduces its volume by $\tilde{\rho}\tilde{u}_x$, which transform into the outside of fluid domain from inside of fluid domain. To ensure mass conservation, the probability distribution function at resting node should be corrected as

$$\tilde{f}_0(\tilde{\mathbf{r}},\tilde{t}+1)=\tilde{f}_0^c(\tilde{\mathbf{r}},\tilde{t}+1)+\sum_{\beta\in U}\tilde{f}_{\bar{\beta}}^c(\tilde{\mathbf{r}},\tilde{t}+1)-\sum_{\beta\in U}\tilde{f}_\beta(\tilde{\mathbf{r}},\tilde{t}+1)-\tilde{\rho}\tilde{u}_x(\tilde{\mathbf{r}},\tilde{t}+1) \tag{247}$$

thus, the density at $\tilde{t}+1$ step reads

$$\tilde{\rho}(\tilde{\mathbf{r}},\tilde{t}+1)=\frac{\tilde{f}_0^c(\tilde{\mathbf{r}},\tilde{t}+1)+\sum_{\beta\in U}\tilde{f}_{\bar{\beta}}^c(\tilde{\mathbf{r}},\tilde{t}+1)+\sum_{\alpha\notin U}\tilde{f}_\alpha(\tilde{\mathbf{r}},\tilde{t}+1)}{1+\tilde{u}_x(\tilde{\mathbf{r}},\tilde{t}+1)} \tag{248}$$

in which $\bar{\beta}$ stands for the opposite direction of β direction. Summation of β is carried out over all directions, which come out from unknown nodes(solid wall nodes plus nodes outside the fluid domain), while summation of α is carried out over all directions, which come out from fluid nodes (pure fluid nodes and other boundary nodes). If $\tilde{\rho}$ prescribed on inlet boundary, velocity $\tilde{\mathbf{u}}(\tilde{\mathbf{r}},\tilde{t}+1)$ can be calculated by

$$\tilde{u}_x(\tilde{\mathbf{r}},\tilde{t}+1)=\frac{\tilde{f}_0^c(\tilde{\mathbf{r}},\tilde{t}+1)+\sum_{\beta\in U}\tilde{f}_{\bar{\beta}}^c(\tilde{\mathbf{r}},\tilde{t}+1)+\sum_{\alpha\notin U}\tilde{f}_\alpha(\tilde{\mathbf{r}},\tilde{t}+1)}{\tilde{\rho}(\tilde{\mathbf{r}},\tilde{t}+1)}-1 \tag{249}$$

Outlet cell

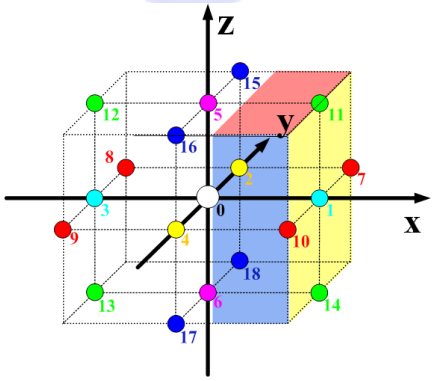

Figure 17: Middle outlet cell

Outlet cells can be treated in a similar way as in the inlet cell. We only take middle outlet cells here as an example to show how to implement boundary conditions as the same as inlet cells. As shown in Figure 17, Nodes 1, 7, 10, 11 and 14 are outside of the simulation domain. In the streaming step, the distribution function on inlet node towards direction 3,8,9,12 and 13 dependent upon the value on unknown nodes 1, 7, 10, 11 and 14, therefore they are in need to be reconstructed. Assume $\tilde{\mathbf{u}} = \left(\tilde{u}_x, \tilde{u}_y, \tilde{u}_z\right)$ is specified on the boundary. All other probability distribution function $\tilde{f}_i \quad \left(i \neq 3,\ 8,\ 9, 12, 13\right)$ can be obtained through the streaming step from neighbored fluid nodes.

Similar to section 8.1, we have

$$\begin{cases} \tilde{f}_3 = \tilde{f}_1 - \dfrac{\rho\tilde{u}_x}{3} \\ \tilde{f}_8 = \tilde{f}_{10} - \dfrac{\rho\tilde{u}_x}{6} + \dfrac{\rho\tilde{u}_y}{2} + \dfrac{\left(\tilde{f}_4 + \tilde{f}_{16} + \tilde{f}_{17}\right) - \left(\tilde{f}_2 + \tilde{f}_{15} + \tilde{f}_{18}\right)}{2} \\ \tilde{f}_9 = \tilde{f}_7 - \dfrac{\rho\tilde{u}_x}{6} - \dfrac{\rho\tilde{u}_y}{2} - \dfrac{\left(\tilde{f}_4 + \tilde{f}_{16} + \tilde{f}_{17}\right) - \left(\tilde{f}_2 + \tilde{f}_{15} + \tilde{f}_{18}\right)}{2} \\ \tilde{f}_{12} = \tilde{f}_{14} - \dfrac{\rho\tilde{u}_x}{6} + \dfrac{\rho\tilde{u}_z}{2} + \dfrac{\left(\tilde{f}_6 + \tilde{f}_{17} + \tilde{f}_{18}\right) - \left(\tilde{f}_5 + \tilde{f}_{15} + \tilde{f}_{16}\right)}{2} \\ \tilde{f}_{13} = \tilde{f}_{11} - \dfrac{\rho\tilde{u}_x}{6} - \dfrac{\rho\tilde{u}_z}{2} - \dfrac{\left(\tilde{f}_6 + \tilde{f}_{17} + \tilde{f}_{18}\right) - \left(\tilde{f}_5 + \tilde{f}_{15} + \tilde{f}_{16}\right)}{2} \end{cases} \tag{250}$$

The mass sent into unknown nodes (nodes 1, 7, 10, 11, 14) from the current node in the last collision step is $\tilde{f}_1^c + \tilde{f}_7^c + \tilde{f}_{10}^c + \tilde{f}_{11}^c + \tilde{f}_{14}^c$. The mass sent out from unknown nodes into the current node is $\tilde{f}_3 + \tilde{f}_8 + \tilde{f}_9 + \tilde{f}_{12} + \tilde{f}_{13}$. Due to the moving of outlet boundary, current voxel increases the volume by $\tilde{\rho}\tilde{u}_x$. To keep mass conservation, the probability function at the resting node could be set as

$$\tilde{f}_0 = \tilde{f}_0^c + \left(\tilde{f}_1^c + \tilde{f}_7^c + \tilde{f}_{10}^c + \tilde{f}_{11}^c + \tilde{f}_{14}^c\right) - \left(\tilde{f}_3 + \tilde{f}_8 + \tilde{f}_9 + \tilde{f}_{12} + \tilde{f}_{13}\right) + \tilde{\rho}\tilde{u}_x \tag{251}$$

Substituting Eq.(251) into Eq.(28),

$$\tilde{\rho} = \tilde{\rho}\tilde{u}_x + \tilde{f}_0^c + \left(\tilde{f}_1^c + \tilde{f}_7^c + \tilde{f}_{10}^c + \tilde{f}_{11}^c + \tilde{f}_{14}^c\right) \left(\tilde{f}_1 + \tilde{f}_7 + \tilde{f}_{10} + \tilde{f}_{11} + \tilde{f}_{14}\right) + \tilde{f}_2 + \tilde{f}_4 + \tilde{f}_5 + \tilde{f}_6 + \tilde{f}_{15} + \tilde{f}_{16} + \tilde{f}_{17} + \tilde{f}_{18} \tag{252}$$

the total density reads

$$\tilde{\rho} = \frac{\left[\begin{array}{c} \tilde{f}_0^c + \tilde{f}_2 + \tilde{f}_4 + \tilde{f}_5 + \tilde{f}_6 + \tilde{f}_{15} + \tilde{f}_{16} + \tilde{f}_{17} + \tilde{f}_{18} \\ \left(\tilde{f}_1^c + \tilde{f}_7^c + \tilde{f}_{10}^c + \tilde{f}_{11}^c + \tilde{f}_{14}^c\right) + \left(\tilde{f}_1 + \tilde{f}_7 + \tilde{f}_{10} + \tilde{f}_{11} + \tilde{f}_{14}\right) \end{array}\right]}{1 - \tilde{u}_x} \tag{253}$$

If $\tilde{\rho}$ is given

$$\tilde{u}_x = 1 - \frac{\left[\begin{array}{c} \tilde{f}_0^c + \tilde{f}_2 + \tilde{f}_4 + \tilde{f}_5 + \tilde{f}_6 + \tilde{f}_{15} + \tilde{f}_{16} + \tilde{f}_{17} + \tilde{f}_{18} \\ \left(\tilde{f}_1^c + \tilde{f}_7^c + \tilde{f}_{10}^c + \tilde{f}_{11}^c + \tilde{f}_{14}^c\right) + \left(\tilde{f}_1 + \tilde{f}_7 + \tilde{f}_{10} + \tilde{f}_{11} + \tilde{f}_{14}\right) \end{array}\right]}{\tilde{\rho}} \tag{254}$$

Compare Eq.(161) or Eq.(250) with Eq. (25) in Zou and He [1], it is easy to found that Zou and He [1] model is just 2D special case of the present model. Zou and He [1] called their model as bouncy back non-equilibrium part model, therefore $\tilde{Q}_{212}^{non} = \tilde{Q}_{313}^{non} = 0$ is just 3D generousness of bouncy back non-equilibrium part model. Therefore, the bouncy back non-equilibrium part model is a particular case of zero off-equilibrium third-order moments of the distribution function model.

Case study

In this section, we will use two examples, fluid flow in a round and rectangular cylinder along the x direction, to demonstrate that slip velocity result from bouncy back boundary condition is viscosity dependent. Simulation results using two different boundary conditions are compared.

Fluid flow in a rectangular cylinder

Consider a steady flow within a square cylinder along x direction, general Navier-Stokes equation

$$\rho\left(\frac{\partial \mathbf{v}}{\partial t} + \mathbf{v} \cdot \frac{\partial \mathbf{v}}{\partial \mathbf{r}}\right) = \mathbf{F} - \frac{\partial p}{\partial \mathbf{r}} + \mu\Delta\mathbf{v} \tag{255}$$

Reduce to

$$\begin{cases} \left.\dfrac{\partial^2 u}{\partial y^2}+\dfrac{\partial^2 u}{\partial z^2}\right|_{\Omega} = -\dfrac{F_x}{\mu} \\ u\big|_{\partial\Omega}=0 \end{cases} \tag{256}$$

in which

$$\Omega=(-H,H)\times(-H,H) \tag{257}$$

From the Appendix, we know that the analytic solution of Eq. (256) reads

$$u=\frac{F_x H^2}{\mu}\left[\frac{H^2-z^2}{2H^2}-\frac{16}{\pi^3}\sum_{n=1,3,5}^{\infty}\frac{1}{n^3}\frac{\sinh\left(n\pi\frac{H+y}{2H}\right)+\sinh\left(n\pi\frac{H-y}{2H}\right)}{\sinh(n\pi)}\sin\left(n\pi\frac{H+z}{2H}\right)\right] \tag{258}$$

Introduce

$$\tilde{\rho}_l=\frac{\rho_l}{\rho_c},\quad \tilde{u}(\tilde{y},\tilde{z})=\frac{u(y,z)}{c},\quad \tilde{F}_x=\frac{F_x\Delta t}{\rho_c c},\quad \hat{y}=\frac{y}{H},\quad \hat{z}=\frac{z}{H},\quad \tilde{H}=\frac{H}{\Delta x} \tag{259}$$

Note that the kinematic viscosity in Lattice Boltzmann Model may be expressed as

$$\mu=\rho_l\nu=\frac{2\tilde{\tau}^*-1}{6}\rho_l\Delta t c^2 \tag{260}$$

then the analytic solution Eq.(258) reads

$$\tilde{u}=\frac{6\tilde{F}_x\tilde{H}^2}{(2\tilde{\tau}^*-1)}\left[\frac{1-\hat{z}^2}{2}-\frac{16}{\pi^3}\sum_{n=1,3,5}^{\infty}\frac{1}{n^3}\frac{\sinh\left(n\pi\frac{1+\hat{y}}{2}\right)+\sinh\left(n\pi\frac{1-y}{2}\right)}{\sinh(n\pi)}\sin\left(n\pi\frac{1+z}{2}\right)\right] \tag{261}$$

In lattice Boltzmann simulation, the fluid domain is assumed as

$$1\le\tilde{x}\le 20;\quad 0\le\tilde{y}\le 200;\quad 0\le\tilde{z}\le 200; \tag{262}$$

Therefore the corresponding parameter in the analytic solution was set as $\tilde{H}=100$. Other parameters were set as: $\tilde{\rho}_l=1$; $\tilde{\tau}^*=2$; $\tilde{F}_x=0.00001$. Nonslip condition at the solid wall was introduced through the method proposed in section 7. In the inlet ($\tilde{x}=1$) and outlet ($\tilde{x}=20$), periodic boundary condition was used along x direction, the velocity profile was shown in Figure 18. The results of the numerical simulation consists with analytic solution very well; the comparison of numerical simulation with the analytic solution is shown in Figure 19.

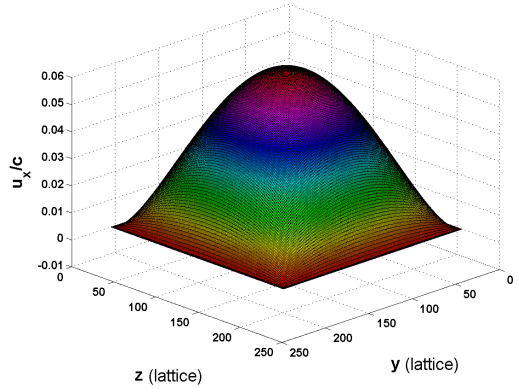

Figure 18: Velocity profile for $\tilde{\tau}^*=2$

For the inlet ($\tilde{x}=1$) and outlet ($\tilde{x}=20$), the alternative boundary condition was prescribed velocity $\mathbf{v}=(\tilde{u},0,0)$, in which $\tilde{u}$ was given in Eq.(261). These given velocity boundary conditions also can be introduced through the method proposed in section 7. Numerical simulation shows by prescribing analytic velocity at the inlet and outlet boundary give the same result as a periodic boundary condition.

If $\tilde{\tau}^*\le 2$, replacing solid wall boundary condition by bounce-back boundary condition will not be changed simulation results significantly. However, as $\tilde{\tau}^*$ increases, the bounce-back boundary condition will produce apparent slip velocity at the solid wall, while the nonslip boundary condition given in section 7 gives exactly zero velocity.

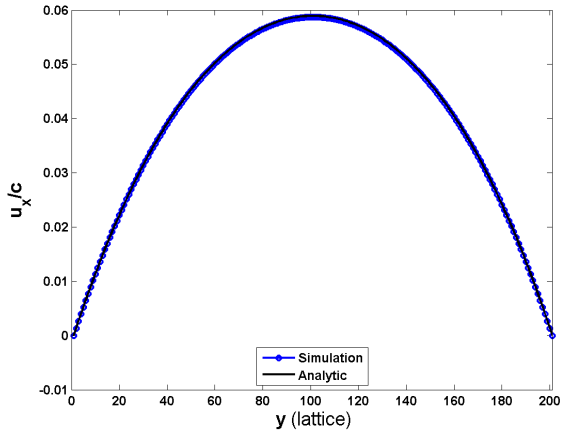

Figure 19: Intersection of velocity profile with $\tilde{z} = 100$ plan

Velocity profile with the bouncy back boundary condition for $\tilde{\tau}^* = 20$ was shown in Figure 20. Simulation results show that the slip velocity produced by the bounce back boundary condition in a rectangular cylinder is not uniform. The slip velocity reaches its minimum value at the corners of the cylinder while it reaches its maximum at the middle of the edge. Figure 21 shows the details of the slip velocity at the solid wall boundary $\tilde{z} = 0$ produced by the bounce-back boundary condition. If increase the viscosity (or the value of $\tilde{\tau}^*$) future, the slip velocity monotonically increases with the viscosity. The velocity profile and slip velocity with bouncy back boundary condition for $\tilde{\tau}^* = 40$ were shown in Figure 22 & 23.

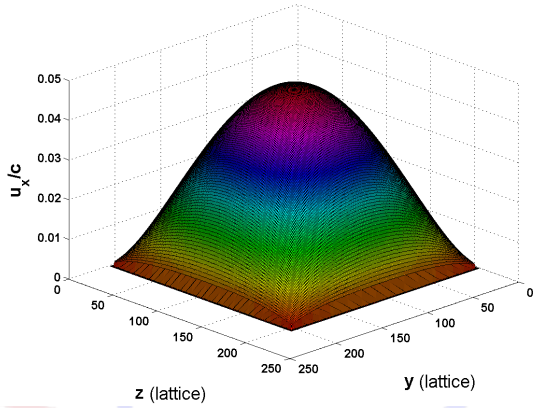

Figure 20: Velocity profile with the bouncy back boundary condition for $\tilde{\tau}^* = 20$

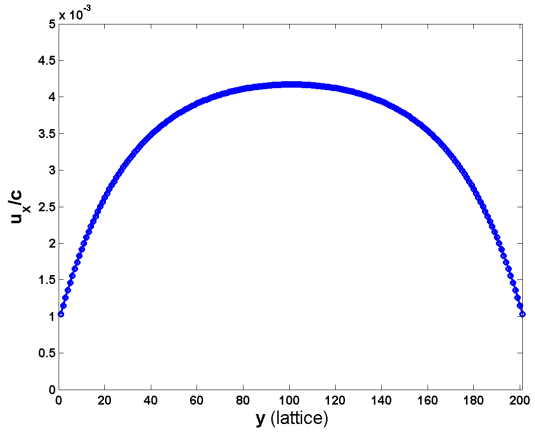

Figure 21: Intersection of velocity profile with bouncy back boundary condition at $\tilde{z} = 0$ plan

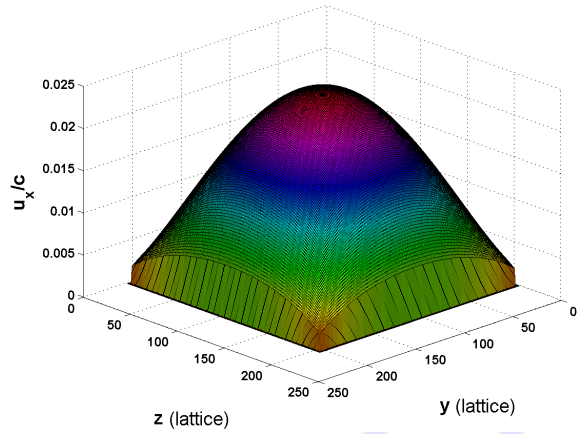

Figure 22: Velocity profile with bouncy back boundary condition for $\tilde{\tau}^{*} = 40$

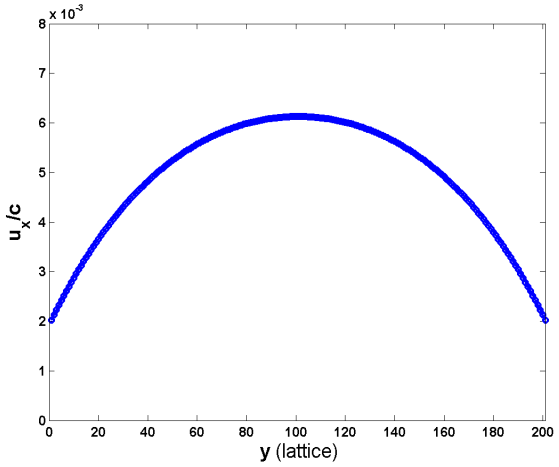

Figure 23: Intersection of the velocity profile with bouncy back boundary condition at $\tilde{z} = 0$ plan

Poiseuille flow in a round cylinder

Let us consider the Poiseuille flow in a round tube (Figure 24 & 25). The analytic solution reads

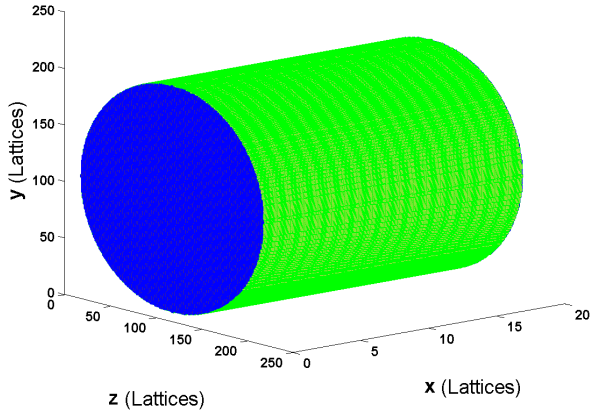

Figure 24: Sketch of cylinder Structure

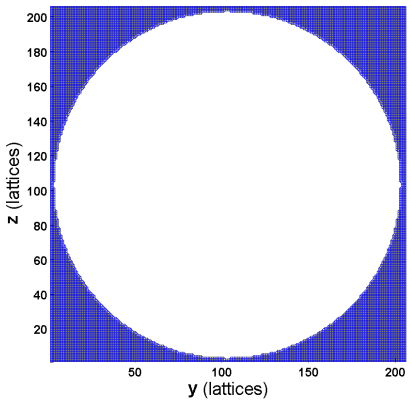

Figure 25: Intersection of tube

$$u(r)=\frac{F_x}{4\mu}\left(R^2-r^2\right) \tag{263}$$

Substituting Eq. (260) into Eq.(263) we have

$$u(r)=\frac{3}{\left(4\tilde{\tau}^*-2\right)\rho_l\Delta t c^2}F_x\left(R^2-r^2\right) \tag{264}$$

Introduce

$$\tilde{\rho}_l=\frac{\rho_l}{\rho_c},\quad \tilde{u}(r)=\frac{u(r)}{c},\quad \tilde{F}_x=\frac{F_x\Delta t}{\rho_c c},\quad \tilde{R}=\frac{R}{\Delta x},\quad \tilde{r}=\frac{r}{\Delta x} \tag{265}$$

then the analytic solution reads

$$\tilde{u}(\tilde{r})=\frac{3\tilde{F}_x}{\left(4\tilde{\tau}^*-2\right)\tilde{\rho}_l}\left(\tilde{R}^2-\tilde{r}^2\right) \tag{266}$$

In our simulation, wet nodes are within the domain

$$\begin{cases}\left(\tilde{y}-101\right)^2+\left(\tilde{z}-101\right)^2\le\tilde{R}^2=100^2\\ 1\le\tilde{x}\le 20\end{cases} \tag{267}$$

Other parameters are

$$\tilde{\rho}_l=1 \tag{268}$$

i.e.

$$\rho_c=\rho_l \tag{269}$$

$$\tilde{\tau}^*=2,\quad 20,\quad 40 \tag{270}$$

Respectively

$$\tilde{F}_x=0.001 \tag{271}$$

At y axis, i.e. $\tilde{z}=101$ and $\tilde{x}=10$, fluid domain reads

$$\left(\tilde{y}-101\right)^2\le\tilde{R}^2=100^2 \tag{272}$$

Thus, the velocity of fluid in x direction reads

$$\tilde{u}(\tilde{r})=\frac{0.003}{\left(4\tilde{\tau}^*-2\right)}\left[100^2-\left(\tilde{y}-101\right)^2\right] \tag{273}$$

In our simulation, the periodical boundary condition is used for inlet ($\tilde{x}=1$) and outlet ($\tilde{x}=20$) boundary. In the wall node of the tube, the bouncy back boundary condition and the nonslip boundary condition developed in section 7 are used respectively for comparison. The simulation results show that, if the viscosity (or $\tilde{\tau}^*$) is small (refer to Figure 26 and Figure 27), bouncy back boundary condition could be a good approximation, however, as shown in Figure 28-37, if $\tilde{\tau}^*$ is large, the error may be significant. If we define slip velocity as the difference between the velocity of Lattice Boltzmann simulation and analytical velocity, i.e.

$$\tilde{u}_{slip} = \tilde{u}_{LBM} - \tilde{u}_{Analytic} \quad (274)$$

The simulation result shows that, in a round cylinder, the bouncy back boundary condition almost produces uniform slip velocity across the whole intersection of the cylinder.

The three dimension velocity profiles under two different boundary conditions are shown in Figure 36 & 37, respectively.

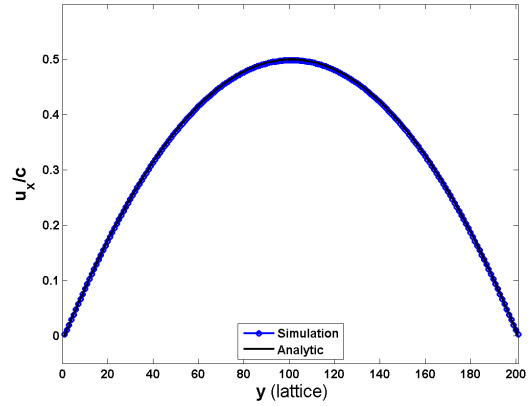

Figure 26: Velocity profile with Bouncy back boundary condition for $\tilde{\tau}^* = 2$

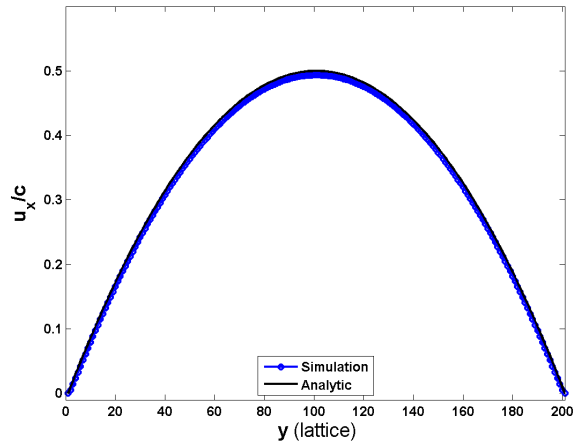

Figure 27: Velocity profile with nonslip boundary condition for $\tilde{\tau}^* = 2$

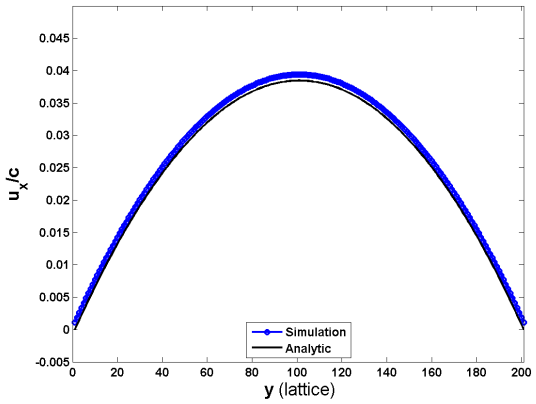

Figure 28: Velocity profile with Bouncy back boundary condition for $\tilde{\tau}^* = 20$

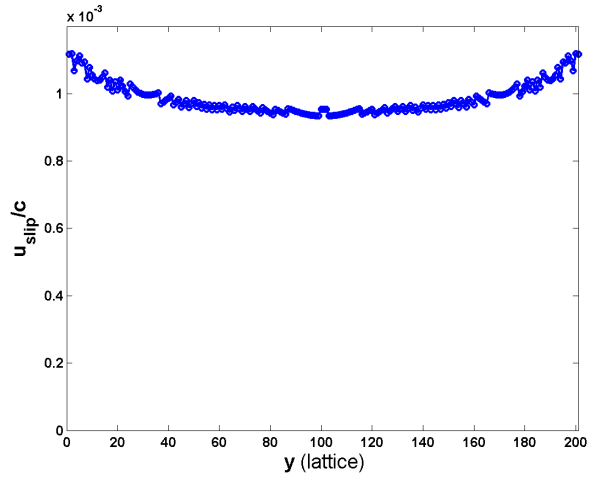

Figure 29: Slip velocity with Bouncy back boundary condition for $\tilde{\tau}^* = 20$

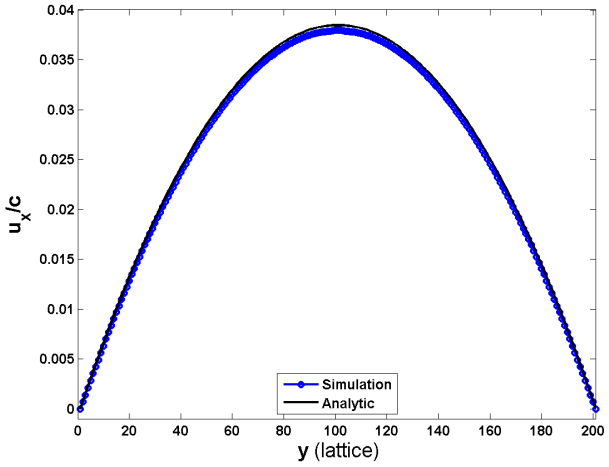

Figure 30: Velocity profile with nonslip boundary condition for $\tilde{\tau}^* = 20$

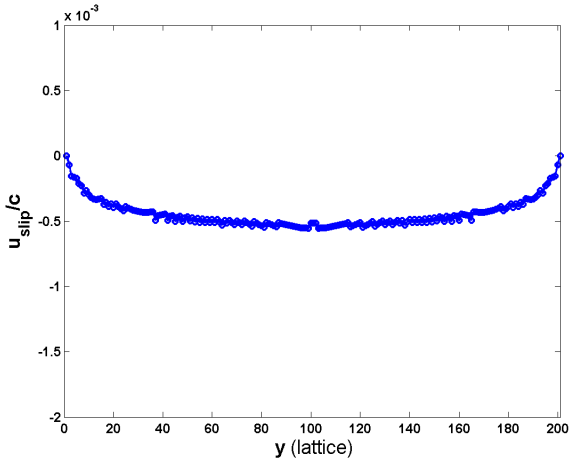

Figure 31: Slip velocity of nonslip boundary condition for $\tilde{\tau}^* = 20$

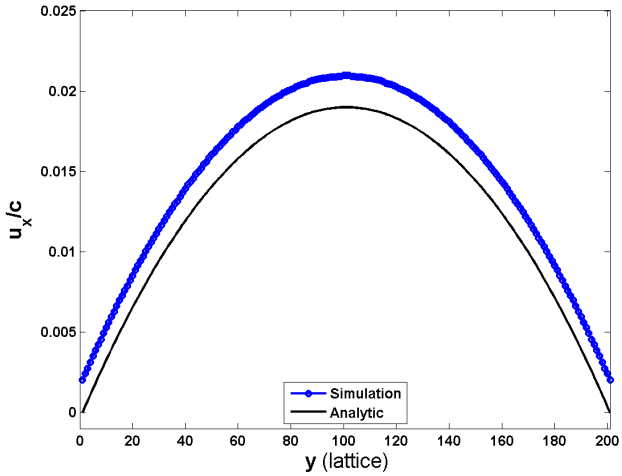

Figure 32: Velocity profile of Bouncy back boundary condition for $\tilde{\tau}^* = 40$

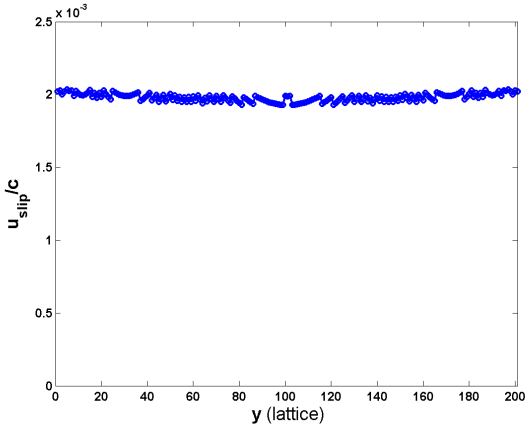

Figure 33: Slip velocity with Bouncy back boundary condition for $\tilde{\tau}^* = 40$

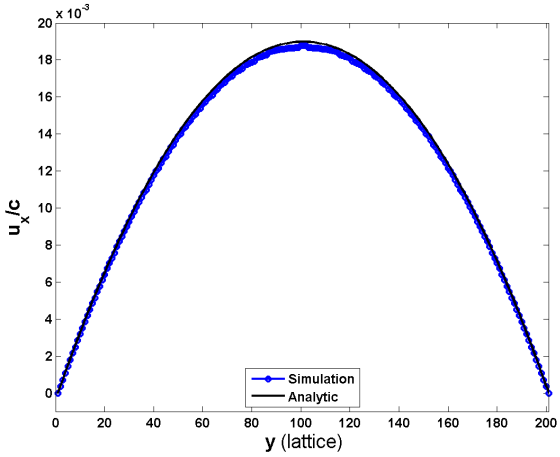

Figure 34: Velocity profile of nonslip boundary condition for $\tilde{\tau}^* = 40$

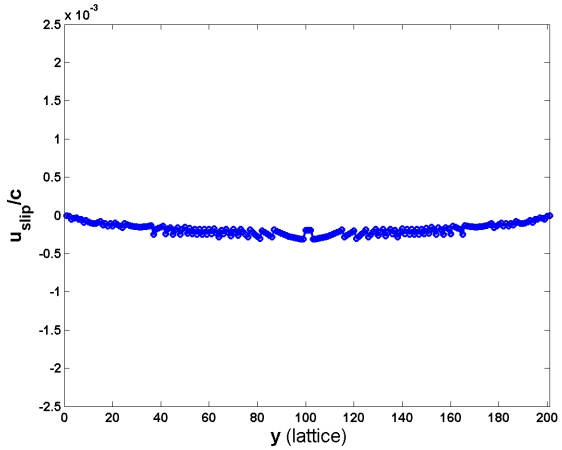

Figure 35: Slip velocity of nonslip boundary condition for $\tilde{\tau}^* = 40$

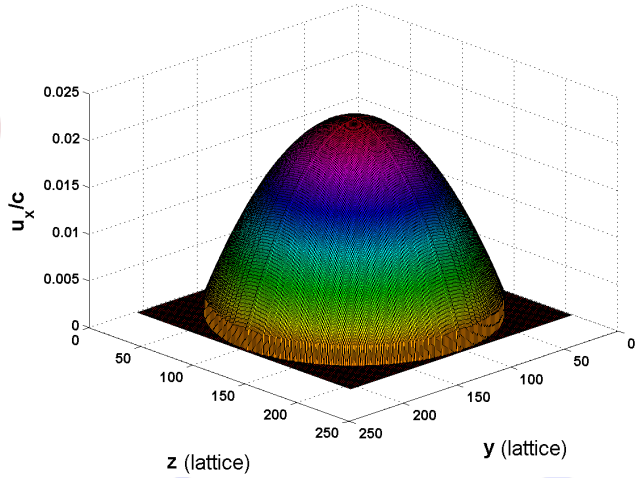

Figure 36: 3D Velocity profile with Bouncy back boundary condition for $\tilde{\tau}^* = 40$

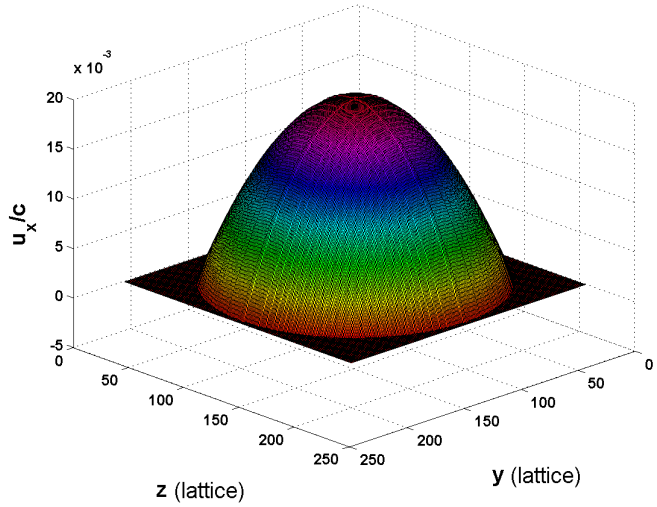

Figure 37: 3D Velocity profile with nonslip boundary condition for $\tilde{\tau}^* = 40$

Conclusion

Up to third-order moment analysis were entirely carried out. A third-order moments boundary reconstruction were proposed for D3Q19 lattice; Zero node particle population correction was introduced so that mass conservation is exactly satisfied on reconstructed boundary; Proposed boundary reconstruction can exactly satisfy not only for nonslip solid wall boundary condition, but also for prescribed velocity (or density) boundary condition, including inlet or outlet boundary; Proposed boundary reconstruction keeps all known particle populations, proposed boundary condition also is on-site, and it reconstructs unknown particle population only in terms of information on the current lattice site, it is of great advantage for parallel computing; Some new boundary configurations were reconstructed; Proposed third-order moments boundary reconstruction can be easily extended to thermal lattice Boltzmann model (we will address this issue in another paper), especially isothermal boundary, where nonzero heat flux is essential; Proposed boundary reconstruction was used for case study, simulation results shown proposed method can exactly satisfy prescribed boundary condition while bounce-back boundary condition cannot.

Acknowledgment

Many thanks to Dr. Jingsheng Ma for his kind help. He provided the author with constructive suggestions and dissuasion, and more ever, he spent a lot of time to revise the manuscript. Many thanks to the High Education funding of Guangdong Province （No.2018KZDXM07）for financial support.

References

1. Zou QS & He XY (1997) On pressure and velocity boundary conditions for the lattice Boltzmann BGK model. Physics of Fluids 9: 1591-1598.
2. Ma J, Wu K, Jiang Z, Couples GD (2010) SHIFT: An implementation for lattice Boltzmann simulation in low-porosity porous media. Phys Rev E 81: 056702.
3. Mei R, Shyy W, Yu D, Luo LS (2000) Lattice Boltzmann method for 3-D flows with curved boundary. J Comput Phys 161(2): 680-699.
4. Mei RW, Luo LS, Shyy W (1999) An accurate curved boundary treatment in the lattice Boltzmann method. J Comput Phys 155(2): 307-330.
5. Verschaeve JCG, Muller B (2010) A curved no-slip boundary condition for the lattice Boltzmann method. J Comput Phys 229(19): 6781-6803.
6. Strack OE, Cook BK (2007) Three-dimensional immersed boundary conditions for moving, solids in the lattice-Boltzmann method. International Journal for Numerical Methods in Fluids 55: 103-125.
7. Noble DR, Torczynski JR (1998) A lattice-Boltzmann method for partially saturated computational cells. Int J Mod Phys C 9: 1189-1201.
8. Holdych DJ, Noble DR, Georgiadis JG, Buckius RO (2004) Truncation error analysis of lattice Boltzmann methods. J Comput. Phys 193(2), 595-619.
9. Hecht M, Harting J (2010) Implementation of on-site velocity boundary conditions for D3Q19 lattice Boltzmann simulations. J Stat Mech.-Theory Exp P01018.
10. Skordos PA (1993) Initial and Boundary-Conditions for the Lattice Boltzmann Method. Physical Review E 48: 4823-4842.
11. Latt J, Chopard B, Malaspinas O, Deville M, Michler A (2008) Straight velocity boundaries in the lattice Boltzmann method. Physical Review E 77.
12. Yoon H, Kang Q, Valocch AJ (2015) Lattice Boltzmann-Based Approaches for Pore-Scale Reactive Transport. Reviews in Mineralogy and Geochemistry 80: 393-431
13. Chen C, Packman AI, Gaillard JF (2008) Pore-scale analysis of permeability reduction resulting from colloid deposition. Geophysical Research Letters 35.
14. Chen L, Kang Q, Pawar R., He YL, Tao WQ (2015) Pore-scale prediction of transport properties in reconstructed nanostructures of organic matter in shales. Fuel 158: 650-658.
15. Bianchi F, Wittel FK, Thielmann M, Trtik P, Herrmann HJ (2018) Tomographic Study of Internal Erosion of Particle Flows in Porous Media. Transport in Porous Media 122, 169-184.
16. He XY., Zou QS, Luo LS, Dembo M (997) Analytic solutions of simple flows and analysis of nonslip boundary conditions for the lattice Boltzmann BGK model. Journal of Statistical Physics 87: 115-136.
17. Ansumali S, Karlin IV, Arcidiacono S, Abbas A, Prasianakis NI (2007) Hydrodynamics beyond Navier-Stokes: Exact solution to the lattice Boltzmann hierarchy. Physical Review Letters 98: 124502.
18. Kim SH, Pitsch H (2008) Analytic solution for a higher-order lattice Boltzmann method: Slip velocity and Knudsen layer. Phys Rev E 78(1): 016702.
19. Feng Z, Lim HC (2018) Mass-Conserved Wall Treatment of the Non-Equilibrium Extrapolation Boundary Condition in Lattice Boltzmann Method. Energies 11: 1.
20. Ma J (2016) Pore-Scale Characterization of Gas Flow Properties in Shale by Digital Core Analysis. Chapter 4, Unconventional Oil and Gas Resources Handbook, Pp: 127-150.
21. Inamuro T, Yoshino M, Ogino F (1995) A Non-Slip Boundary-Condition for Lattice Boltzmann Simulations. Physics of Fluids 7: 2928-2930.
22. Noble DR, Georgiadis JG, Buckius RO (1995) Direct Assessment of Lattice Boltzmann Hydrodynamics and Boundary-Conditions for Recirculating-Flows. Journal of Statistical Physics 81: 17-33.
23. Maier RS, Bernard RS, Grunau DW (1996) Boundary conditions for the lattice Boltzmann method. Physics of Fluids 8: 1788-1801.

24. Chopard B, Dupuis A (2003) A mass conserving boundary condition for lattice Boltzmann models. International Journal of Modern Physics B 17: 103-107.

25. Bao J, Yuan P, Schaefer L (2008) A mass conserving boundary condition for the lattice Boltzmann equation method. J Comput Phys 227: 8472-8487.

26. Malaspinas O, Deville M, Chopard B (2008) Towards a physical interpretation of the entropic lattice Boltzmann method. Physical Review E 78.

27. Kruger T, Varnik F, Raabe D (2009) Shear stress in lattice Boltzmann simulations. Physical Review E 79.

28. Hollis AP, Halliday I, Care CM (2008) An accurate and versatile lattice closure scheme for lattice Boltzmann equation fluids under external forces. J Comput Phys 227(7): 8065-8082.

29. Hollis A, Halliday I, Care CM (2006) Enhanced, mass-conserving closure scheme for lattice Boltzmann equation hydrodynamics. J Phys A-Math Gen 39: 10589-10601.

30. Halliday I, Hammond LA, Care CM (2002) Enhanced closure scheme for lattice Boltzmann equation hydrodynamics. J Phys A-Math Gen 35: L157-L166.

31. Bennett S, Asinari P, Dellar PJ (2012) A lattice Boltzmann model for diffusion of binary gas mixtures that includes diffusion slip. International Journal for Numerical Methods in Fluids 69(1): 171-189.

32. Taheri P, Torrilhon M, Struchtrup H (2009) Couette and Poiseuille microflows: Analytical solutions for regularized 13-moment equations. Physics of Fluids 21.

33. He XY, Shan XW, Doolen GD (1998) Discrete Boltzmann equation model for nonideal gases. Physical Review E 57, R13-R16.

Appendix

Appendix A: Boundary Configurations in 2D

Suppose we have a binary image of porous soil structure, as shown in Figure 38, where each blue pixel defines solid while white pixel stands fir pore. Given a binary image, there are three approaches to define the fluid domain and lattice. The first approach is shown in Figure 39, where each node is allocated at the center of each pixel. The first fluid node near the solid wall is considered as a boundary node. The nonslip (or prescribed velocity) boundary condition is assigned to the boundary (first fluid) node. The disadvantage of this approach is that the zero velocity is at the center of the first fluid pixel rather than on the exact boundary.

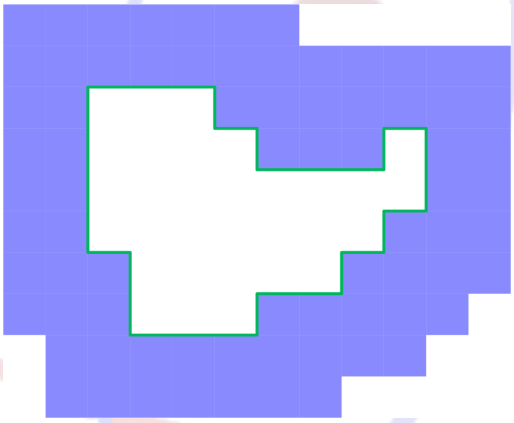

Figure 38: Binary CT image of soil structure

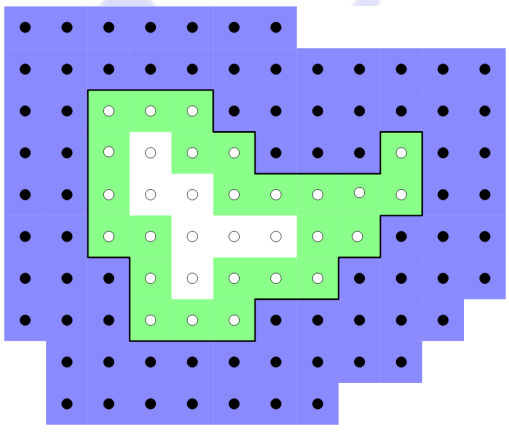

Figure 39: The first approach: node is in the center of the pixel. The first fluid node is a boundary node. No extension on fluid domain.

The second approach is shown in Figure 40, where each node is located at the center of the pixel. The first solid node near the reconstructed fluid node is considered as a boundary node. The nonslip (or prescribed velocity) boundary condition is assigned to the boundary (first solid) node. Both collision and streaming steps will be implemented on the boundary node. Thus, the second approach is equivalent to extend the fluid domain by one pixel towards a solid wall. The disadvantage of this approach is that the zero velocity is at the center of the first solid pixel, rather than on the exact boundary. The third approach is shown in Figure 41, where each node is located at the corner of each pixel. The boundary node is exactly at the original boundary. However, since both the collision and streaming steps will be implemented on the boundary node, thus the whole pixel associated with that boundary node has to be filled with fluid, otherwise streaming between the boundary node and neighboring pure fluid node is not fully specified. Therefore the fluid domain has to be extended by half pixel wide towards the solids wall. The dark green area in Figure 41 is the original solid area, which is replaced by the fluid area. From the implementation point of view, there is no difference between the white area, green area, or dark green area. Thus Figure 41 is equivalent to Figure 42

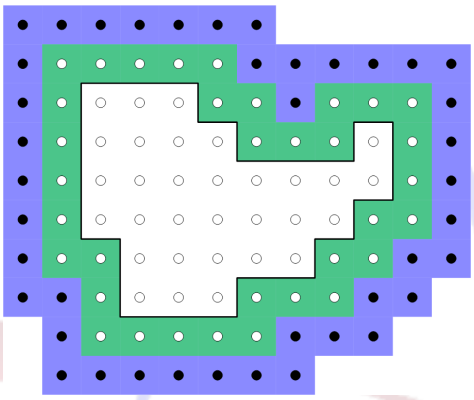

Figure 40: The second approach: node is in the center of the pixel. The first solid node is a boundary node. Fluid domain is extended by one pixel towards a solid wall.

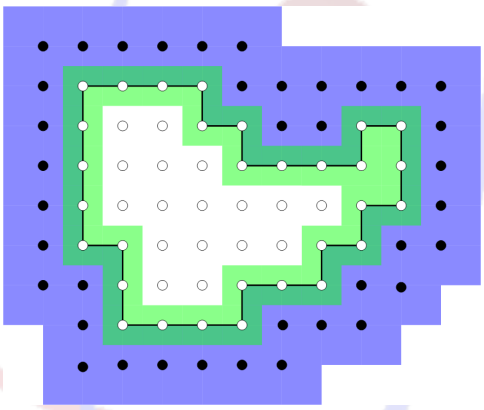

Figure 41: Third approach: node is on the edge of the original pixel. Fluid domain is extended by half a pixel towards a solid wall

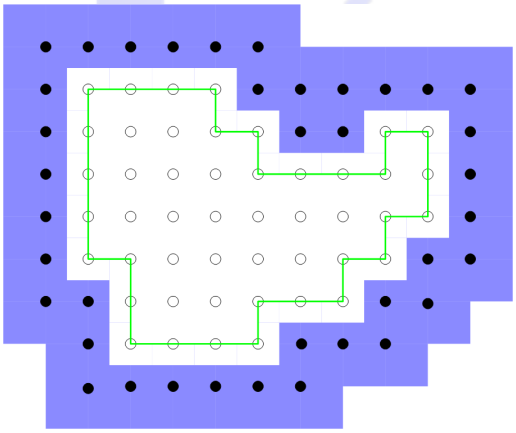

Figure 42: Extended fluid domain based on the third approach.

Note that in the third approach, after the fluid domain is extended, the minimum width of the pore is at least 2 pixels. In this paper, we assume that the resolution of the image is fine enough so that both the minimum width of grain and pore is at least 2 pixels.

To summarize, with the third approach, there are totally 6 different boundary configurations in 2D, as shown in Figure 43. Of course, any 90^0 rigid body rotation of a configuration above is also a possible configuration. We consider the two configurations to be identical if one of them can be obtained by a rigid body rotation from another one.

If the particle population that comes out from a solid node is represented by a hollow double arrow and the particle population that comes from fluid or boundary node is drawn as a solid arrow, then corresponding 6 boundary configurations in Figure 43 can be abstracted as Figure 44.

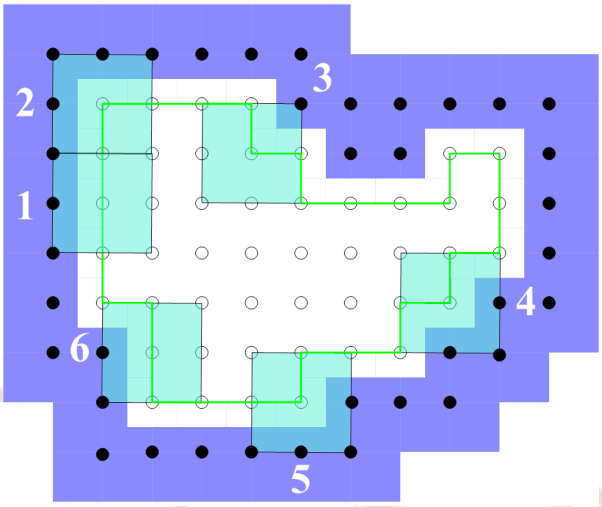

Figure 43: Boundary configurations based on the third approach.

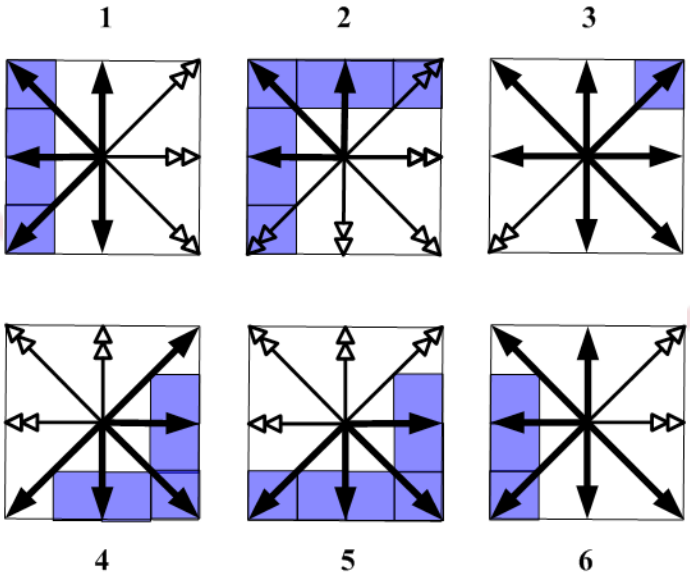

Figure 44: All possible boundary configurations based on the third approach

Appendix B: Solution of Poisson's Equation in A Square Domain

Consider Poisson's equation

$$\begin{cases} \left.\dfrac{\partial^2 u}{\partial y^2}+\dfrac{\partial^2 u}{\partial z^2}\right|_{\Omega} = -1 \\ u|_{\partial\Omega} = 0 \end{cases} \qquad \text{(B.1)}$$

in which

$$\Omega=(-1,1)\times(-1,1) \tag{B.2}$$

Introduce unknown function transformation

$$u(y,z)=v(y,z)+\frac{1-z^2}{2} \tag{B.3}$$

Then Eq.(B.1) becomes into

$$\begin{cases}\left.\dfrac{\partial^2 v}{\partial y^2}+\dfrac{\partial^2 v}{\partial z^2}\right|_{\Omega}=0\\ v|_{\partial\Omega}=\dfrac{z^2-1}{2}\end{cases} \tag{B.4}$$

Eq. (B.4) is a Laplace's equation, separate variables method is applicable, let

$$v(y,z)=\sum_{n=0}^{\infty}f_n(y)g_n(z) \tag{B.5}$$

then

$$\frac{\partial^2 v(y,z)}{\partial y^2}=\sum_{n=0}^{\infty}f_n''(y)g_n(z) \tag{B.6}$$

$$\frac{\partial^2 v(y,z)}{\partial z^2}=\sum_{n=0}^{\infty}f_n(y)g_n''(z) \tag{B.7}$$

Substituting Eq. (B.6) and (B.7) into Eq. (B.4)

$$\sum_{n=0}^{\infty}f_n''(y)g_n(z)+f_n(y)g_n''(z)=0 \tag{B.8}$$

A sufficient condition of Eq. (B.8) is

$$\frac{f_n''(y)}{f_n(y)}+\frac{g_n''(z)}{g_n(z)}=0 \tag{B.9}$$

Therefore, each term in Eq.(B.9) have to be constant. It is easy to prove first term is positive, thus

$$\frac{f_n''(y)}{f_n(y)}=-\frac{g_n''(z)}{g_n(z)}=c_n^2 \tag{B.10}$$

The boundary condition in Eq.(B.4) reads

$$\begin{cases}v(\pm1,z)=\sum_{n=0}^{\infty}f_n(\pm1)g_n(z)=\frac{z^2-1}{2}\\ v(y,\pm1)=\sum_{n=0}^{\infty}f_n(y)g_n(\pm1)=0\end{cases} \tag{B.11}$$

$$\begin{cases}g_n''(z)+c_n^2g_n(z)=0\\ g_n(\pm1)=0\\ \sum_{n=0}^{\infty}g_n(z)=\frac{z^2-1}{2}\end{cases} \tag{B.12}$$

$$g_n(z)=A_n\cos c_nz+B_n\sin c_nz \tag{B.13}$$

$$g_n(-1)=A_n\cos c_n-B_n\sin c_n=0 \tag{B.14}$$

$$A_n=B_n\frac{\sin c_n}{\cos c_n}=D_n\sin c_n \tag{B.15}$$

$$g_n(z) = B_n \frac{\sin c_n}{\cos c_n} \cos c_n z + B_n \sin c_n z = D_n \left[\sin c_n \cos c_n z + \cos c_n \sin c_n z \right] \tag{B.16}$$

$$g_n(z) = D_n \sin\left[c_n (1+z) \right] \tag{B.17}$$

$$g_n(1) = D_n \sin[2c_n] = 0 \tag{B.18}$$

$$c_n = \frac{n\pi}{2} \tag{B.19}$$

$$g_n(z) = D_n \sin\left(n\pi \frac{1+z}{2} \right) \tag{B.20}$$

$$\sum D_n \sin\left(n\pi \frac{1+z}{2} \right) = \frac{z^2-1}{2} \tag{B.21}$$

$$\int_{-1}^{1} \sin^2\left(n\pi \frac{1+z}{2} \right) dz = 1 - \frac{\sin(2n\pi)}{2n\pi} = 1 \tag{B.22}$$

$$\int_{-1}^{1} \sin\left(n\pi \frac{1+z}{2} \right) \sin\left(k\pi \frac{1+z}{2} \right) dz = \frac{2\left[\mathrm{ncos}(n\pi)\sin(k\pi) - \cos(k\pi)\sin(n\pi) \right]}{\pi\left(k^2 - n^2\right)} = 0 \tag{B.23}$$

$$D_n \int_{-1}^{1} \sin^2\left(n\pi \frac{1+z}{2} \right) dz = \int_{-1}^{1} \frac{z^2-1}{2} \sin\left(n\pi \frac{1+z}{2} \right) dz \tag{B.24}$$

$$D_n = \int_{-1}^{1} \frac{z^2-1}{2} \sin\left(n\pi \frac{1+z}{2} \right) dz = \frac{4\sin(n\pi)}{(n\pi)^2} + \frac{8\left[\cos(n\pi) - 1 \right]}{(n\pi)^3} \tag{B.25}$$

$$D_n = \begin{cases} 0 & \text{if } n \text{ is even} \\ -\dfrac{16}{(n\pi)^3} & \text{if } n \text{ is odd} \end{cases} \tag{B.26}$$

$$\frac{1-z^2}{2} = \frac{16}{\pi^3} \sum_{k=0}^{\infty} \frac{1}{(2k+1)^3} \sin\left[(2k+1)\pi \frac{1+z}{2} \right] \tag{B.27}$$

$$\begin{cases} f_n''(y) - \left(\dfrac{n\pi}{2} \right)^2 f_n(y) = 0 \\ f_n(\pm 1) = 1 \end{cases} \tag{B.28}$$

$$f_n(y) = \frac{\sinh\left(n\pi \frac{1+y}{2} \right) + \sinh\left(n\pi \frac{1-y}{2} \right)}{\sinh(n\pi)} \tag{B.29}$$

$$u = \frac{1-z^2}{2} \tag{B.30}$$

$$-\frac{16}{\pi^3} \sum_{k=0}^{\infty} \frac{\sinh\left[(2k+1)\pi \frac{1+y}{2} \right] + \sinh\left[(2k+1)\pi \frac{1-y}{2} \right]}{\sinh\left[(2k+1)\pi \right]} \frac{\sin\left[(2k+1)\pi \frac{1+z}{2} \right]}{(2k+1)^3}$$

$$\text{or } u = \frac{1-z^2}{2} - \frac{16}{\pi^3} \sum_{n=1,3,5}^{\infty} \frac{1}{n^3} \frac{\sinh\left(n\pi \frac{1+y}{2} \right) + \sinh\left(n\pi \frac{1-y}{2} \right)}{\sinh(n\pi)} \sin\left(n\pi \frac{1+z}{2} \right) \tag{B.31}$$